REGULATION OF THE NEURONAL K^+-Cl^- COTRANSPORTER KCC2 BY PROTEIN ASSOCIATED WITH MYC

By

Nicole Jodela Garbarini

Dissertation

Submitted to the Faculty of the

Graduate School of Vanderbilt University

in partial fulfillment of the requirements

for the degree of

DOCTOR OF PHILOSOPHY

in

Neuroscience

May, 2008

Nashville, Tennessee

Approved:

Professor Eric Delpire

Professor Randy Blakely

Professor Louis DeFelice

Professor Anne Kenworthy

Professor Bih-Hwa Shieh

To Mom and Dad, for all their love and support throughout the years

and

In memory of Roger England,

for supporting everyone in our lab,

and for his 40 years of dedication to research at Vanderbilt.

ACKNOWLEDGEMENTS

Many people have provided me with support throughout my graduate school and academic career. I would like to first thank my advisor, Eric, for training me in the lab, and always being very kind, patient, and receptive as we both learned the ropes of the successful mentor/mentee relationship. I also appreciate his encouragement and support when I have investigated other scientific career paths, particularly in regard to my AAAS Mass Media Fellowship. My thesis committee chair, Randy Blakely, provided exceptional leadership and advice, and always made time to meet with me and discuss my progress. Lou DeFelice, Anne Kenworthy, and Bih-Hwa Shieh also were enthusiastic participators in my committee meetings, and I thank them for their commitment to helping my project. The American Heart Association supported my thesis project via a predoctoral grant award, and I thank them for their generous contribution to my research.

I thank the members of the Delpire Laboratory, past and present, for valuable discussions and advice. I would particularly like to thank our postdoctoral fellows: Kerstin Piechotta, for training me in yeast two-hybrid and other laboratory techniques, and Kenneth Gagnon, for enthusiastic discussions of data and models, as well as for helping me prepare for my defense.

The Neuroscience Graduate Program has grown tremendously over my time at Vanderbilt, and I truly appreciate the many opportunities this program provided. Elaine Sanders-Bush and Lou DeFelice, who both served in the role of Director of Graduate Studies, enhanced my graduate school experience though their openness, personal support and advice on many occasions. I also appreciate the help of program staff and

administration, particularly Mary Early-Zald, Shirin Pulous, and Mary Michael-Woolman.

Prior to graduate school, I have had the great fortune of having wonderful teachers who inspired me to achieve and be my very best. I would particularly like to thank Beverly Cardino, my high school English teacher who remains a friend to this day, as well as Dr. Philip Zinsmeister, my undergraduate advisor at Oglethorpe University, who inspired me to pursue biology through his mentorship and example.

I am very fortunate to have had the enduring love and support of family and friends. I would like to thank my parents, Ray and Nieves, for loving me and caring for me through all of my life. I can always count on them for checking in on me, supporting my academic endeavors, and unhesitatingly sharing my successes to anyone with an open ear. I thank them for instilling me with ambition and independence, as well as kindness and good judgment, and I gladly share my achievements with them.

There are so many friends who have contributed to my graduate school experience. I thank Brandon Smith for his continuous love, support, and comfort. Leigh Carmody and Ashley Brady have been great sources of technical advice for my thesis project, tips for staying afloat, and above all, friendship. Several other fellow IGP friends, especially Angela Boutte and Efrain Garcia, have also stood alongside me for both work and play; I count myself lucky to have had such a warm, open, and intelligent group of companions throughout my graduate school career. Last but not least, I would like to thank Kerry Crowe, Gabriela Peters-Cuellar, Sean Jewett, Blake Stabler, Heidi Blackwell, and Casey Dryden for also giving me their unconditional love and support in everything I do.

TABLE OF CONTENTS

LIST OF FIGURES

Page

LIST OF TABLES

CHAPTER I

INTRODUCTION

Chloride regulation in GABAergic signaling and inhibitory neurotransmission

The regulation of intracellular neuronal chloride is essential to proper neurotransmission. In the nervous system, excitatory neurotransmitters generate action potentials by causing a depolarization of the neuronal membrane potential. Inhibitory neurotransmission propagated by the neurotransmitters glycine and GABA are required to balance and fine tune this system. GABA is the predominant inhibitory neurotransmitter in the adult nervous system, acting primarily through the ionotropic $GABA_A$ receptors. The $GABA_A$ receptor primarily transports chloride ions, with some bicarbonate ions transported through the channel as well. When GABA stimulates the $GABA_A$ receptor, an inhibitory response is generated by the hyperpolarization caused by chloride ions moving into the cell due to the low intracellular chloride concentration. Thus, it is this low intracellular chloride concentration which allows GABA to have an inhibitory effect. When internal chloride concentrations are higher than the external milieu, GABA instead acts as an excitatory neurotransmitter.

The regulation of intracellular chloride concentration in neurons is governed primarily by a family of ion cotransporters known as the cation chloride cotransporters, or CCCs.

Cation-chloride family of transporters

Seven CCCs have been identified: one Na+-Cl- cotransporter (NCC), two Na+-K+-Cl- cotransporters (NKCC1 and NKCC2), and four K+-Cl- cotransporters (KCC1-4) (Figure 1). The Na-Cl cotransporter is inhibited by thiazide diuretics, whereas the Na-K-2Cl and the K-Cl cotransporters are inhibited by the loop diuretics bumetanide and furosemide. NCC and NKCC2 are renal-specific, while the remaining five cotransporters are all found in the brain (Delpire, 2000). Furosemide and bumetanide are loop diuretics that target the cation-chloride cotransporters, but they are very unspecific. The KCC family includes four isoforms (KCC1-4). They all share an approximate 30% amino acid identity to other members of the CCC family. KCCs transport K^+ to Cl^- in a 1:1 ratio, allowing for electroneutral transport (Lauf et al., 1992; Jennings and Adame, 2001). All KCCs are sensitive to changes in cell volume and are activated by cell swelling (Gillen et al., 1996; Hiki et al., 1999; Mount et al., 1999; Race et al., 1999). Upon cell swelling, KCCs extrude K^+ and Cl^- ions from the cell, returning cell volume to control values. KCC1 is a ubiquitously expressed protein, with a 'housekeeping' role in cell volume maintenance and regulation. KCC3 and KCC4 are widely but not universally expressed. They are both found predominantly in kidney, heart, skeletal muscle and brain (Hiki et al., 1999; Mount et al., 1999; Race et al., 1999; Pearson et al., 2001).

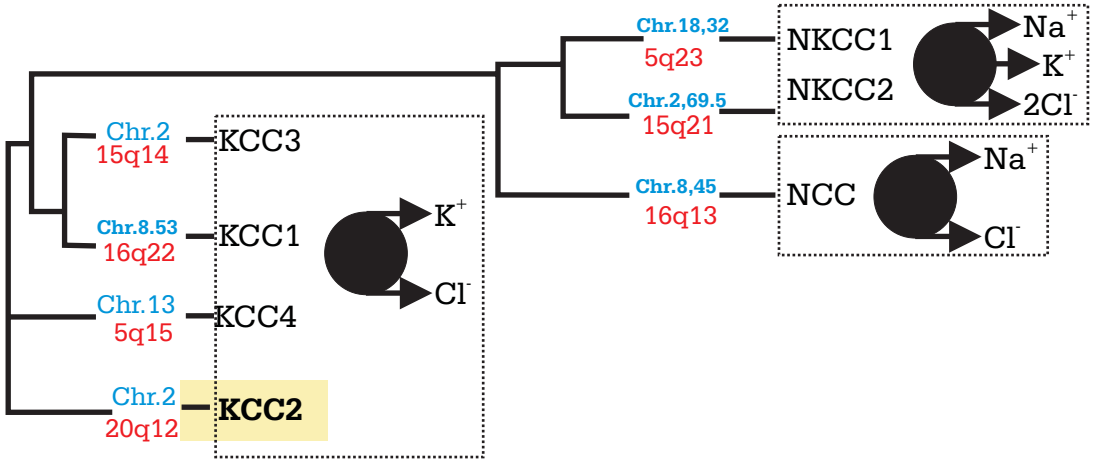

Figure 1. Tree of cation-chloride cotransporter family.
Homology tree of the cation chloride cotransporter (CCC) family. There are four potassium chloride cotrasnporter (KCC) isoforms, with the greatest similarity between KCC1 and KCC3, and KCC2 and KCC4. The only sodium chloride cotransporter (NCC) and the two isoforms of sodium-potassium-chloride cotransporters (NKCC1, and NKCC2) are likewise shown. Next to each isoform, mouse and human chromosome locations are shown. Murine, upper/blue text; human lower/red text.

KCC2 background

Structure

KCC2 has a high (~67%) amino acid identity to the other KCCs, with the greatest homology to KCC4 (Payne et al., 1996; Mount et al., 1999). All members of the CCC family have twelve transmembrane domains with cytoplasmic N' and C' terminal regions (Lauf and Adragna, 2000). KCCs are set apart from other CCCs by a large predicted extracellular loop with 4 putative N-glycosylation sites, present between transmembrane domains 5 and 6 (Payne et al., 1996) (Figure 2). The KCCs also have a number of putative protein kinase C phosphorylation sites in the C terminus (Payne et al., 1996). KCC2 and KCC4 share a tyrosine kinase consensus phosphorylation site in the C' terminus (Payne et al., 1996; Mount et al., 1999). It has been shown that this tyrosine residue (Y1087) is critical for KCC2 function, yet amino acid substitutions and pharmacological studies show no regulatory role for tyrosine residue phosphorylation (Strange et al., 2000). KCC2 has a 34 amino acid region, also located in the carboxyl terminus, which is unique from the other KCC isoforms (Payne et al., 1996; Hiki et al., 1999; Mount et al., 1999). Although there was only known isoform of KCC2 for over a decade, we now know there are two isoforms of this cotransporter. KCC2b, which had been first cloned in 1996, is the most prominent and well-studied isoform of the transporter -- it is the isoform which has been shown to have very little expression early in life, but is upregulated during development. KCC2b is also the most abundant during maturity. Most recently, Uvarov, et al. discovered an alternative promoter and first exon located upstream of the previously identified start of KCC2b. This novel KCC2 isoform, KCC2a, differs by 40 amino acids in the N-terminal region. The KCC2a isoform makes

up almost 50% of the low KCC2 levels present after birth, but only 5-10% of the total KCC2 in the mature cortex (Uvarov et al., 2007).

Several reports contribute to the hypothesis that KCC2 likely exists as functional homomultimers. NKCC1 has been reported to exist as a dimer (Moore-Hoon and Turner, 2000) and dominant negative effects by truncated KCC1 coexpressed with wild type KCC suggest that the KCCs function as multimers, as well (Casula et al., 2001). Analysis of rat brain proteins taken at different ages have also been analyzed by SDS-PAGE/Western blot in different concentrations of cross-linking and reducing agents. This study suggested that oligomerization of KCC2 is age-dependent, with monomeric inactive KCC2 present to a small extent in early development, and active homodimers present in mature brain (Blaesse et al., 2006). Yeast two-hybrid and pull-down assays of heterologously expressed CCCs have suggested that the KCC isoforms, as well as NKCC1, could possibly exist in heteromultimers, although further work needs to be done to demonstrate this *in vivo* and explain its possible physiological role (Simard et al., 2007).

Spatial and temporal KCC2 Expression

KCC2 is unique to all the KCCs in that it is only expressed in neurons. A Neuronal Restrictive Silencing Element found in the KCC2 gene is proposed to confer neuron-specific KCC2 expression (Karadsheh and Delpire, 2001). Analysis of KCC2 gene regulation identified several potential transcription factor binding sites in the KCC2 promoter region. One of these proposed transcription factors, Early growth response 4 (Egr4) has been demonstrated in cultured neurons as having a functional effect on KCC2 transcription (Uvarov et al., 2005; Uvarov et al., 2006). KCC2 is expressed highly

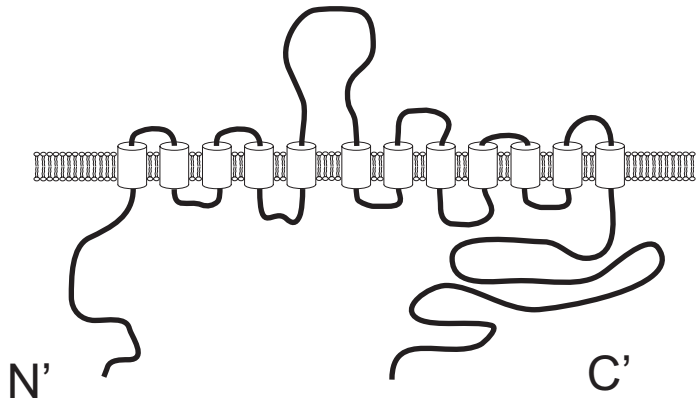

Figure 2. Predicted topology of KCC2.
Kyle-Doolittle hydropathy plot analysis of KCC2 predicts a twelve transmembrane domain protein with intracellular N' and C' terminal tails, as reported in Payne et al., 1996. A large extracellular loop with four predicted N-glycosylation sites occurs between transmembrane domains 5 and 6. All members of the CCC family share this 12 transmembrane domain and intracellular N' and C' tail structure.

throughout the central nervous system, and enriched in GABAergic and glycinergic neurons, including pyramidal neurons of the hippocampus and Purkinje neurons and granular cells of the cerebellum, as exemplified in Figure 3 (Payne et al., 1996; Lu et al., 1999; Williams et al., 1999). In the granule cell layer of the cerebellum, KCC2 exhibits distinct colocalization with the β2/β3-subunits of the $GABA_A$ receptor (Williams et al., 1999). In terms of subcellular localization, immunolocalization studies in rat cerebellum, spinal cord, and hippocampus show that KCC2 is primarily expressed at neuronal soma and dendrites (Williams et al., 1999; Gulyas et al., 2001; Hubner et al., 2001). Although KCC2 is closely linked with GABAergic signaling, it is not, however, confined to the vicinity of inhibitory synapses. KCC2 shows subcellular localization near excitatory synaptic inputs in the adult rat hippocampus, potentially in correlation to the presence of extrasynaptic $GABA_A$ receptors expressed on the shafts of dendritic spines (Gulyas et al., 2001).

KCC2 expression overlaps with gonadotropin-releasing hormone (GnRH) in approximately 35% of GnRH-neurons, and there appears to be sexual dimorphism in KCC2 expression during development. Only females exhibit a gradient of KCC2 expression in GnRH-cells from the rostral to caudal sides of the brain. Males, however, maintain a consistent level of KCC2 localization (Leupen et al., 2003). At postnatal day 15, KCC2 expression in the substantia nigra pars reticulate is significantly lower in male rats than female rats. Electrophysiology experiments using cells from this age and brain region show the functional effect of this difference, as application of the $GABA_A$ agonist

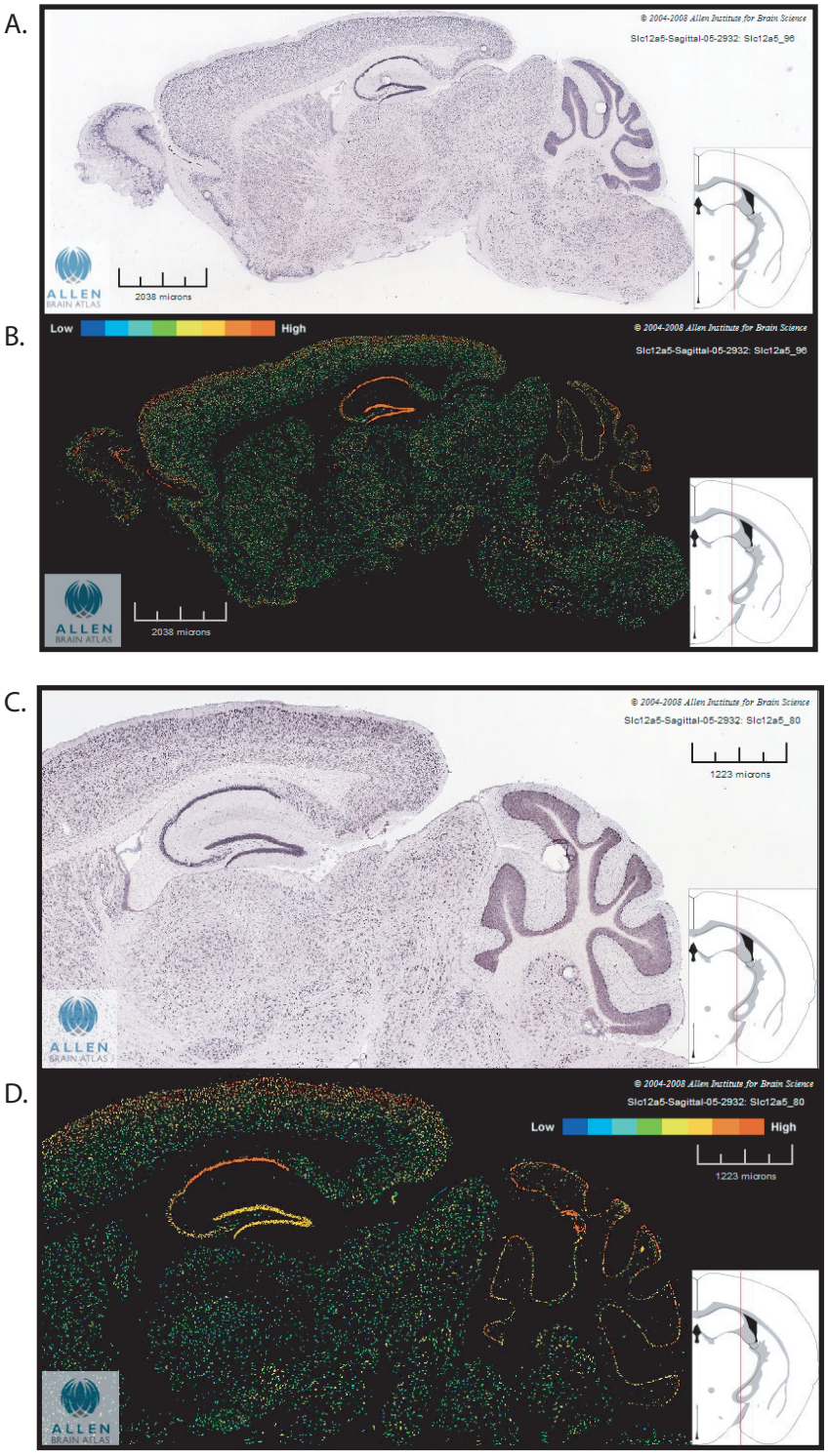

Figure 3. KCC2 expression in the brain.
Sagittal sections of adult male C57BL/6J mouse brains show KCC2 gene expression throughout the brain, by *in situ* hybridization (A, C) and shown with corresponding color map of gene expression (B, D). Insets show position of slices from coronal perspective. A, B: position 2000. C, D. position 2400. Images obtained from Allen Brain Atlas [Internet]. Seattle (WA): Allen Institute for Brain Science, 2007.

muscimol depolarizes male neurons, but hyperpolarizes female neurons (Galanopoulou and Moshe, 2003). Similar differences in KCC2 levels have also been reported in neurons of the developing hippocampus and developing hypothalamus (Nunez and McCarthy, 2007; Perrot-Sinal et al., 2007) Such differences between males and females are an interesting field of expanded studies, in light of predisposition of males to developmental disorders associated with GABA signaling, and male susceptibility to brain injury (McCarthy et al., 2002; Galanopoulou and Moshe, 2003).

KCC2 expression is upregulated throughout development, with the greatest expression during adulthood. Minimal amounts of KCC2 RNA and protein are expressed during birth, and it has been recently shown that the isoform which is present is the less-common KCC2a isoform, as discussed earlier (Lu et al., 1999; Uvarov et al., 2007).

The upregulation of KCC2 expression is coincident with a change in GABAergic responses. In early development, GABA is an excitatory, depolarizing neurotransmitter. GABA signaling later transitions to inhibitory and hyperpolarizing; this the most prominent GABAergic effect during adulthood. The role of KCC2 in GABAergic signaling will be discussed later in the introduction.

KCC2 activity and regulation

Like the other KCCs, KCC2 is an electroneutral cation-chloride cotransporter. A direct estimate of KCC stoichiometry in erythrocytes suggests a 1:1 ratio of K^+ ions and Cl^- ions are transported together across the cell membrane (Jennings and Adame, 2001), and numerous electrophysiological experiments likewise indicate that KCC2 function does not affect the membrane potential. This electroneutral stoichiometry makes it ideal for establishing intracellular $[Cl^-]$, as it can alter $[Cl^-]_i$ without changing the resting

membrane potential of the cell. While all the KCCs are activated by cell swelling, KCC2 is unique in that it is constitutively active in isotonic conditions (Payne et al., 1996; Payne, 1997; Williams et al., 1999).

There are several known pharmacologic stimulators and inhibitors of KCC2 activity, although they are not specific for KCC2 in particular. The alkylating agent N-ethylmaleimide (NEM) has been shown to activate ^{86}Rb uptake by KCC2. The loop diuretics furosemide and bumetanide are known inhibitors of this KCC2 activity, with KCC2 having a higher sensitivity to furosemide than bumetanide (inhibition constant (K_i) of ~25 μM and ~55 μM, respectively). Furthermore, compounds known to inhibit K-Cl transport in red blood cells likewise have been shown to inhibit KCC2. The stilbene disulfonic acid DIDS (4,4'-diisothiocyanostilbene-2,2'-disulfonic acid) and the alkanoic acid DIOA ([(dihydroindenyl)oxy]alkanoic acid) have been shown to inhibit approximately 80% of furosemide-sensitive flux at a concentration of 100 μM. (Payne, 1997)

KCC2 regulation is influenced by phosphorylation and dephosphorylation, although the exact mechanisms and pathways involved are not precisely understood (Figure 4). PKC activation has been previously shown to decrease KCC2 surface expression and activity when expressed in oocytes (Bergeron et al., 2006). However, a recent study has shown that, in HEK293 cells and cultured neurons, protein kinase C phosphorylation of a serine residue in the carboxyl terminus increases KCC2 cell surface expression by decreasing the rate of transporter endocytosis (Munoz et al., 2007).

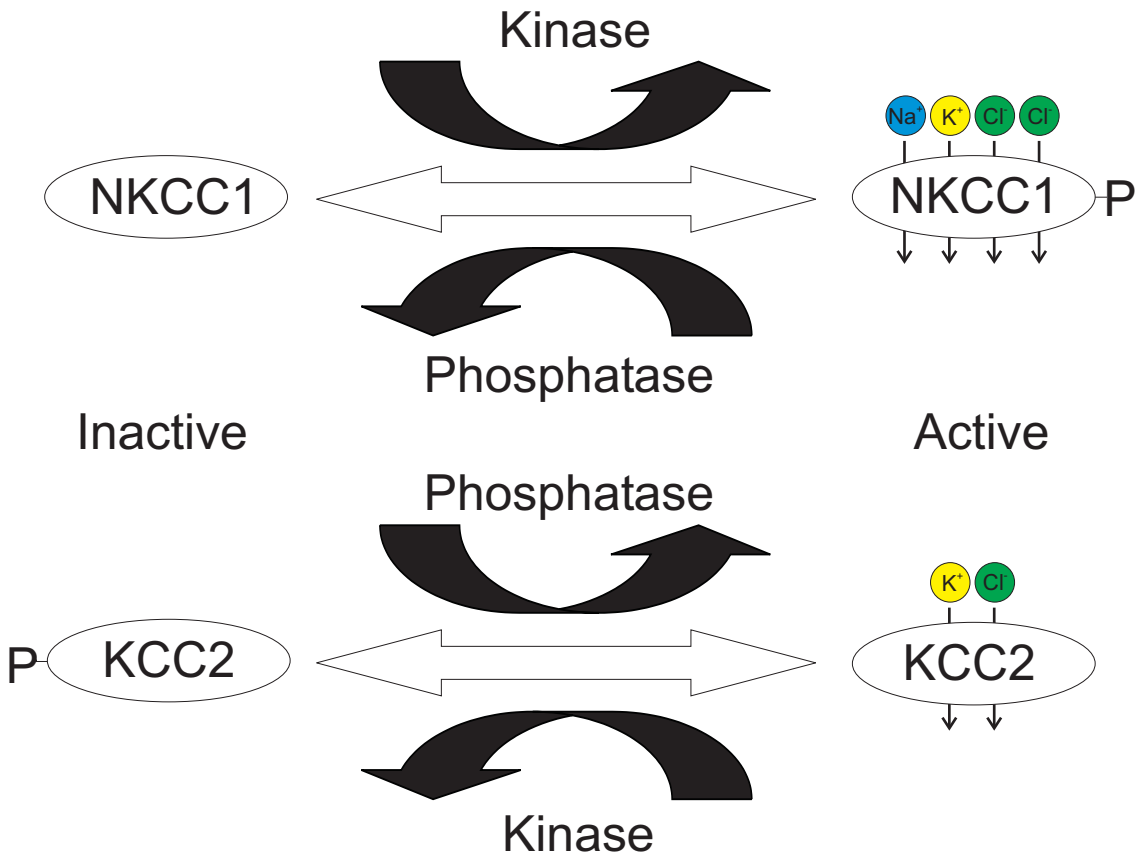

Figure 4. NKCC1 and KCC2 are regulated by phosphorylation/dephosphorylation.
NKCC1 and KCC2 are regulated by opposing phosphorylation pathways. NKCC1 is activated by phosphorylation, whereas KCC2 is activated by dephosphorylation.

Co-application of IGF-1 and c-src has been shown to rapidly activate KCC2, post-translationally, in immature neurons, suggesting that protein tyrosine phosphorylation pathways are key to KCC2-mediated transport (Kelsch et al., 2001).

Another interesting emerging story is the effect of SPAK (Ste20-related proline-alanine-rich kinase) and WNK (With No Lysine/(K)) kinases on KCC2 function. SPAK was first identified as an interactor with the N-terminus of KCC3. Piechotta et al identified the SPAK binding motif on the cotransporter as [R/K]-F-x-[V/I] and subsequent analysis of the other CCCs identified two SPAK binding sites on NKCC1.(Piechotta et al., 2002) Yeast two-hybrid library screening with SPAK identified WNK4 and other proteins related to the stress-response pathway as potential interactors. This data, along with further characterization of SPAK binding and NKCC1 function, suggested a role of SPAK as not just a kinase, but as a scaffolding protein as well (Piechotta et al., 2003). The current working model of NKCC1 activation suggests WNK phosphorylates SPAK, which in turn leads to SPAK translocation to the membrane for phosphorylation and activation of NKCC1 (Gagnon et al., 2006; Delpire and Gagnon, 2008).

Yeast two-hybrid has demonstrated that the N-terminus of KCC2b, the original, and most prevalent KCC2 isoform, still interacts with the kinase even though it lacks a [R/K]-F-x-[V/I] motif (Gagnon et al., 2006). Additionally, strong evidence suggests that SPAK and WNK also have an effect on KCC2 activity. KCC2 activity is significantly decreased by coexpression of SPAK and WNK4 in both isosmotic and hyposmotic conditions. Interestingly, in isosmotic conditions, a switch to kinase-dead SPAK causes a significant increase in flux compared to KCC2 alone. However, in hyposmotic

conditions, a switch to inactive SPAK or omitting SPAK expression altogether leads to a decrease in KCC2 flux compared to KCC2 alone (Gagnon et al., 2006). Considering the opposing roles KCC2 and NKCC1 have in regulating intracellular chloride, it seems fitting that while SPAK and WNK4 contribute to NKCC1 activation, these same kinases can in turn cause KCC2 deactivation.

The newly identified isoform of KCC2, KCC2a, contains a putative SPAK binding motif in the 40 amino acids unique to this isoform of KCC2 (Uvarov et al., 2007). Experiments testing the effects of SPAK on KCC2a are yet to be performed, but it will be interesting to learn how SPAK affects this KCC2 isoform.

BDNF and KCC2

The neurotrophin BDNF has been shown to modulate KCC2, but with seemingly paradoxical effects. BDNF overexpressing mice exhibit increased KCC2 expression (Aguado et al., 2003). On the other hand, exogenous application of BDNF causes a dose-dependent and time-dependent (length of exposure) downregulation of KCC2 mRNA and protein levels (Rivera et al., 2002).

Rivera et al. have also studied stimulation of GABAergic inputs to CA1 neurons, and have demonstrated that rat hippocampal slices bathed in BDNF were depolarizing, as opposed to hyperpolarizing responses seen in control conditions (Rivera et al., 2002; Rivera et al., 2005). In a follow-up study, the same group further elucidates this mechanism of BDNF-mediated alterations in KCC2 expression and GABAergic response. When hippocampal slices were incubated in Mg^{2+}- free solution to generate continuous interictal activity, there was a decrease in KCC2 mRNA and KCC2 protein.

Slices in Mg^{2+}- free solution containing NBQX (1,2,3,4-Tetrahydro-6-nitro-2,3-dioxo-benzo[f]quinoxaline-7-sulfonamide) and AP-V (DL-2-Amino-5-phosphonopentanoic acid) to block seizure-like interictal activity do not show the same KCC2 decreases, demonstrating that it is the activity, rather than Mg^{2+} withdrawal alone, that causes this downregulation of KCC2, primarily in the CA1 region. Using biotinylation experiments, the authors also show that the turnover and degradation of cell-surface KCC2 is increased in Mg^{2+}- free solution, due to interictal activity. Fitting with their previous data, when they measure IPSPs in the CA1 region of hippocampal slices, Mg^{2+}-free solution and consequent activity causes a depolarizing shift in the IPSP reversal potential. They also show that the BDNF's effect on KCC2 occurs via the tyrosine kinase receptor B (TrkB). Transgenic mice with mutant TrkB lacking either the Phospholipase C or Shc docking sites do not undergo the same amount of KCC2 downregulation compared to control mice (Rivera et al., 2004; Rivera et al., 2005).

Protein interactions with KCC2

At the initiation of this project, there were no known protein-protein interactions with KCC2. Since then, two novel interactions have been reported. The first, reported in 2004, is the interaction between KCC2 and brain creatine kinase (CKB) (Inoue et al., 2004). The functional significance of this interaction was explored in a follow-up functional study using HEK293 cells and cultured cortical neurons. Heterologous expression of dominant negative CKB, glycine receptors, and KCC2 in HEK cells causes a depolarizing shift in the reversal potential of glycine. In neurons, application of the creatine kinase inhibitor, 2,4-dinitrofluorobenzene (DNFB), caused a depolarizing shift in

the GABA reversal potential (Inoue et al., 2006). Thus, it is suggested that one native role of CKB is to activate KCC2 activity.

Second, the cytoskeleton-associated binding protein 4.1N has been found to bind to KCC2, as well. Neurons cultured from KCC2 knockout mice have abnormal dendritic spine morphology and fewer functional dendritic synapses as compared to controls. In KCC2 -/- neurons, this phenotype is rescued by transfecting KCC2 mutant lacking the carboxyl terminus. Conversely, transfection of KCC2-CT alone into wild type neurons causes long dendritic spine protrusions similar to those seen in KCC2-/- mice. This led Li et al to examine KCC2-CT binding partners by immunoprecipitation and immune blotting for several proteins highly enriched in dendritic spines, from which they identified 4.1N as a KCC2 binding partner. The authors suggest that KCC2 in association with 4.1N may act as a synchronizing factor for synaptogenesis, perhaps by governing the neuron's response to glutamatergic and GABAergic signaling, and thus coordinating formation of inhibitory and excitatory synapses (Li et al., 2007).

Physiological significance of KCC2 function

KCC2 and GABAergic signaling

Because of its unique kinetic properties in isotonic conditions, KCC2 is proposed to serve as a buffer for external K^+ concentration in the direct vicinity of neurons, and to maintain intracellular Cl^- concentrations necessary for inhibitory GABA and glycine responses (Payne, 1997; Lu et al., 1999; Rivera et al., 1999; DeFazio et al., 2000; Delpire, 2000; Vardi et al., 2000).

The role of KCC2 in GABAergic neuronal communication is one of the more well-studied aspects of KCC proteins. The GABA response in immature brain is excitatory due to large depolarizing responses, whereas in the mature brain it is inhibitory. At birth, KCC2 expression is minimal, and increases markedly during postnatal development. This upregulation coincides with the switch of GABA and glycine responses from depolarizing to hyperpolarizing (Lu et al., 1999; Rivera et al., 1999). Viewed in light of KCC2 localization in GABAergic neurons and colocalization with the β2/β3-subunits of the $GABA_A$ receptor (Payne et al., 1996; Williams et al., 1999), such data support KCC2 as the neuronal Cl^- extruder which establishes the low $[Cl^-]_i$ and modulates GABA-stimulated responses (Figure 5).

Several studies have provided evidence for the role of KCC2 in modulating intracellular Cl- (Kakazu et al., 1999; Rivera et al., 1999; DeFazio et al., 2000; Kakazu et al., 2000; Vardi et al., 2000; Nabekura et al., 2002; Ueno et al., 2002; Zhu et al., 2005). For instance, in bipolar retinal neurons $GABA_A$ receptors are distributed equally among dendrites. However, the localized dendritic expression of KCC2 allows GABA to produce different effects on opposite poles of the same neuron (Vardi et al., 2000). Development in the retinotectal circuit is dependent on the shift in intracellular chloride ($[Cl^-]_i$) and targeted KCC2 expression in these developing neurons by electroporation is sufficient to prematurely shift $[Cl^-]_i$ and interfere with GABAergic signaling, and also with synaptic development of the retinotectal circuit (Akerman and Cline, 2006).

In some situations, GABA can act as an excitatory neurotransmitter even in mature neurons with normal adult levels of $[Cl^-]_i$. Coincident stimulation of neurons at dendrites and soma can create a shunting effect, resulting in a net depolarization due to

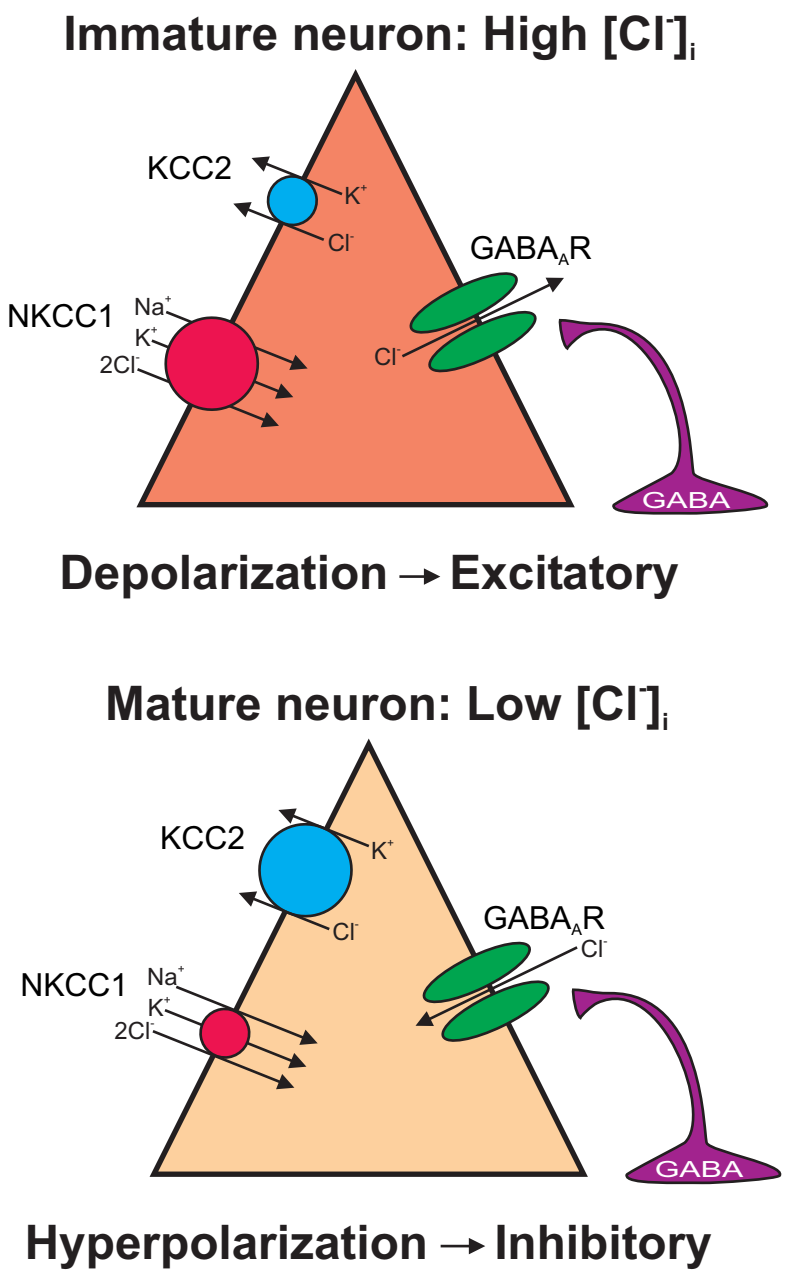

Figure 5. Intracellular Cl^- is altered by CCC expression.
Top panel: Model of an immature neuron illustrating higher expression of the Na-K-2Cl cotransporter than KCC2 cotransporter, thus resulting in a high intracellular Cl^- concentration (dark shading). Release of GABA then results in Cl^- exit through the ionotropic $GABA_A$ receptor, membrane depolarization, and excitatory neurotransmission. Bottom panel: In a mature neuron, expression of the KCC2 K-Cl cotransporter is greater than NKCC1, resulting in a lower intracellular Cl^- concentration (light shading). Thus, release of GABA results in Cl^- movement into the cell, membrane hyperpolarization, and inhibition.

bicarbonate transport by the $GABA_A$ receptor (Gulledge and Stuart, 2003). However, KCC2 subcellular distribution in cortical neurons can similarly affect the membrane potential response to GABA in mature cells. For instance, axon initial segments of pyramidal neurons are almost exclusively innervated by GABAergic axo-axonal cells. Absence of KCC2 in this localized region causes GABA to be depolarizing, even in mature neurons (Szabadics et al., 2006)

Cortical neurons from transgenic KCC2 knockout mice having 3 to 5% of normal KCC2 expression, unlike their wild type controls, show no developmental decreases in $[Cl^-]_i$. Moreover, when challenged with membrane depolarization, neurons lacking KCC2 cannot maintain existing intracellular chloride levels, or regulate chloride when challenged with chloride loading (Zhu et al., 2005). Expression of KCC2 is upregulated by increased spontaneous GABAergic activity and downregulated following blockade of $GABA_A$ receptors, demonstrating that GABA-mediated depolarization itself can then increase KCC2 expression and promote the maturation of the inhibitory response (Ganguly et al., 2001).

Animal models of KCC2 dysfunction

Studies of animal models with disruptions in KCC2 also indicate that this cotransporter plays an important role in neuronal communication. A full knockout of KCC2 in mice resulted in death shortly after birth, due to respiratory failure and consequent hypoxia (Hubner et al., 2001; Stein et al., 2004).

Mice with a targeted deletion of the exon 1b of KCC2 resulted in a 95% knockdown of KCC2 expression. Homozygous mice have tonic-clonic type seizures,

consisting of generalized limb stiffness, and die early, approximately two weeks after birth. These seizures could be induced by handling of the mice, as well. Homozygotes also had a decrease of KCC2 in parvalbumin-expressing interneurons in the brain, which follows previous reports of a loss of these neurons after seizures.

Common anti-convulsant pharmacologic agents were tested in these mice, as well. The $GABA_A$ agonist diazepam temporarily alleviated seizure activity, but was ineffective for long-term use or for prevention of future seizures. Phenytoin, another commonly used anti-convulsant drug, had a more lasting effect on alleviating seizures than diazepam, and also curbed the growth deficiencies seen in these KCC2 lacking mice. However, phenytoin efficacy decreased after approximately 12 days after birth. Seizures were exaggerated by administration of picrotoxin, a blocker of $GABA_A$ receptors. Heterozygote mice did not have an obvious phenotype but were more susceptible to seizures due to administration of the $GABA_A$ blocker pentylenetetrazole (Woo et al., 2002).

A *Drosophila* homologue to the mammalian KCC2 has also been identified through a screen for seizure-enhancing mutations. Named *kazachoc* (*kcc*), after the Slavic dance in which dancers squat and stiffly kick out alternating legs, this gene reduces seizure threshold in flies, functioning via $GABA_A$ mediated pathways (Hekmat-Scafe et al., 2006).

KCC2 and ischemia

Following stroke, brain damages include an overload of potassium due to K^+ release, and seizure susceptibility. As a neuronal transporter of both potassium and chloride, KCC2 is well situated to be involved in post-ischemic brain damage, and several studies support this notion, as well. In rat models, global ischemia causes seizures in response to intense auditory stimulation. The loop diuretics furosemide and bumetanide, inhibitors of KCC2, temporarily blocked seizure susceptibility, whereas the osmotic diuretic mannitol did not. Furosemide and bumetanide, however, does not prevent seizures induced by the $GABA_A$ receptor antagonist bicuculline. Also, it is noted that these chemical agents, which are not specific to KCC2, would not be clinically useful due to their potent diuretic effects (Reid et al., 2000). Another study has shown that ischemia raises levels of KCC2 mRNA which more strongly links post-ischemia seizure-susceptibility to alteration of KCC2 expression and/or function (Reid et al., 2001).

KCC2 and human disease

Changes in KCC2 levels in various forms of epileptic diseases suggest that the cotransporter plays a role in these disease states. Hippocampal sclerosis (cell loss) is often seen in patients of temporal lobe epilepsy. Normal patient hippocampi exhibit a high level of NKCC1 and KCC2 colocalization throughout the hippocampus, but in epileptic patients, NKCC1 and KCC2 are colocalized in the non-sclerotic regions (CA4 and subiculum) but 20% less so in the sclerotic CA1 region and the subiculum-CA1 border areas (Munoz et al., 2007).

Patients with malformations in cortical development (e.g., focal cortical dysplasia, ganglioglioma, hemimegalencephaly) have altered KCC2 distribution, with low KCC2 immunoreactivity in the neuropil, but high levels of staining localized to cell somas in dysplastic cells (Aronica et al., 2007).

Temporal lobe epilepsy patients show upregulated NKCC1 and slightly downregulated KCC2 in the hippocampal regions, as compared to neocortex. Injecting oocytes with membranes preps made from hippocampal tissues from these patients causes oocytes to depolarize in response to GABA. This can be blocked by adding bumetanide, an inhibitor of NKCC1, further suggesting that the E_{GABA} shift seen in oocytes is due to the altered NKCC1 expression in the TLE patient brain tissues (Palma et al., 2006).

Searching the NIH-NCBI database for reported human single nucleotide polymorphisms, there are six SNPs in human KCC2 which are nonsynonymous (resulting in an amino acid change) and fall within coding regions. None of these SNPs have had any further testing or examination, but this is indeed an avenue worth exploring, either studying the functional effect of these mutations in experimental laboratory models, or in human population studies which might link these mutations to diseases such as epilepsy.

KCC2 and pain

KCC2 has been implicated in playing a role in pain perception. Injury in rat facial neurons and dorsal motor neurons of the vagus nerve imparted by transection of axons causes a downregulation in dendritic KCC2 expression, subsequent increase in $[Cl^-]_i$, and a depolarizing shift in the GABA response (Nabekura et al., 2002; Toyoda et al., 2003).

Sciatic nerve constriction in rats causes an ipsilateral decrease in KCC2 expression and increased E_{GABA} in spinal lamina I neurons. Nociceptive threshold was also decreased by antisense KCC2 mRNA administration into the spinal cord (Coull et al., 2003). Injury evoked by formalin injection into the rat hindpaw also causes a downregulation of KCC2 in spinal cord neurons, coincident with increases in flinching, a behavior indicative of heightened sensitivity to pain (Nomura et al., 2006). Further study of peripheral nerve injury, using loose ligation of rat sciatic nerve, demonstrates that KCC2 protein decreases are accompanied by increases in BDNF, and early behavioral signs of pain are attenuated by pretreatment with tyrosine kinase blocking drug or BDNF-sequestering scavenger proteins. The KCC2 protein changes and TrkB-mediated effects are, however, immediate and transient. One week after injury, KCC2 protein levels match controls and no chemical or scavenger protein disruption of the BDNF pathway attenuates pain behavior (Miletic and Miletic, 2007). Two mechanisms thought to be involved in KCC2's contribution to neuropathic pain include disinhibition of non-nociceptive fibers synapsing on spinal neurons, or perhaps the conversion of normally inhibitory low-action potential threshold GABA pathways to excitatory (Price et al., 2005).

Summary

KCC2, a member of the cation-chloride cotransporter (CCC) family, is a critical modulator of neuronal function, chiefly through its involvement in chloride regulation and GABAergic signaling. As an electroneutral cotransporter of potassium and chloride, it is an ideal establisher of the intracellular chloride concentration in neurons. Powered by the potassium gradient set by the Na^+-K^+ pump, KCC2 extrudes chloride from

neurons, resulting in a low internal chloride concentration without changing the reversal potential of the cell. This in turn causes the neurotransmitter GABA to have a hyperpolarizing effect, as the $GABA_A$ receptor is an ionotropic receptor primarily selective for chloride.

A full knockout of KCC2 expression in mice leads to death shortly after birth, while a knockdown of KCC2 expression results in a seizure phenotype, and death approximately two weeks after birth. A genetic screen for seizure-enhancing mutations in *Drosophila* demonstrates that KCC2 disruption contributes to seizure susceptibility, as well. These animal models demonstrate that KCC2 is essential to preventing overexcitability in the nervous system.

Ischemic injury, pain states, and seizure disorders have been linked to KCC2 function and expression. Post-mortem studies of epilepsy patients show that KCC2 levels are altered in patients. Given the knowledge that KCC2 is important to inhibition in the nervous system, it seems likely that this KCC2 downregulation is the origin of epileptiform activity. However, electrophysiological experiments in rat brain slices seem to indicate that interictal activity causes a downregulation of KCC2 expression. It is possible that KCC2 can be involved with the origin as well as response and/or propagation of epileptiform activity, but more studies will need to be done to make these distinctions.

Given the importance of KCC2, relatively little is known about its regulation. Net dephosphorylation leads to stimulation of cotransporter activity, yet specific targets and kinases are yet to be definitively established. Stress-signaling pathways may affect

KCC2 via the Ste20-related kinase SPAK. BDNF and TrkB signaling likewise play a role in KCC2 activation.

Understanding protein interactions of membrane-bound transporters is a key aspect to understanding how these transporters are regulated. At the initiation of this project, no known interactors with KCC2 had been identified. Thus, this thesis project aims to determine and characterize novel protein interactions with KCC2, as described by the following hypotheses and specific aims.

Hypothesis and specific aims:

Very little is known about the regulation of KCC2, especially considering many convincing studies demonstrating its important role in neuronal communication. Regulation of membrane transporters often requires interaction with other proteins, some involved in trafficking, and others in posttranslational modifications. This has led me to explore the first hypothesis:

Hypothesis I.: KCC2 interacts with other proteins on its carboxyl terminus, and these potential interactors affect KCC2 function and/or expression.

- *Specific Aim 1: Identify novel interactors with the KCC2 carboxyl terminus*

As described in Chapter I, a yeast two-hybrid screen identified PAM/Phr1 as a potential interactor with the KCC2-CT. This potential interactor is interesting for several reasons, as described in Chapter II. Since PAM is a large protein, I used only the portion of the protein identified in the screen in the following experiments, from now on called RCC1/PAM. This leads me to my second hypothesis:

Hypothesis II.: RCC1/PAM binds to KCC2 and affects its function.

- *Specific Aim 1:Investigate effect of RCC1/PAM on KCC2 activity and expression in HEK293 cells*
- *Specific Aim 2: Characterize PAM binding to create a targeted point mutation disrupting interaction between PAM and the KCC2-CT*
- *Specific Aim 3: Compare mutant KCC2 expression and activity to wild type KCC2 in the presence of RCC1/PAM*

CHAPTER II

IDENTIFICATION OF PROTEIN INTERACTORS OF THE KCC2 CARBOXYL TERMINUS USING YEAST TWO-HYBRID

Introduction

There are many paths to begin the journey to understanding the physiological role of a particular protein. These paths take many forms, from transgenic methods, such as deleting a gene from a model organism, to genomic meta-analyses, such as studying SNPs in humans afflicted by a particular disease. Screening a protein for potential binding partners also can be a particularly rewarding and fruitful beginning, as it can uncover obscure or unexpected associations between two proteins, thus potentially linking together two or more signaling pathways, and contributing to a greater understanding of both proteins.

The yeast two-hybrid system is a powerful method of screening for novel protein-protein interactions. Developed in the late 1980s, it has been utilized by many researchers for identification of novel protein interactions. Stanley Fields, developer of the yeast two-hybrid system, attributes yeast two-hybrid's power and subsequent popularity to its elemental implications, stating, "The two-hybrid system addresses one of life's fundamental questions: How does one find a meaningful partner?"

The yeast two-hybrid system can be used to test interaction between two known proteins, or to use a protein to screen a library for novel interactors. In both cases, transcription factor assembly and reporter gene expression act as a read-out of protein-protein interaction. In a library screen to identify novel interactors, the protein of

interest, the "bait," is fused to one half of a yeast transcription factor, the activating domain or the binding domain. The "fish" proteins are made from a cDNA library and fused to the remaining half of the transcription factor. If the bait and fish proteins interact, the transcription factor domains come in close proximity, thus allowing binding to specific promoter region, and activation of reporter genes downstream of this promoter, engineered into the yeast strain's genome (Figure 6). Such reporter genes include beta-galactosidase or various amino acid auxotrophy genes. Conversely, proteins which do not interact do not bring the transcription factor activating and binding domains together, and thus no reporter gene transcription can occur.

Since its inception, the yeast two-hybrid system has been further modified to enhance its capabilities. For example, a mammalian two-hybrid system utilizes mammalian cells, as opposed to yeast, which is ideal if factors native to mammalian cell nuclei need to be present for binding to occur (Feng and Derynck, 2001). Three-hybrid systems can be used to identify interactions which necessitate three binding partners, such as two proteins and an interaction-regulating factor (e.g., kinase, phosphatase, methylase) (Sandrock et al., 2001). The yeast split-ubiquitin system can be used to study protein interaction in the membrane or cytosol (Thaminy et al., 2004; Mockli et al., 2007). However, the core concept of the original yeast two-hybrid system remains in these variations.

Our lab has previously had success using yeast two-hybrid to identify interactions in library screens, such as with KCC3 and SPAK (Piechotta et al., 2002) and SPAK, WNK, and apoptosis associated tyrosine kinase (AATYK) (Piechotta et al., 2003)

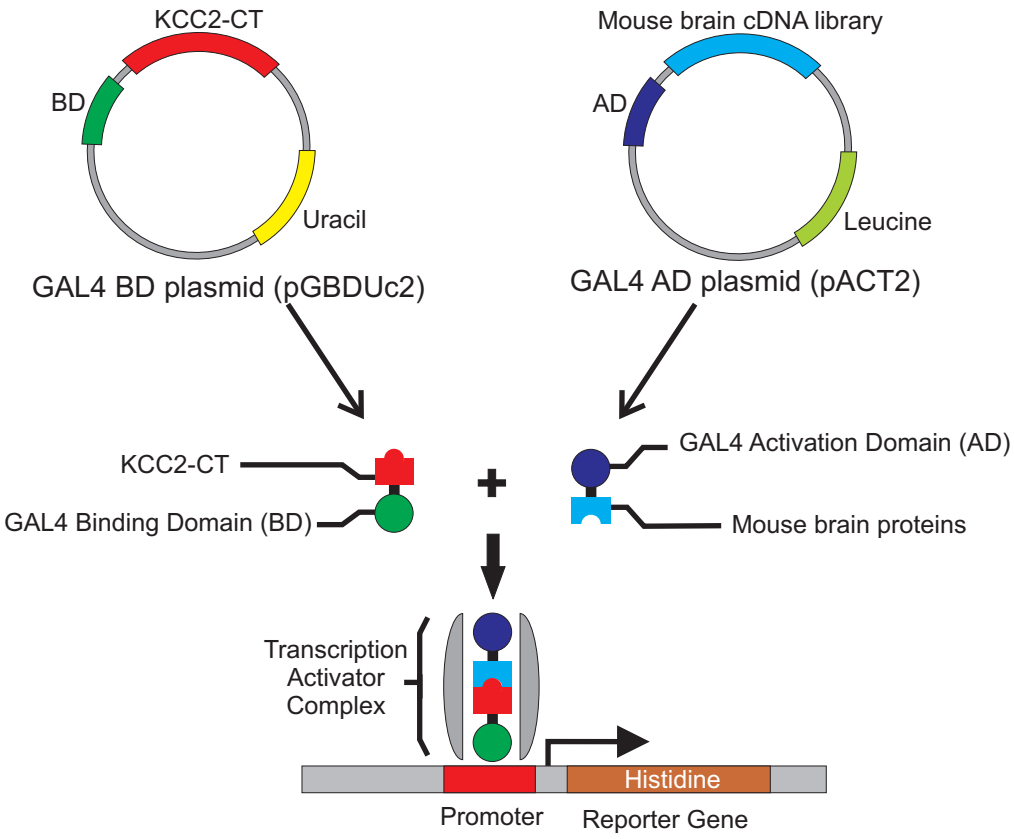

Figure 6. Yeast two-hybrid as a test of protein interaction.
The carboxyl terminus of KCC2 (KCC2-CT) was subcloned into the yeast two-hybrid vector pGBDUC2 which contains a Gal 4 binding domain. cDNA clones from a mouse brain library were fused to the Gal 4 activating domain in pACT2. Protein interaction between KCC2-CT and the protein, or partial protein, produced from the cDNA library clone will likewise bring together Gal 4 activating and binding domains, forming a transcription activator complex which can then activate transcription of yeast reporter genes.

(Delpire and Gagnon, 2007), as well as in testing specific proteins with small-scale yeast two-hybrid transformations. Thus, based on past successes of the laboratory, the same yeast two-hybrid reagents and protocols were utilized for identifying novel interactors with KCC2.

The KCC2 carboxyl-terminal tail (KCC2-CT) was chosen as the "bait" protein for this screen because it contains several interesting characteristics which make it a likely interface for transporter regulation (Figure 7). The intracellular carboxyl tail of KCC2 is very large, making up approximately 45% of the entire protein. The KCC2-CT contains several putative protein kinase C phosphorylation sites, one which has been recently shown to affect cotransporter stability at the cell surface (Payne et al., 1996; Munoz et al., 2007). The KCC2 carboxyl tail contains a unique 34 amino acid sequence of the KCC2 C'-terminus, which is not conserved in other KCC isoforms. Heterologous expression of KCC2, KCC1, and KCC1/KCC2-CT chimeras suggest this sequence is responsible for its constitutive activity in isotonic conditions (Mercado et al., 2006). Additional KCC2 chimera studies demonstrate that proximal, central, and distal regions of the C terminus play a role in ion transport aside from PKC-mediated effects (Bergeron et al., 2006). In addition, a tyrosine residue on the C' tail located at position 1087 is necessary for KCC2 function, however, not via phosphorylation (Strange et al., 2000). Taken together, these facts suggest that the carboxyl terminus is an important contributor to KCC2 function and a likely site for multiple protein-protein interactions. This has led me to explore the identification of novel KCC2 interactors, specifically focusing on the carboxyl terminus.

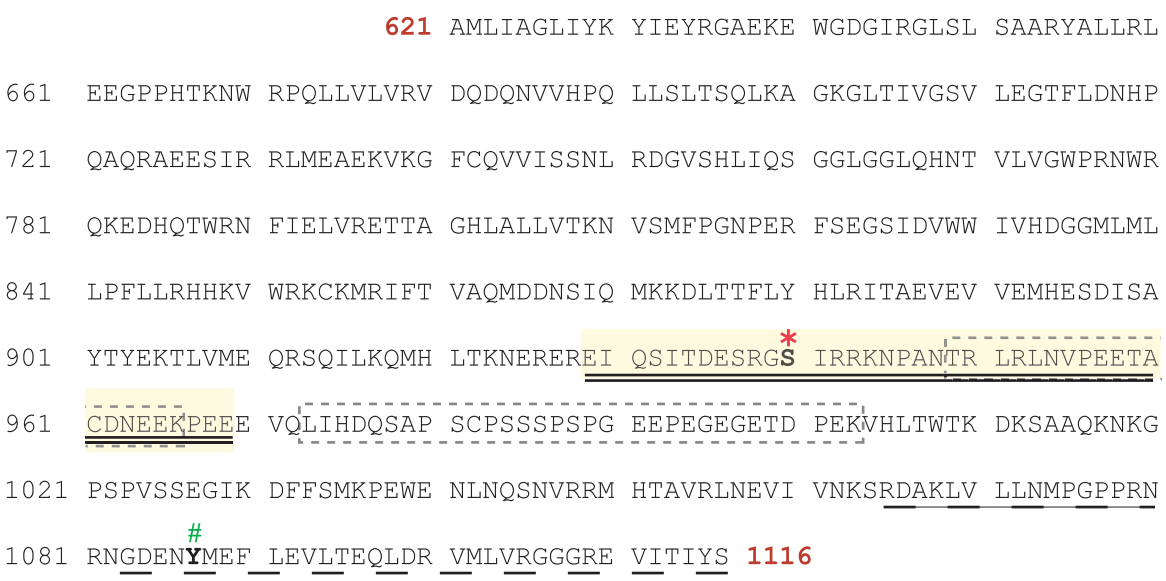

Figure 7. Domains and features of the KCC2 carboxyl terminus.
The KCC2 carboxyl terminus sequence, shown here, contains many regions of interest. A KCC2-specific sequence in double underscored and highlighted in yellow. Two PEST sequences are outlined by a dotted box. Asterisk indicates a serine residue verified as a PKC phosporylation site. The pound sign denotes a tyrosine residue critical for function, but not via phosphorylation. The dashed underline indicates a predicted GGDEF domain, which is a domain homolgous to adenylyl cyclase.

Methods

Amplification of mouse brain cDNA library

The mouse brain cDNA library in the pACT2 vector in *E. coli* was obtained from Clontech (Mountain View, CA). The library was amplified such that the total number of colony forming units (cfu) plated would be greater or equal to three times the target number of cDNA library clones to be screened. The Clontech titer of their library equals 10^8 cfu/ml, and the target number of clones to be screened was 3.5×10^6. Therefore, 120 µl of bacteria was resuspended in 50 mL LB medium, and 200 µl of this diluted library was plated on 250 150-mm LB/agar plates (250 plates x ~40,000 cfu/plate = 11×10^6 cfu). Bacteria plates were grown for 2 days at 30°C, then scraped and pelleted for DNA isolation using the Qiagen MegaPrep Kit 2500. The titer results indicated 20,000 cfu/plate.

Generation of bait/KCC2 carboxyl terminus

To perform a yeast two-hybrid screen, a protein fragment or polypeptide needs to be inserted into a yeast vector, such that it is in frame with the GAL4 binding domain. To do so, a sense oligonucleotide PCR primer was designed with a restriction site allowing ligation in the proper frame and an anti-sense oligonucleotide PCR primer is designed with a stop codon followed by a restriction site. Thus, a portion of the carboxyl terminus of the rat KCC2 (KCC2-CT) was amplified by PCR using an existing rat KCC2 cDNA clone and primers 8S and 9A. PCR fragment was ligated into the pGEM vector, and pGEM clones were checked with restriction enzyme mapping before sequencing with ABI Prism Big Dye Terminator (Applied Biosystems, Foster City, CA) using the 8S, 9A,

T7 and SP6 primers (see Table 1). The PCR fragment was removed by digestion with *BamHI* and *SalI* DNA restriction enzymes, and then ligated into the pGBDUC2 vector (x*BamHI,* x*SalI*) in frame with the Gal4 binding domain. All sequences in pGBDUC2 were checked using the GB1 and GB2 primers.

Table 1: Primers used for yeast two-hybrid DNA constructs

Primer Name	***Primer Sequence (5' to 3')***
8S	CGGAATTCCGGGGGGCAGAGAAGGAGTGGGG
9A	GAAGATCTTCAGGAGTAGATGGTGATGACCTC
T7	AATACGACTCACTATAG
SP6	ATTTAGGTGACACTATAG
GB1	ATAAGTGCGACATCATCATCG
GB2	TTCAGTATCTACGATTCATAG

Yeast culturing

The yeast strain PJ69-4A was used for all yeast two-hybrid work (Pramfalk et al., 2004), as this is a widely used two-hybrid strain with several reporter genes engineered into its genome. Additionally, protocols for this particular strain are well-established in our laboratory. All yeast cultures were grown at 30°C, and stored short-term at 4°C. Yeast cells, untransformed with any plasmids, were grown on YPDA plates which contained all essential amino acids for growth. Yeast transformed with pACT2 vectors were maintained on -Leucine plates, and those transformed with pGBDUC2 vectors were maintained on -Uracil plates. For long term storage, yeast cells were resuspended in 25% glycerol and stored at -80°C.

Library screen

Sequential yeast transformations were performed to introduce the bait and fish plasmids into the yeast. First, the KCC2-CT- pGBDUC2 plasmid was transformed into PJ69-4A yeast cells (Pramfalk et al., 2004). This transformed yeast was then used in another library-scale transformation in order to screen the amplified mouse brain cDNA library in pACT2 vector. Transformed yeast from the screen were subject to nutritional selection, first by plating the yeast cells on 150mm -Uracil/-Leucine/-Adenine plates, then by two rounds of picking and restreaking surviving clones onto -Uracil/-Leucine/-Histidine + 2 mM 3-amino-1,2,4-triazole (3-AT) plates. All plates were incubated at 30°C, and in plastic bags to avoid drying. Surviving colonies were picked 4 and 9 days after transformation or restreaking.

Library titer

A library titer was performed in order to estimate how many yeast colony forming units (cfu) were successfully transformed with both the bait/pGBDUC2 and fish/pACT2 plasmids. The library transformation suspension was serially diluted in 1:10, 1:100 and 1:1000 ratios, and 100 µl of each dilution spread on a -Uracil, -Leucine drop-out media plate. The transformation efficiency was calculated by counting cfus growing on the -Uracil, -Leucine plates containing 30-300 cfus.

$$\frac{cfu \times \text{total suspension vol. } (\mu l)}{[\text{Vol. plated } (\mu l)] \times [\text{dilution factor}] \times [\text{amount DNA used}(\mu g)]} = cfu/\mu g \text{ DNA}$$

Liquid LacZ Assays

As an additional level of stringency to use in conjunction with Histidine and Adenine auxotrophy, yeast clones were assayed for LacZ/beta-galactosidase activity. For this assay, several colonies from one clone were picked to grow overnight in 14 mL -Uracil, -Leucine, -Histidine liquid media at 30°C. 1 ml of the overnight culture (at stationary phase, ODλ600>1.5) was transferred into 4 ml of YPDA medium, and incubated at 30°C at 250 rpm for approximately 3 hrs, until ODλ600 = 0.5 ± 0.1. Following two spin/wash cycles with 1x PBS, pelleted yeast cells were lysed with lysis buffer and incubated at 37°C for 3 hrs with ONPG assay buffer (120 mM Na_2HPO_4, 80 mM NaH_2PO_4, 2 mM $MgCl_2$, 100 mM β-mercaptoethanol, 1.33 mg/ml ONPG (Sigma)). The reaction was stopped by addition of Na_2CO_3, centrifuged, then read in a spectrophotometer at λ420nm.

Clone identification

Yeast clones with the highest β-galactosidase expression were lysed with 10µl 5x Reporter Lysis Buffer (Promega, Madison, WI) for 10 minutes at 37°C then subjected to PCR using the YST1 and YST2 primers and the ExpandLong Template PCR kit (Roche, Indianapolis, IN).

Amplified PCR fragments were then sequenced with ABI Prism Big Dye Terminator (Applied Biosystems, Foster City, CA) using the YSEQ primer.

In situations where direct PCR of lysed yeast cells did not yield readable sequences, clone plasmids were rescued from yeast cells by incubation in 10µl lyticase, heat shock at 37°C for 1 hour, incubation with 10µl 20% SDS, and one freeze-thaw

cycle. DNA was then extracted with phenol:chloroform:isoamyl and ethanol precipitation, then transformed into competent *E. coli* cells. *E. coli* clones were picked and grown on duplicate nitrocellulose filter paper grids, then subject to Southern blotting using ^{32}P-labelled cDNA probes made from the pACT2 plasmid. Positive *E. coli* clones containing pACT2 were picked from the duplicate plate, then grown and miniprepped for DNA, and then sequenced with the YSEQ and GB2 primers (see Table 2). The sequences which were in frame with the Gal binding domain were identified using BLAST on the NIH-NCBI website.

Table 2: Primers for Clone Identification

Primer Name	***Primer Sequence (5' to 3')***
YST1	GAAGTGAACTTGCGGGGTTTTTCAGTATCTACG
YST2	CTATTCGATGATGAAGATACCCCACCAAAC
YSEQ	CCATACGATGTTCCAGATTACGCTAGC
GB2	TTCAGTATCTACGATTCATAG

Results

Library titer plates made of -Uracil, -Leucine media were used to control for transformation efficiency, as well as to calculate the number of mouse brain library clones screened. The library titer plates grew 91 clones (1:1000 dilution) and 968 clones (1:100 dilution) and the entire library screen transformation was plated on 65 plates. Therefore an estimated range of 5,915,000 to 6,292,000 total library clones were screened. $[65*(91x10^3 + 968x10^2)]$

An initial pool of approximately 900 clones was retrieved from the initial selection by plating on -Uracil/-Leucine/-Adenine plates. Following nutritional selection by picking and restreaking onto -Uracil/-Leucine/-Histidine +3-AT plates, twice in succession, the pool of clones was narrowed to 50 candidates. These surviving clones were then assayed using a liquid LacZ colorimetric assay to assess the level of expression of the beta-galactosidase reporter gene. After selecting the clones with the highest LacZ values, we arrived at a final pool of candidate proteins. These were sequenced and identified using BLAST searches (NIH-NCBI). Clones were excluded if they encoded for known false positives in the yeast two-hybrid system (e.g., elongation factors, heat shock proteins), as well as if they were not in the same translational frame as the Gal4 Activating domain, or if they encoded 3'UTR regions. Figure 8 shows the top list of candidates identified which meet this criteria (upper panel) as ranked by the galactosidase activity determined from the liquid LacZ assays (lower panel).

Rank	Clone #	[Gal]	Protein
1	7	7.633	Protein Associated with Myc
2	106	6.616	Protein Associated with Myc
3	469	4.132	Protein Associated With Myc
4	3	1.954	Ran Binding Protein 9
5	44	1.491	KIAA1140/Tetratricopeptide repeat protein 7A
6	430	0.900	KIAA1140/Tetratricopeptide repeat protein 7A
7	446	0.794	KIAA1140/Tetratricopeptide repeat protein 7A
8	442	0.656	Brain Creatine Kinase
9	102	0.400	KIAA1140/Tetratricopeptide repeat protein 7A
10	26	0.340	Ran Binding Protein 9
11	424	0.277	Brain Creatine Kinase
12	341	0.270	Brain Creatine Kinase

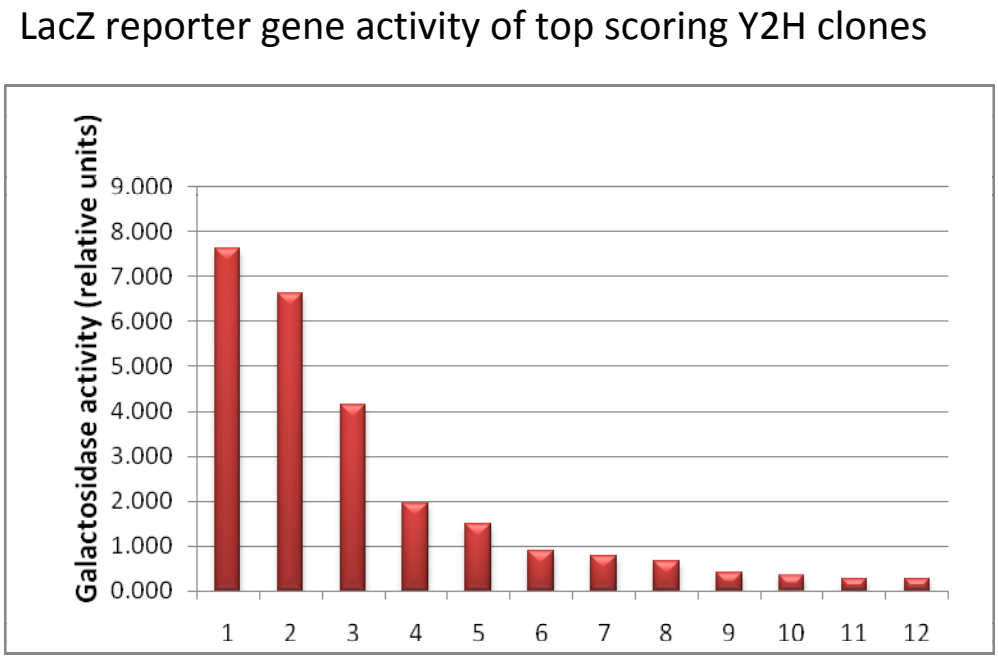

Figure 8. Candidates from yeast two-hybrid screen and LacZ assay data. Candidates from the yeast two-hybrid screen went through several rounds of selection, included plating/restreaking on media lacking Adenine or Histidine. Surviving clones were the tested further in liquid LacZ assays to measure β-galactosidase activity, as well. After sequencing high-activity clones to eliminate common false positives (e.g. elongation factors), proteins that were out of frame, and cDNAs from non-coding regions, a final list of candidates was created (upper panel) and ranked based on values obtained in LacZ assays (bottom panel).

Discussion

Our library titer demonstrated that approximately 6 x 10^6 library clones were screened. This is a good number, as it is recommended that yeast two-hybrid screens of mammalian cDNA libraries should cover a minimum of 5 x 10^6 clones in order to have full coverage and saturation of representative cDNAs (Van Criekinge and Beyaert, 1999).

"The greatest hits"

The top scoring candidates in this library screen included several very interesting candidates (Figure 8). Of these, the highest LacZ activity came from a portion of Protein Associated with Myc, or PAM. This protein is particularly intriguing due to the phenotypes of PAM homologue mutants in the fly and worm, as further discussed in detail in the next chapter.

Another protein which appeared several times in our screen was the putative protein KIAA1140, or tetratricopeptide repeat domain protein 7A (TTC7). This protein was identified during a sequencing and protein prediction screen of large proteins expressed in the brain (Hirosawa et al., 1999). Tetratricopeptide repeat (or, TPR) domain-containing proteins are characterized by a degenerate 34 amino acid consensus sequence forming a helical secondary structure, and proteins with this domain are involved in a variety of cell processes, from mitosis to protein scaffolding (Lamb et al., 1995; Blatch and Lassle, 1999). More studies on TTC7 were reported in 2005, in a study attempting to identify genes involved in iron homeostasis. TTC7 was found to be mutated in two mouse mutant strains, one with an anemic phenotype, and the other with a flaky skin phenotype. Speculation about TTC7's role include that it may be a candidate gene for

psoriasis, and may bind to iron transporters, however its exact function is not known (Helms et al., 2005; White et al., 2005).

Another protein which came up several times in this screen is brain creatine kinase, or CKB. Creatine kinase activity has been generally characterized in skeletal muscle cells. It participates in intracellular energy storage and synthesis by phosphorylating creatine, consuming adenosine triphosphate (ATP) and producing adenosine diphosphate (ADP) in the process. Brain creatine kinase likewise is a phosphoprotein which associates with mitochondria and participates in the energy cycle and ADP/ATP conversion and localization (Booth and Clark, 1978; Mahadevan et al., 1984). Increase of plasma CKB levels in humans is suggestive of brain injury, and CKB rate constants increase before and during induced seizure activity in adult rats (Somer et al., 1975; Holtzman et al., 1997; Haskins et al., 2005). CKB changes have also been recently linked to bipolar disorder, amphetamine use, and Alzheimer's disease, although it is not clear if changes in CKB activity are indicative of or resulting from progression of these conditions. (Castegna et al., 2002; Streck et al., 2008)

Brain creatine kinase expression is highest in the brain, specifically in glial cells. However, its expression is not confined to the brain, but widespread through several tissue and cell types. It is hypothesized that CKB acts as a rapidly reactive participant in energy synthesis, which is recruited into action for energy demanding processes, such as cell growth and development (Kuzhikandathil and Molloy, 1994; Willis et al., 1999). There have been several links between CKB and cancer, as well. CKB expression is highly upregulated in many tumor cell lines and CKB has been shown to be repressed by p53. CKB upregulation is present in 78% of colon tumors, suggesting its use as a

biomarker for cancerous tumors, such as in the case of colorectal cancer (Kaddurah-Daouk et al., 1990; Zhao et al., 1994; Kuzhikandathil and Molloy, 1999; Balasubramani et al., 2006).

The same interaction I identified between KCC2 and brain creatine kinase was later confirmed by another group's yeast two-hybrid screen using the KCC2-CT (Inoue et al., 2004). They further explored this interaction in a follow-up functional study of glycine-receptor expressing HEK293 cells and cultured cortical neurons. HEK cells cotransfected with KCC2 and dominant negative CKB show a depolarizing shift in the glycine reversal potential. In neurons, the application of a creatine kinase inhibitor, 2,4-dinitrofluorobenzene (DNFB), caused a depolarizing shift in the GABA reversal potential (Inoue et al., 2006). Thus, it is suggested that one native role of CKB is to activate KCC2 activity.

Considerations of the yeast two-hybrid system

Yeast two-hybrid is a useful method for identifying novel protein-protein interactions, and has been used with success by our laboratory, and many other laboratories, in the past. There are, however, some pitfalls and drawbacks worth noting. The size and region of the bait protein impacts the fruitfulness of the yeast two-hybrid screen. Bait and candidate proteins cannot contain any transmembrane domains, as these hydrophobic structures will cause transport into the nuclear membrane, thus preventing it from activating the yeast reporter genes. Initially, I had sought out to identify interactors with the KCC2-specific region of the KCC2 carboxyl terminus (rKCC2 residues 929 to 969). I also used both this region, as well as a larger region encompassing the KCC2-

specific region in library-scale yeast two-hybrid screen. However, these regions were possibly too small, as they did not result in many hits for these screens.

Yeast two-hybrid screens are also known to result in many false positives. Some aspects of our screening protocol help in evading such false leads. We use two different auxotrophy reporter genes as selection markers for positives: Adenine and Histidine, driven by two different Gal promoters. Thus, candidate proteins which may independently act as a transcription factor would have to be able to bind to both promoters in order to pass through to the next stage of clone selection. Additionally, we use liquid LacZ assays as yet another level of stringency in selecting positive candidate interactors.

However, confirming positives outside of the yeast system is also necessary. In the next chapter, I examine the candidate interactor PAM more closely, and use GST pull-down assay and coimmunoprecipitation assays for confirmation outside the yeast system.

CHAPTER III

VALIDATION OF KCC2 AND RCC1/PAM INTERACTION

Introduction

Portion of PAM identified

The carboxyl-terminal tail of rat KCC2 (KCC2-CT) was used to screen a two-hybrid mouse brain cDNA library. Among the positive clones, a portion of the RCC1 homology domain of Protein Associated with Myc (PAM, residues 551-874) was identified as a potential interactor of KCC2-CT. These 323 amino acids are a relatively small portion of the entire PAM protein (Figure 9). This portion of PAM is located in a region similar to the Regulator of Chromatin Condensation 1 domain, or RCC1 domain. As its name suggests, the RCC1 domain was first characterized in the RCC1 protein for its cell cycle related effects in the nucleus. The RCC1 protein binds to DNA and acts as a regulator for the initiation of chromosome condensation by catalyzing the exchange of guanine nucleotides on Ran GTPase (Ohtsubo et al., 1989; Bischoff and Ponstingl, 1991). X-ray crystallography of human RCC1 protein demonstrated that the structure of RCC1 consists of a seven-bladed propeller formed by internal repeats of 51 to 68 amino acid residues per propeller blade. The residues of RCC1 are not conserved in comparison to the WD-40 repeats found in the similarly shaped beta subunit of the heterotrimeric G-proteins. However, this propeller blade structure is in general highly similar, and could potentially indicate an evolutionary conservation of the propeller structure among superfamilies of GTP-binding proteins (Renault et al., 1998).

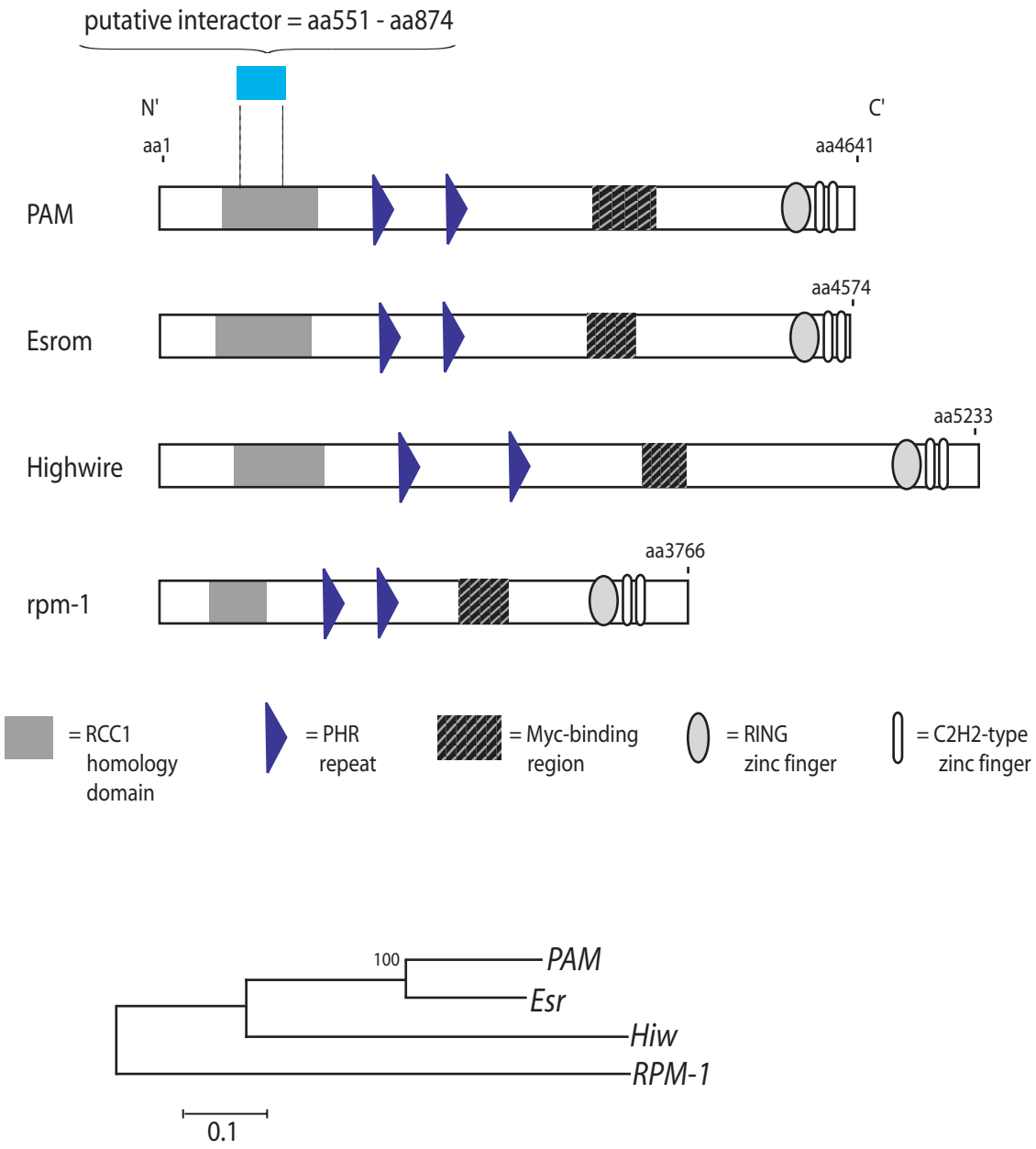

Figure 9. RCC1/PAM clone compared to full length PAM and homologues. A. The portion of PAM pulled from the KCC2-CT yeast two-hybrid screen is shown in relation to full length PAM. Full length PAM and its various domains are depicted, along with PAM homologues in *Danio rerio* (Esrom), *Drosophila* (highwire), and *C. elegans* (rpm-1). B. Phylogenetic tree depicting similarities between proteins. Figure compiled and adapted from Schaefer et al., 2000 and D'Souza et al., 2005.

RCC1-like domains have been found in several other cytoplasmic proteins besides PAM. One such protein is alsin, the product of the ALS2 gene. Mutations in ALS2 are predominantly linked to a juvenile-onset form of amyotrophic lateral sclerosis (ALS) and juvenile primary lateral sclerosis (PLS). Alsin contains three domains with GTPase function, one of which is an N'-terminal RCC1 domain. Several of the aforementioned ALS2 mutations cause a short form of the alsin protein, prematurely ending the protein in the middle of the RCC1 domain and thus deleting the other GTPase domains (Hadano et al., 2001; Yang et al., 2001; Gros-Louis et al., 2006). In the cell, alsin plays many roles, not only in protein scaffolding and trafficking, but most significantly as an activator of rab/rac-mediated signaling pathways which control endocytosis, macropinocytosis, protein transport and neurite outgrowth and survival (Otomo et al., 2003; Tudor et al., 2005; Devon et al., 2006; Hadano et al., 2006; Jacquier et al., 2006; Hadano et al., 2007; Kunita et al., 2007). Alsin's RCC1 domain is responsible for alsin distribution in the cytoplasm, and the RCC1 domain also acts as a binding site for several proteins (Yamanaka et al., 2003; Hadano et al., 2007). For instance, the RCC1 domain of alsin binds to glutamate receptor associated protein GRIP1, and alsin has been functionally linked to AMPA receptor distribution and susceptibility to glutamate toxicity in neurons (Lai et al., 2006).

Another RCC1-domain containing protein is Retinitis Pigmentosa GTPase Regulator protein, or RPGR. Individuals with X-linked retinitis pigmentosa, a severe form of macular degeneration, were found to have several in-frame deletions and nonsense and missense mutations clustered in the RCC1 region of the RPGR gene (Meindl et al., 1996; Buraczynska et al., 1997; Bauer et al., 1998; Miano et al., 1999;

Vervoort et al., 2000; Vervoort and Wright, 2002; Jin et al., 2005; Neidhardt et al., 2007). Later investigations into RPGR interactors showed that several proteins bound to RPGR though this RCC1 domain, such as the delta subunit of the photoreceptor-localized cyclic GMP phosphodiesterase (PDEδ), and several microtubule motor proteins localized to the cilia of photoreceptor cells (Linari et al., 1999; Roepman et al., 2000; Khanna et al., 2005). Additionally there is data demonstrating that the RPGR - RCC1 domain can independently traffic from basal to ciliary membranes after ciliogenesis in MDCKII cells (He et al., 2008). Collectively, this data demonstrates that the importance of the RCC1 domain for protein-protein interactions, and possibly for protein transport and localization within the cell.

PAM background

PAM is a very large protein, with an estimated length of 4641 amino acids, and many groups report a molecular weight estimate of 510 kiloDaltons (Guo et al., 1998). One group has recently reported two molecular weights of PAM, an approximately 410 kDa form unique to embryonic rat tissues and rat-derived cell lines, and a 350 kDa which is the most prominent isoform in the postnatal and adult stages (Santos et al., 2006). PAM has several distinct protein domains (Figure 9). As aforementioned, near the N-terminus of the protein is a domain with high homology to the Regulation of Chromatic Condensation domain. This domain has a characteristic seven-bladed propeller structure, and in PAM this characteristic 7-fold repeat is retained, but divided in half by a 134 aa sequence. PAM also has two signature 91 aa repeated sequences, termed the PAM/Highwire/RPM-1 (PHR) repeats. Closer to the C-terminus is the myc-binding

domain. Alternative splicing leads to six isoforms of this particular region, and affects binding affinity to myc. In the extreme C-terminus, two C2H2 domains are clustered near a RING zinc-finger domain, a domain characteristic of E3 ubiquitin ligase proteins (Guo et al., 1998; Peterson et al., 2002; Burgess et al., 2004). Given the size of this protein, and its many specialized domains, it is likely that PAM plays a part in many physiological roles in the cell -- an idea supported by the variety of findings about PAM function which have since been reported in the research literature.

PAM (also known as Phr1 (Burgess et al., 2004) or MycBP2 in GenBank) was originally characterized as a myc binding protein (Guo et al., 1998). However, later studies have shown that PAM is found in the cytosol during M and G_1 phases of the cell cycle (Scholich et al., 2001). In neurons, it has been described as having subcellular localization in soma, axons and dendrites (Murthy et al., 2004) however, it is widely expressed and present in both neuronal and non-neuronal cell types.

Several factors made PAM an intriguing potential candidate interactor with KCC2. One example is that PAM and KCC2 have an interesting overlap in spatial and temporal expression. In mice, both PAM and KCC2 undergo developmental upregulation during the first two weeks after birth (Yang et al., 2002). Additionally, PAM is highly expressed, and developmentally upregulated in the pyramidal cells of the hippocampus, granule cells of the dentate gyrus and cerebellum, as well as Purkinje cells of the cerebellum — regions in which KCC2 likewise has high levels of expression. Furthermore, both PAM and KCC2 have been linked in having a role in the spinal nociceptive pathway (Coull et al., 2003; Ehnert et al., 2004).

Later reports of mice with a disruption in the PAM/Phr1 gene likewise increased our interest in this protein. One such report came from an analysis of the piebald deletion complex in mouse chromosome 14. These mice have chromosomal abnormalities surrounding the endothelin B receptor. PAM/Phr1 was identified as a candidate gene in this region contributing to the piebald phenotype (Peterson et al., 2002). Mice with a deletion in the Phr1 gene have a similarity to the KCC2 knockout mouse phenotype, in that after birth they both exhibit respiratory distress and subsequently, death. This respiratory distress is in part attributed to incomplete sensory innervations of the diaphragm muscle, abnormal synapses of the phrenic nerve on the diaphragm, and dysmorphic synapses on intercostal muscles (Burgess et al., 2004).

Recently, two groups have independently published studies on the role of PAM/Phr1 in mice. In the first report, Bloom et al describe that constitutive Phr1 knockout mice, like the piebald mice, do not begin breathing and die at birth, and have aberrant phrenic nerve innervations of the diaphragm. Additionally, the Phr1 mice lack innervation of the thalamus by retinal nerves. In the brain, the anterior commissure is absent, the corpus callosum is narrower, and there is a significant decrease in GABAergic neurites (but not cell bodies) as compared to control mice.

Many brain morphology defects present in the constitutive knockout, including enlarged lateral ventricles, dysmorphic hippocampi and narrow corpus callosi, carried over to a conditional knockout with Phr1 function deleted in excitatory neurons of the cortex and hippocampus. Further analysis suggests that these defects are due to cortical neurons losing their ability to project their axons. In western blot analyses, they observe

no appreciable difference in DLK protein in these mice. In the fly and worm, Highwire and RPM-1 downregulate DLK through ubiquitination (Bloom et al., 2007).

However, another group also studied PAM/Phr1 function in mice after it was identified as a candidate gene for neurodevelopment regulation in a forward genetic screen in mice with motor axon projection defects. The Magellan mutation, which inserts a stop codon in PAM upstream of the zinc finger domains, causes extensive errors in motor and sensory neuron axon growth, particularly at major axonal choice points. They further localized PAM as associating with the tubulin cytoskeleton in the axon, but not in normal growth cones. They additionally used siRNA knockdown of Phr1 in neurons, and showed that neurons in culture phenocopied the axonal deficits shown in the Magellan mice. Subcellular immunostaining analysis of DLK expression shows that Magellan mice have upregulated amounts of DLK protein, and the authors suggest that PAM does in fact target DLK for ubiquitination. The authors also report that application of BDNF to Magellan mutant neurons leads to enhanced axonal branching, and they suggest that a shift in PAM to the distal end of the neuron may cause synapse formation when the proper axonal target is reached (Lewcock et al., 2007).

Studies of PAM function suggest that this protein has many varied functions in the cell, as is fitting for a protein of such an enormous size, with many different protein motifs/domains, and with ubiquitous expression. One report of autoantibodies in schizophrenics identifies anti-Protein Associated with Myc antibodies present in patient serum (Balakrishnan et al., 2003). Scholich et al demonstrate that the N-terminal RCC1 domain of PAM, due to its similar structure to $G\alpha_i$ and G-$\beta\gamma$ proteins, can function as an inhibitor of adenylyl cyclases, specifically ACI, ACV, ACVI and ACVII isoforms

(Scholich et al., 2001). Sphingosine-1-phosphate, a GPCR ligand and signaling factor, plays a role in translocating PAM to the membrane to induce this adenylyl cyclase activity (Pierre et al., 2004). A C-terminal portion of PAM encompassing the RING zinc finger domain has been reported to bind on an SH3 domain on tuberin, a protein encoded by TSC2, a gene mutated in the human disease Tuberous Sclerosis (Murthy et al., 2004).

Homologues of PAM in other species

PAM also initially intrigued us as a potential interactor due in part to the phenotypes of PAM homologues mutants in the worm and fly. PAM has high homology to Highwire (Hiw) in *Drosophila* (Wan et al., 2000), and Regulator of Presynaptic Morphology 1 (RPM-1) in *C. elegans* (Schaefer et al., 2000; Zhen et al., 2000). *Hiw* mutants show aberrant synaptic structures, in that they have an excess of presynaptic boutons at neuromuscular junctions (Wan et al., 2000). Two identified RPM-1 mutants were shown to have abnormal synaptic organization, with one reported loss of function mutation causing aberrant synapse formation at GABAergic neuromuscular junctions (Schaefer et al., 2000; Zhen et al., 2000). Studies on these proteins, particularly Highwire, have strongly indicated their role in acting as a ubiquitin ligase, targeting presynaptic signaling proteins for degradation, and thus acting as a negative regulator of synaptic growth (DiAntonio et al., 2001; McCabe et al., 2004; Wu et al., 2005). The most recent PAM homologue to be identified is Esrom, present in zebrafish (*Danio rerio).* Like PAM, this vertebrate homologue is expressed widely throughout neurons and other cell types. Esrom mutants have defects in growth cone navigation during development, and also have defects in the projection of retinal axons, potentially due to misregulated

ubiquitination and degradation of tuberin, a tumor suppressor and intracellular signaling molecule (D'Souza et al., 2005; Hendricks et al., 2008). Esrom also controls the synthesis of pteridine, a signaling molecule in part necessary for yellow pigmentation (Le Guyader et al., 2005). These additional roles of Esrom, in comparison to Highwire and RPM-1, suggest vertebrate PAM homologues have more widespread and complex functions in higher organisms.

Further exploration of KCC2 interaction with PAM

As previously mentioned, PAM is a very large protein. At the initiation of this project, no group had cloned full-length PAM. Thus, the project originally included attempts to clone full-length PAM. However, even using PCR protocols for large nucleotide spans, numerous mutations were introduced in the expanded-range PCR process. Additionally, due to its large size, working with this full-length protein would be experimentally challenging, for instance in overexpression in mammalian expression vectors, precipitation/pull-down, transfer to membranes for Western blotting, etc. Thus, the work described here was carried out using only the portion of PAM identified in the yeast two-hybrid library screen, from here on referred to as RCC1/PAM.

Several classic methods were used to verify interaction between KCC2 and RCC1/PAM. Additionally, examination of RCC1/PAM effect of KCC2 function was studied using radioisotope uptake assays in a mammalian cell system. Cation-chloride cotransport by the CCCs has traditionally been assessed using ^{86}Rb fluxes. ^{86}Rb has a much longer half-life than isotopic K^+ and is transported in the same manner as K^+. It

has been reported that KCC2 has a higher estimated affinity for external ^{86}Rb (Michaelis constant (Km) = 5.2 ± 0.9 (SE) mM) than for external Cl^- (Km >50 mM) (Payne, 1997).

Methods

Small-scale Y2H

"Small scale" yeast two-hybrid transformations were used to ensure that RCC1/PAM alone did not activate yeast reporter genes. Such transformations are referred to as "small scale" to differentiate from the library-scale screens to identify novel protein interactors, but much of the methodology remains the same. RCC1/PAM in the pACT2 vector was first transformed into PJ69-4A yeast, and this strain was grown and maintained on -Leucine agar plates. Then, empty pGBDUC2 vector was transformed into this yeast containing the RCC1/PAM-pACT2 plasmid. Yeast transformations were plated on -Uracil, - Leucine plates, as a positive control to ensure successful expression of both plasmids in the yeast cells, as well as plated or restreaked on - Uracil, -Leucine, -Histidine + 2 mM 3-amino-1,2,4-triazole plates to assess interaction.

DNA constructs

In order to create KCC2-CT fused to a GST fusion protein, KCC2-CT was subcloned into the pGEXT vector, directly following the GST sequence, and in the same translation frame. For expression of RCC1/PAM in HEK cells, the mammalian expression vector pCDNA3 was used, and a HA tag was introduced for antibody recognition.

Western blotting

For Western Blots, proteins were first denatured in sample buffer containing SDS and 5% beta-mercaptoethanol for 15 minutes at 72°C. They were then loaded onto SDS-polyacrylamide gels for electrophoresis, and transferred to polyvinylidene fluoride membrane (Millipore, Bedford, MA) using a semidry transfer apparatus. Membranes were then blocked in 5% non-fat milk/TBST for two hours at room temperature before incubation with antibody in milk/TBST overnight at 4°C. Antibody dilutions were as follows: KCC2, 1:1000 dilution; HRP-conjugated HA, 1:1000 (Roche, Indianapolis, IN).

GST pull-down

In order to create Glutathione S-Transferase (GST) fusion proteins, KCC2-CT cDNA was cloned into the pGEX4T1 vector (Pharmacia, Piscataway, NJ) inserted after the vector's GST encoding sequence. KCC2-CT-pGEX4T1 or empty pGEX4T1 (for GST only controls) were transformed into a protease-deficient strain of *Escherichia coli*. During growth, protein production was induced with isopropyl β-D-1-thiogalactopyranoside (IPTG, 24mg/ml), and bacteria were lysed by freeze-thawing, sonication, and incubation with 20% Triton X-100. Lysates were centrifuged, and supernatants incubated with 50% Sepharose-Glutathione bead slurry. Following three spin/wash cycles, the pull-down assay was performed as previously described (Piechotta et al., 2002), incubating GST protein-bound beads with HEK cell lysates.

Cell culture and transfection

Human Embryonic Kidney (HEK293) or HEK293FT cells were maintained and routinely passaged in DMEM-F12 medium supplemented by 10% fetal bovine serum and 1% Penicillin/Streptomycin (Invitrogen, Carlsbad, CA). Transfections were performed with Fugene 6 (Roche) on cells that were approximately 50-70 percent confluent.

Coimmunoprecipitation

Transfected HEK293FT cells (Invitrogen) were lysed with 1% Triton X-100 lysis buffer (150 mM NaCl, 10 mM Tris, 2 mM EDTA, 1% Triton X-100) containing protease inhibitors (Roche) for 30 min on ice. Lysates were scraped into 1.5 ml tubes and microcentrifuged for 10 min at 14,000 rpm at 4°C. KCC2 was immunoprecipitated from the supernatant with 7 µl of polyclonal KCC2 antibody overnight at 4°C. Protein A-Sepharose beads (Santa Cruz Biotechnology, Santa Cruz, CA), pre-washed with lysis buffer, were incubated with the supernatant for 2 hours at 4°C. Antibody-protein complexes were pulled down by centrifugation for 4 minutes at 4,000 rpm. Pelleted beads were subjected to three spin/washes with 1 ml lysis buffer, then resuspended in sample buffer containing 5% β-mercaptoethanol and denatured at 70°C for 20 minutes.

Microsome preparation

Cells grown in 100-mm dishes were scraped in sucrose solution (0.32 M sucrose, 2 mM EDTA, 2.5 mM β-mercaptoethanol, 5 mM Tris-Cl, pH 7.5, and protease inhibitors) and homogenized with a Teflon pestle for 20 strokes on ice. Cell debris was removed by centrifugation at 4,000 x g for 15 min. The recovered supernatant was then

centrifuged for 15 min at 9000 x g. The pellet from a final high-speed centrifugation (100,000 x g) was resuspended in 500 µl sucrose solution.

RT-PCR and semi-quantitative RT-PCR

In order to confirm the presence of PAM in two potential model cell systems, HEK293 cells and oocytes, RT-PCR was used. RNA was retrieved from HEK293 cells and oocytes using the QiaShredder and RNeasy Total RNA extraction kit (Qiagen, Valencia, CA). RNA was also obtained using the Qiagen RNA extraction kit from mouse brain stored in liquid nitrogen, as a control. RNA was then reverse transcribed using Superscript II reverse transcriptase (Invitrogen, Carlsbad CA) using random hexamer primers, and these cDNAs were then subject to PCR. PCR primers for PAM were designed to amplify a 400 bp sequence based on the Celera mouse genome database, human genome sequence, or *Xenopus* ESTs. PCR samples were then run on agarose-TAE gels and visualized by ethidium bromide staining and exposure to UV light.

Semi-quantitative RT-PCR was used to quantitate RNA levels in HEK293 cells. RNA obtained from transiently transfected HEK293 cells was used for reverse transcription, as described above. PCR primers CC1 and CC2 were used to amplify a 412 bp sequence of KCC2 cDNA. Samples were taken out at various PCR cycles, as indicated in the figures, in order to monitor exponential cDNA amplification before reaching saturation. PCR samples were then run on agarose-TAE gels and visualized by ethidium bromide staining and exposure to UV light.

Table 3: PCR primers used in RT-PCR experiments

Target	*Primer Name*	*Primer Sequence (5' to 3')*
rKCC2	CC1	AGGGCGGAAAGAAGAAGCCG
	CC2	TCCCCACTGGCATCTTCTGCC
human PAM	xPAM-PCR1	AAATTTGTGGCCAAGGACAG
	xPAM-PCR2	CAGAAGACTCTTGCCAAGATG
***Xenopus* PAM**	xPAM-PCR1	AAATTTGTGGCCAAGGACAG
	xPAM-PCR2	CAGAAGACTCTTGCCAAGATG
mouse PAM	xPAM-PCR1	AAATTTGTGGCCAAGGACAG
	mPAM-PCR2	CAGAAGGCTCTTGCCAAGATG

$^{86}Rb^{+}$ uptake

In order to observe KCC2 activity, transfected HEK293 cells were used two days post-transfection for $^{86}Rb^{+}$ uptake experiments. Cells were washed twice with room temperature isotonic Na^{+}-free solution (150 mM NMDG-Cl, 5 mM KCl, 2 mM $CaCl_2$, 0.8 mM $MgSO_4$, 5 mM glucose, 5 mM HEPES, pH 7.4) then preincubated for 15 or 20 minutes with Na^{+}-free solution plus 100 µM ouabain. Following preincubation, cells were then incubated with Na^{+}-free solution containing ouabain and $^{86}Rb^{+}$ at a concentration of 1 µCi/µl. Uptake was terminated by three washes with ice cold Na^{+}-free solution. Cells were lysed with 500 µl 1N NaOH for one hour, and then neutralized with 250 µl glacial acetic acid. $^{86}Rb^{+}$ uptake was measured from 150 µl of cell lysate added to 5 ml Biosafe II scintillation cocktail (RPI, Mount Prospect, IL). Protein quantitation of lysates was determined by Bradford assay (BioRad, Hercules, CA). Final measurements were calculated as pmoles K^{+} per µg protein per min. Statistical analyses were performed by One Way ANOVA and Tukey post-test using GraphPad Prism software.

Results

Negative control of yeast two-hybrid tests of interaction

One possibility contributing to false positives is the potential for the identified yeast clone to unspecifically activate the auxotrophy reporter gene. Some candidate proteins isolated from libraries have been shown to bind to the Gal promoter region, thus independently functioning as a transcription factor for yeast auxotrophy genes used in clone selection. In order to test this in the case of RCC1/PAM, RCC1/PAM-pACT2 was tested in a small-scale yeast two-hybrid transformation against the empty pGBDUC2 bait vector. As shown in Figure 10, when plated on the double-dropout -Uracil, -Leucine plate as a control, the transformed yeast survives, indicating that both pACT2 and pGBDUC2 vectors have been successfully transformed into yeast cells. However, when plated on the –Uracil –Leucine – Histidine +2-AT plates, no yeast growth is seen, indicating that RCC1/PAM-pACT2 does not act as an unspecific transcription factor at the Gal promoter region of PJ69-4A, and does not activate yeast reporter genes independent of interaction with KCC2-CT.

KCC2-CT and RCC1/PAM interaction in GST pull-down assays

The interaction between KCC2-CT and RCC1/PAM was confirmed using a GST pull-down assay. Lysates from HEK293 cells expressing HA-tagged RCC1/PAM were incubated with GST-KCC2-CT immobilized on GST-Sepharose beads. As seen in Figure 11, only GST-KCC2-CT was able to pull-down RCC1/PAM (lane 2), whereas GST alone did not pull down RCC1/PAM.

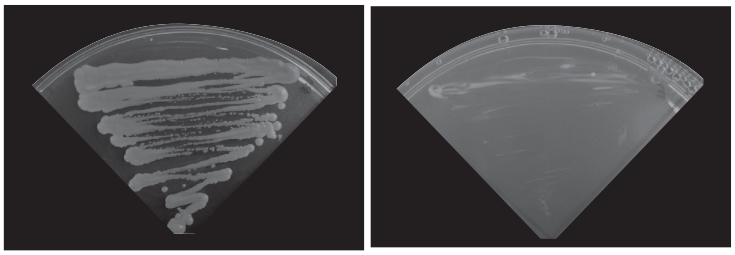

Figure 10. Negative control of RCC1/PAM in yeast two-hybrid.
The partial PAM clone tested in a small scale yeast two-hybrid transformation against the empty bait vector, pGBDUC2. Left, restreak on -Uracil, -Leucine media (control plate); Right, -Uracil, -Leucine, -Histidine +AT media (experimental plate).

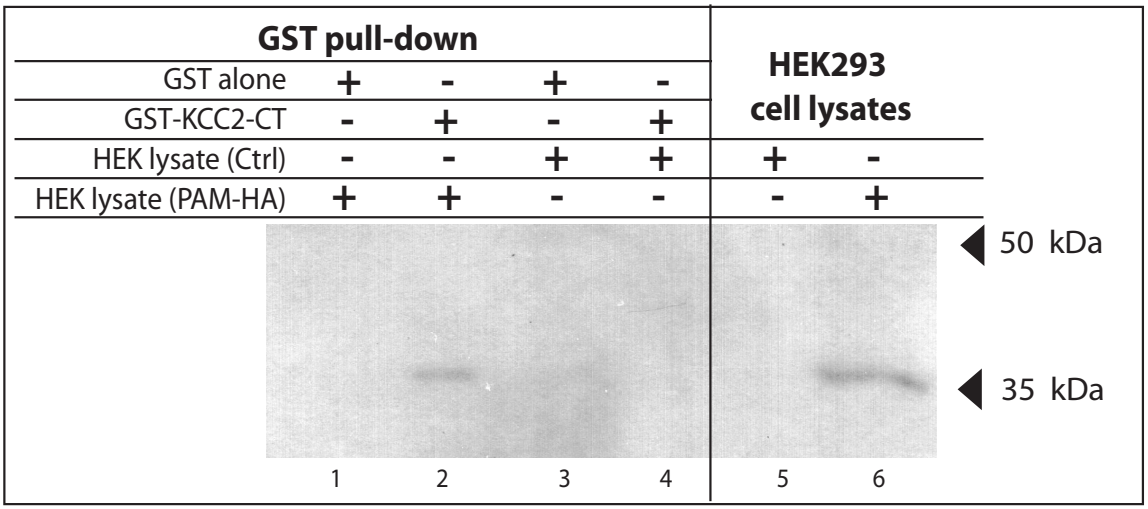

Figure 11. GST pull-down assay demonstrates KCC2-CT binding to RCC1/PAM.

Immunoblot using HRP-conjugated anti-HA antibody. Lanes 1-4: GST pull-down assay using either purified GST or GST-KCC2-CT, incubated with HEK293 cell lysate transfected with either pCDNA3 alone or HA-tagged RCC1/PAM. Lanes 5 and 6: whole cell lysates of transfected HEK293 cells.

CoIP demonstrates RCC1/PAM binding to full-length KCC2

Coimmunoprecipitation assays were used to show that the partial PAM clone also forms a complex with full-length KCC2 in cells. The partial PAM clone was tagged with an HA epitope, and cotransfected into HEK293FT cells with either empty pCDNA3 vector or full-length KCC2. Cell lysates were subjected to immunoprecipitation using the KCC2 antibody, and protein complexes isolated with Protein A-Sepharose beads. Immunoblotting with HA antibody showed that PAM-HA is immunoprecipitated with KCC2 (Figure 12, lane 4). However, no PAM-HA was pulled-down in the absence of KCC2 (Figure 12, lane 2).

Presence of endogenous PAM in HEK cells

PAM has been localized to many different cell lines, such as HeLa cells, and many tissue types. Thus, it was anticipated that PAM would be expressed in HEK293 cells and *Xenopus laevis* oocytes, two heterologous expression systems commonly used by the laboratory. The presence of PAM was confirmed by RT-PCR using RNA isolated from HEK293 cells, *Xenopus* oocytes, and mouse brain (control). Primers were designed based on previously reported sequences, or in the case of *Xenopus*, EST databases, to amplify a 400 bp sequence in the PAM cDNA. As seen in Figure 13, PAM was detected in oocytes, HEK 293 cells, and mouse brain, but no signal was detected in the control (water only).

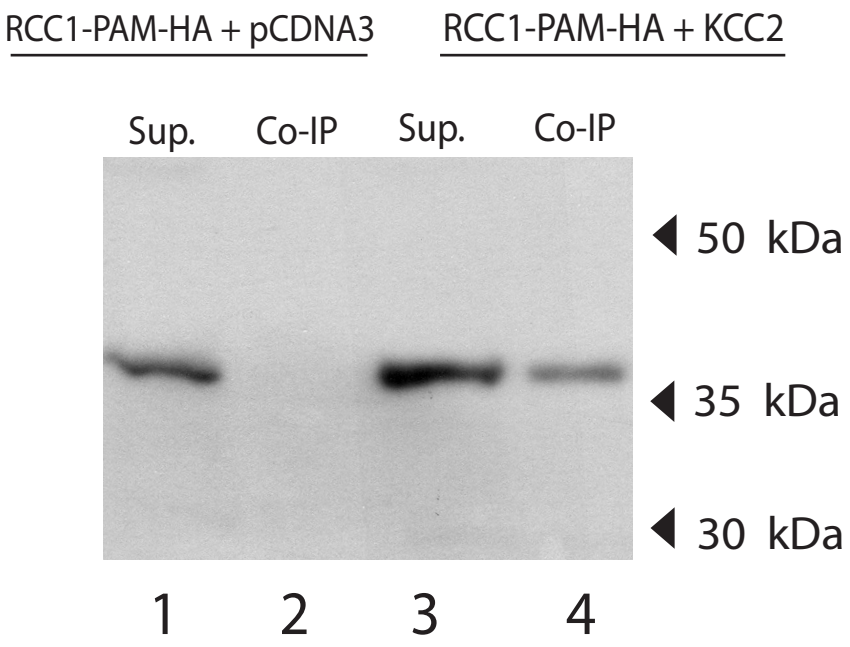

Figure 12. Coimmunoprecipitation of RCC1/PAM with full-length KCC2. Representative Western blot of co-immunoprecipitation experiments. HEK293 cells were transfected with either RCC1/PAM alone, or KCC2 and RCC1/PAM. Anti-KCC2 antibody was used for immunoprecipitation, and HRP conjugated-anti HA antibody was used for immunoblotting.

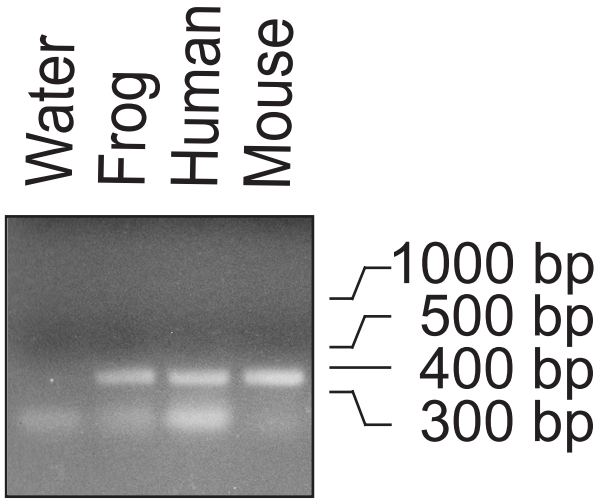

Figure 13. RT-PCR demonstrates PAM is found in HEK293 cells. RNA isolated from *Xenopus laevis* oocytes, HEK293 cells, and mouse brain, was reverse-transcribed and PCR amplified using PAM-specific primers. Note the presence of a ~390 bp PCR fragment in all three samples and not in the negative control (water).

RCC1/PAM increases KCC2-mediated flux

To assess the effect of PAM on KCC2 function, we cotransfected the RCC1/PAM fragment with full length KCC2 in HEK293 cells. Function of the cotransporter was assessed using unidirectional $^{86}Rb^{+}/K^{+}$ uptakes. Cells were transfected with KCC2 and/or RCC1/PAM two days prior to functional assays, and uptakes were measured at 6 min intervals over 30 min. As seen in Figure 14, KCC2 expression in HEK cells resulted in large Na^{+}-independent K^{+} uptake, several fold greater than baseline (empty pCDNA3 transfected). Interestingly, coexpression of the partial PAM clone increased KCC2-mediated flux.

$^{86}Rb^{+}$ flux does not increase with GST coexpression

One possible explanation of this increase in KCC2-mediated flux is that coexpression of any protein results in unspecific upregulation in KCC2 activity. Thus, as an additional control, glutathione S-transferase (GST), which has a molecular weight of approximately 35 kDa was used as a similarly sized, non-relevant protein, for coexpression with KCC2. In $^{86}Rb^{+}$ uptake experiments, coexpression of GST did not result in an increase in KCC2 flux (Figure 15). This supports the evidence that the increase in KCC2 activity seen with RCC1/PAM coexpression is specific to RCC1/PAM, and not merely an artifact resulting from expression of a small ~30 kDa protein.

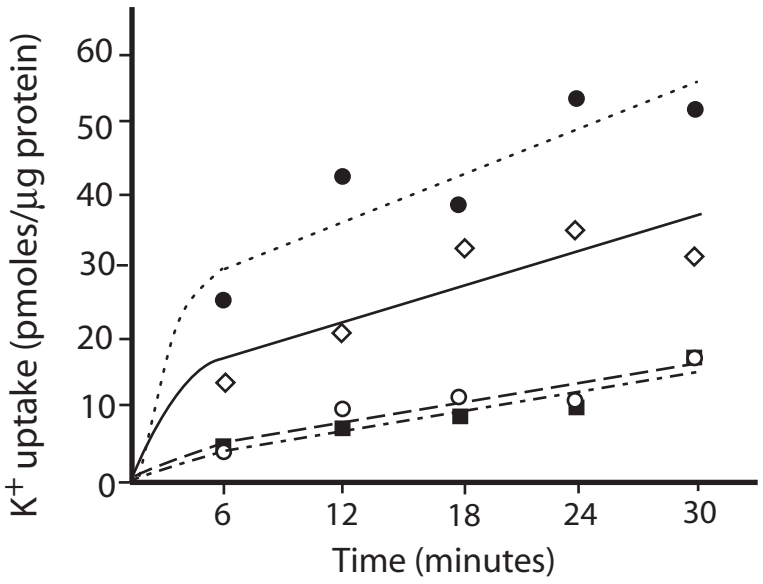

Figure 14. RCC1/PAM increases KCC2-mediated flux in HEK293 cells. Unidirectional $^{86}Rb^{+}$ uptake in HEK293 cells measured at six minute intervals over 30 minutes. Cells were transfected with either: KCC2 and RCC1/ PAM clone (filled circles, dotted line), KCC2 only (open diamonds, solid line), RCC1/PAM only (open circles/dashed line) or empty pCDNA3 vector only (filled squares, dashed/dotted line). Graph shown is representative of three experiments.

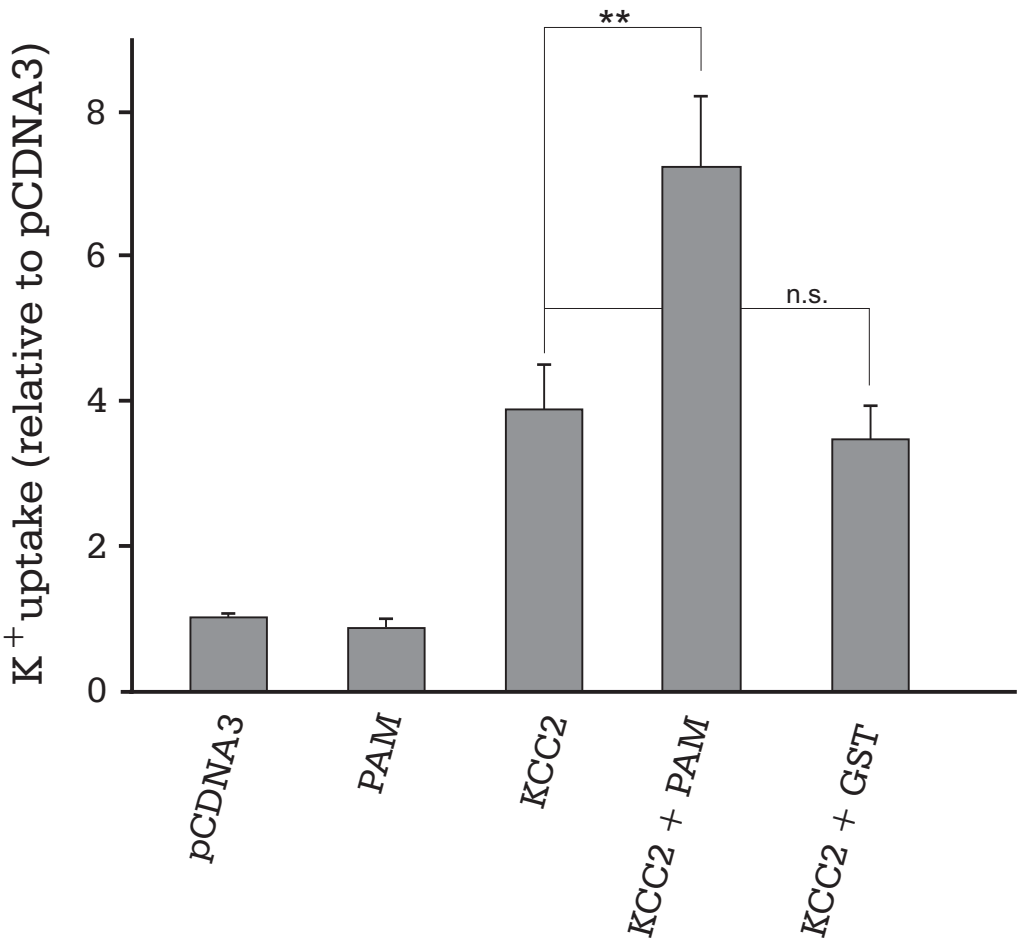

Figure 15. GST does not affect KCC2 activity.
HEK293 cells were transfected with KCC2 alone, KCC2 and RCC1/PAM, or KCC2 and GST. KCC2 uptake activity was measured using unidirectional $^{86}Rb^{+}$ uptake after 10 minutes of incubation with $^{86}Rb^{+}$. ** = $P < 0.01$ (ANOVA, Tukey post-test).

RCC1/PAM effect on KCC2 protein

To account for the increased KCC2 flux, we first considered the possibility that RCC1/PAM affects the amount of functional KCC2 protein. To quantitate the KCC2 protein levels, we prepared HEK293 cell microsomal fractions to enrich for membrane-associated proteins. Microsomes were subjected to Western blot analysis, and probed with anti-KCC2 antibody or with anti-human transferrin antibody to control for unspecific effects by RCC1/PAM. As shown in Figure 16, KCC2 levels increased significantly when the cotransporter was coexpressed with RCC1/PAM. This effect is RCC1-specific, as transfections were controlled for amount of DNA by using empty pcDNA3 vector.

RCC1/PAM effect on KCC2 RNA expression

To determine whether the increased KCC2 protein expression by RCC1/PAM originates from increased transcription, we examined KCC2 RNA levels under the different transfection conditions. Using semi-quantitative RT-PCR with primers specific to KCC2, we showed that RCC1/PAM increases KCC2 RNA levels in HEK293 cells (Figure 17).

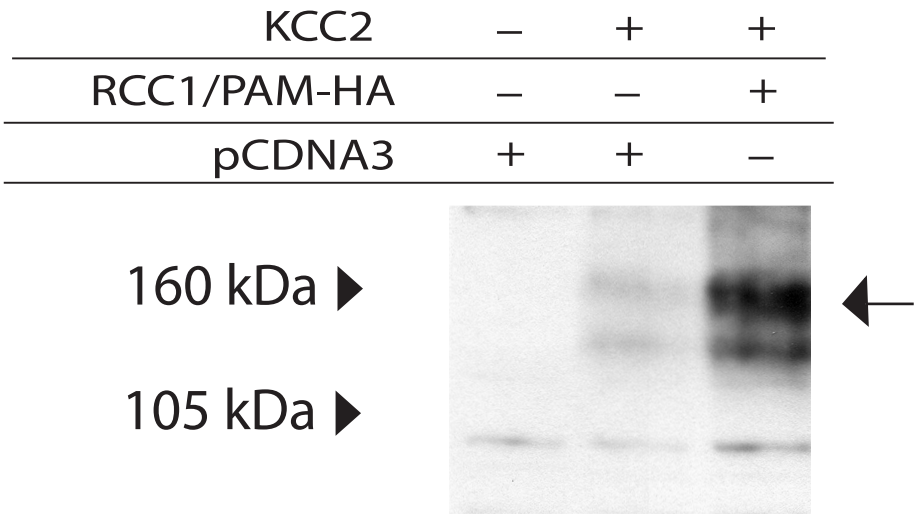

Figure 16. RCC1/PAM increases KCC2 protein in HEK293 cells. HEK293 cells were transfected with rKCC2-pCDNA3 plus empty pCDNA vector or rKCC2 plus RCC1/PAM. Total protein was subject to SDS-PAGE for Western blotting. Membrane was probed with anti-KCC2 antibody. Representative of three separate experiments.

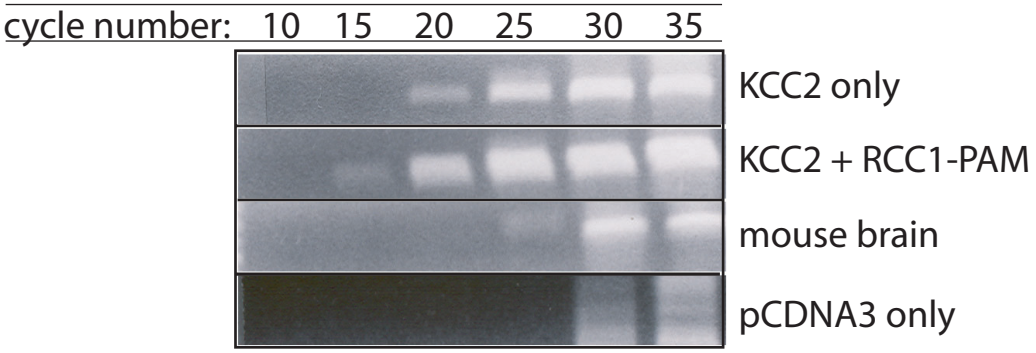

Figure 17. RCC1/PAM increases KCC2 RNA levels in HEK293 cells. RNA was isolated from transfected HEK293 cells, and RNA yield used for reverse transcription. Resulting cDNA was then used for semi-quantitative PCR with reactions taken out at indicated cycles and run on agarose-TAE gels.

Discussion

Validation of interaction using additional in vitro *methods*

The data in this section validates binding between RCC1/PAM and KCC2, as identified in the initial yeast two-hybrid library screen. First, the negative yeast two-hybrid control with empty pGBDUC2 vector demonstrates that RCC1/PAM does not intrinsically activate transcription of reporter genes in the yeast. Second, GST pull-down assays served as an *in vitro* method of testing RCC1/PAM interaction. As described, GST-KCC2-CT fusion protein can effectively pull down HA-tagged PAM expressed in HEK cells, whereas GST protein alone cannot. Finally, binding between full-length KCC2 and RCC1/PAM is demonstrated by coimmunoprecipitation of these proteins following heterologous expression in HEK293 cells. This test of protein interaction is important because it demonstrates that RCC1/PAM can interact with full-length KCC2, as the transporter would exist in its native state. Moreover, this experiment also has greater physiological relevance than the two-hybrid tests in the sense that, whereas two-hybrid interaction takes place inside the nucleus, the protein-protein interaction of the coIP experiments takes place in a more natural cytoplasmic milieu.

Interpretation of flux assays, and increased RNA and protein

In order to explore the functional role of PAM and KCC2 interaction, $^{86}Rb^{+}$ uptake assays on HEK293 cells were used to measure KCC2 activity. The experimental model tested compared expressed KCC2 activity alone or with RCC1/PAM. The logic behind this was that, in lieu of having a full-length PAM clone to express, RCC1/PAM could be used as a dominant negative PAM isoform which would compete with

endogenous PAM for docking on the KCC2-CT. PAM expression is reported in many different cell lines, thus it was expected that it would be present in HEK293 cells. To verify this, RT-PCR was used on HEK cell RNA, and this indeed verified PAM was expressed in the HEK293 cells as well.

HEK cells demonstrated a baseline amount of $^{86}Rb^{+}$ transport over time, and expression of RCC1/PAM alone did not change flux (Figure 14). KCC2 expression increased $^{86}Rb^{+}$ uptake significantly above baseline, and KCC2 coexpression with RCC1/PAM even further increased $^{86}Rb^{+}$ uptake, significantly more than KCC2 alone. In order to rule out the idea that the cotransfection itself caused a flux increase, GST was used as a non-specific protein control, and it did not, in fact, cause an increase in KCC2 flux. This suggests that RCC1/PAM, specifically, is responsible for the increase in KCC2 activity, and not an artifactual effect of cotransfecting two proteins.

There are many points at which RCC1/PAM could be affecting KCC2-mediated flux. One possibility is that RCC1/PAM is changing whole-cell levels of the cotransporter by affecting transcription and/or translation. Alternatively, RCC1/PAM could be changing cell surface levels of the cotransporter (either through protein trafficking and insertion into the membrane, or through endocytosis and/or degradation). Finally, RCC1/PAM could be acting at the cell surface to change cotransporter activity, such as through allosteric modification of the transporter, or post-translational modifications like dephosphorylation.

In order to answer these questions, both RNA and protein levels of KCC2 were quantitated. Not only was there an overall increase in KCC2 protein, but there was also an increase in KCC2 RNA. The effect of RCC1/PAM on KCC2 transcription thus could

account for the increased KCC2 flux observed in Figure 14. This result was puzzling, in light of the fact the initial link between RCC1/PAM and KCC2 stemmed from identifying a protein-protein interaction. It is however possible that RCC1/PAM could affect KCC2 independent of this transcriptional effect. RCC1/PAM could affect transcription, but could also affect KCC2 function through its binding to the carboxyl terminus tail. One way to test this hypothesis is to specifically disrupt RCC1/PAM binding to the carboxyl terminus by creating a mutated KCC2 which disabled binding to the KCC2-CT. In the next chapter, the yeast two-hybrid system is employed once again in an attempt to elucidate the binding site of RCC1/PAM on KCC2, and thus create a binding deficient KCC2 construct.

CHAPTER IV

IDENTIFICATION OF RCC1/PAM BINDING SITES ON KCC2

Introduction

Why build a binding site mutant?

As discussed in the previous chapter, significant evidence exists that RCC1/PAM binds to KCC2. The increase in KCC2 activity seen when cotransfecting RCC1/PAM with KCC2 appeared promising, especially considering that the effect was specific to RCC1/PAM and not to GST, a similarly-sized protein. However, further investigation into the cause of this increased KCC2 activity demonstrated that KCC2 RNA levels likewise increased in the presence of RCC1/PAM. Thus, a new strategy had to be utilized in order to tease apart and isolate the functional effect of the RCC1/PAM and KCC2 protein-protein interaction.

The Delpire laboratory has had success in using the yeast two-hybrid system to identify specific protein binding regions, even down to amino acid residues responsible for binding. The SPAK binding motif present on KCC3 and NKCC1was identified by using yeast two-hybrid, and this motif has been identified in many other SPAK binding partners (Piechotta et al., 2002; Delpire and Gagnon, 2006). Thus, this same methodology was employed in order to further characterize the binding site of RCC1/PAM on KCC2.

RXR motifs

As further described in the Results and Discussion sections of this chapter, a putative RXR motif is present in the KCC2-CT. This is particularly interesting because the RXR motif is a trafficking signal which regulates retention and release from the endoplasmic reticulum (ER). This motif was first identified in the carboxyl terminus of the ATP-sensitive K^+ channel. The K^+ channel motif RKR is masked in tetrameric assembly of the K^+ channel, which then allows release of the complete assembled channel complex to the ER. Conversely, exposed RXR motifs result in ER retention, thus preventing incomplete partial channel complexes from being expressed at the cell surface (Zerangue et al., 1999). This ER retention signal has since been identified in a variety of other membrane transport and receptor proteins, such as the NMDA NR1 subunit, $GABA_B$ receptor , and CFTR transporter (Margeta-Mitrovic et al., 2000; Scott et al., 2001; Hegedus et al., 2006). It has been demonstrated that RXR motif-mediated ER retention can be suppressed by PKC phosphorylation or alternative splicing to introduce an adjacent type-1 PDZ domain (Scott et al., 2001). Thus, the RXR motif is a versatile mechanism for mediating ER retention, and consequently, cell-surface expression of membrane proteins. Clearly, this domain is a particularly interesting feature of the KCC2-CT, especially considering the possibility that PAM may bind to this domain and act as a chaperone protein.

Methods

Small-scale yeast two-hybrid

The yeast two-hybrid system was used to test interaction between RCC1/PAM and various truncations and mutated isoforms of the KCC2-CT. These tests against two known proteins are referred to as small-scale transformations, so as to differentiate from the library-scale screen to identify novel protein interactors. However, much of the methodology remains the same. Many variations of the KCC2-CT were all to be tested against RCC1/PAM, so therefore RCC1/PAM in pACT2 vector was first transformed into PJ69-4A yeast, and this strain was maintained, as previously described, on -Leucine agar plates. Then, regions of the KCC2-CT of varying lengths were subcloned into pGBDUC2 vector, and then transformed into yeast containing the RCC1/PAM-pACT2 plasmid. Yeast transformations were plated on -Uracil, - Leucine plates, as a positive control ensuring a successful expression of both plasmids in the yeast cells, and plated or restreaked on - Uracil, -Leucine, -Histidine +2AT plates to assess interaction.

Small-scale yeast two-hybrid experiments involving KCC1, KCC3, and KCC4 were done in the same fashion, with the cotransporter regions isolated from cDNA by PCR, then inserted into the pGBDUC2 vector for yeast two-hybrid assays against RCC1/PAM-pACT2 in PJ69-4A yeast.

DNA constructs

Truncations of the KCC2-CT were generated by using restriction sites located in the carboxyl terminus, as well as PCR and Expand Long PCR (Roche, Indianapolis, IN) with overhangs allowing for subcloning into the desired vectors. For sequences under 40

base pairs in length, annealed oligonucleotides were designed, again with overhangs to allow for subcloning into yeast two-hybrid vectors. To generate the RXR KCC2 mutant, a 513 bp *Sph*I-*Cla*I fragment consisting of the last 56 amino acids of rat KCC2, some 3'UTR and some polylinker were subcloned into a modified pBSK vector containing a *Sph*I restriction site. The codon encoding the second arginine (CGC) of the RXR motif was mutated into an alanine (GCC) using QuikChange (Stratagene, La Jolla, CA). After sequencing, the *SphI-ClaI* fragment was reintroduced into the wild type clone to produce the mutant KCC2 cDNA.

Table 4: PCR primers and adapters for KCC2-CT truncation mutants as per Figure 18

Construct	*Primer Name*	*Primer Sequence (5' to 3')*
Bait8 (b)	B8S	CGGAATTCCGGGGGGCAGAGAAGGAGTGGGG
	B8A	GAAGATCTTCAGTAGGTGTATGCTGAGATGTCGC
Bait9 (c)	B9S	GCCAATTGATTACTGCAGAGGTGGAAGTCGTGG
	B9A	GAAGATCTTCAGGAGTAGATGGTGATGACCTC
Bait6 (d)	B6S	CGGAATTCCACGACGGGGGCATGCTCATG
	B6A	CGGGATCCTTAGGGCATGTTGAGCAACAC
Bait4 (e)	B4	CGCAATTGTTGGTGTTGCTCAACATGCCC
	B4A	CGGGATCCTTAGGAGTAGATGGTGATGACCTC
Bait4B (g)	B4	CGCAATTGTTGGTGTTGCTCAACATGCCC
	NG14	GCGTTACCTCTACTTTTGATGTACACTCCTAGGGC
Bait4D (h)	B4	CGCAATTGTTGGTGTTGCTCAACATGCCC
	NG15	GGAGGGGCGTTGGCGTTACCTCTAACTCCTAGGGC
Bait4E (i)	NG13	CGGAATTCAACATGCCCGGGCCTCCCCGCAAC
	NG14	GCGTTACCTCTACTTTTGATGTACACTCCTAGGGC

Table 5: Adapter oligonucleotides for KCC sequences used in Figure 19

Construct	*Primer Name*	*Primer Sequence (5' to 3')*
Figure 19A		
KCC1 (a)	K1PB1	AATTCCTGGTCCTACTGAACATGCCCGGCCCCCCTAAGAACAGTGAGGGTGAT GAGAACTACATGTGAG
	K1PB2	GATCCTCACATGTAGTTCTCATCACCCTCACTGTTCTTAGGGGGGCCGGGCAT GTTCAGTAGGACCAGG
KCC2 (b)	K2PB1	AATTCCTAGTTTTGCTCAACATGCCCGGGCCTCCCCGCAACGCCAATGGGGAT GAAAACTACATGTGAG
	K2PB2	GATCCTCACATGTAGTTTTCATCCCCATTGGCGTTGCGGGGAGGCCCGGGCAT GTTGAGCAAAACTAGG
KCC3 (c)	K3PB1	AATTCCTGGTTTTGTTGAATATGCCAGGACCACCCCGGAACCCTGAAGGTGAT GAAAACTACATGTGAG
	K3PB2	GATCCTCACATGTAGTTTTCATCACCTTCAGGGTTCCGGGGTGGTCCTGGCAT ATTCAACAAAACCAGG
KCC4 (d)	K4PB1	AATTCCTGGTCCTGCTGAATATGCCAGGCCCCCCAAAAAGTCGGCAGGGGGAC GAGAACTACATGTGAG
	K4PB2	GATCCTCACATGTAGTTCTCGTCCCCCTGCCGACTTTTTGGGGGGCCTGGCAT ATTCAGCAGGACCAGG
Figure 19B		
KCC3-RXR (d)	K3PB3	AATTCCTGGTTTTGTTGAATATGCCAGGACCACCCCGGAACCGTGAAGGTGAT GAAAACTACATGTGAG
	K3PB4	GATCCTCACATGTAGTTTTCATCACCTTCACGGTTCCGGGGTGGTCCTGGCAT ATTCAACAAAACCAGG
KCC2, RXRE (e)	K2RXREf	GAATTCTTGGTGTTGCTCAACATGCCCGGGCCTCCCCGCAACCGCGAAGGAGA TGAAAACTACATGTGAG
	K2RXREr	GGATCCTCACATGTAGTTTTCATCTCCTTCGCGGTTGCGGGGAGGCCCGGGCA TGTTGAGCAACACCAAGAATT
KCC2, RXPN (f)	K3RXPNf	GAATTCCTGGTTTTGTTGAATATGCCAGGACCACCCCGGAACCCTAATGGTGA TGAAAACTACATGTGAG
	K3RXPNr	GGATCCTCACATGTAGTTTTCATCACCATTAGGGTTCCGGGGTGGTCCTGGCA TATTCAACAAAACCAGGAATT

Results

KCC2-CT truncations narrow down RCC1/PAM binding site on KCC2-CT

In order to isolate the functional effect of RCC1/PAM binding to KCC2-CT, and distinguish to from the influence of RCC1/PAM on KCC2 transcription, the binding site of RCC1/PAM on KCC2-CT was further characterized by creating truncation mutants of the KCC2-CT. These were then tested in small-scale yeast two-hybrid transformations against the PAM library clone (Figure 18A-C). Using this method, a 20 amino acid stretch of the KCC2-CT, which retains the ability to bind RCC1/PAM, was identified (Figure 18A-C, g). This 20 amino acid sequence did not fall within the 34 amino acid KCC2-specific region which has been reported to confer KCC2 activity in isotonic conditions, a feature unique to KCC2 as opposed to the other KCC isoforms (Mercado et al., 2006).

Y1087A point mutant still retains binding to RCC1-PAM

Located in this 20 amino acid stretch is a tyrosine residue, Y1087, which had previously been shown to be critical for KCC2 function via a mechanism independent of phosphorylation (Strange et al., 2000). Hypothesizing that PAM binding to KCC2 might also involve this tyrosine residue, and thus be responsible for the phosphorylation-independent control of KCC2 function, a subclone of KCC2-CT was made from a mutant KCC2 cDNA, in which this tyrosine residue was replaced with an alanine residue. This Y1087A KCC2-CT construct was then used in a yeast two-hybrid assay to test for a change in binding. However, as seen in Figure 18, RCC1/PAM binding to KCC2-CT was unaffected by this mutation (Figure 18A-C, k).

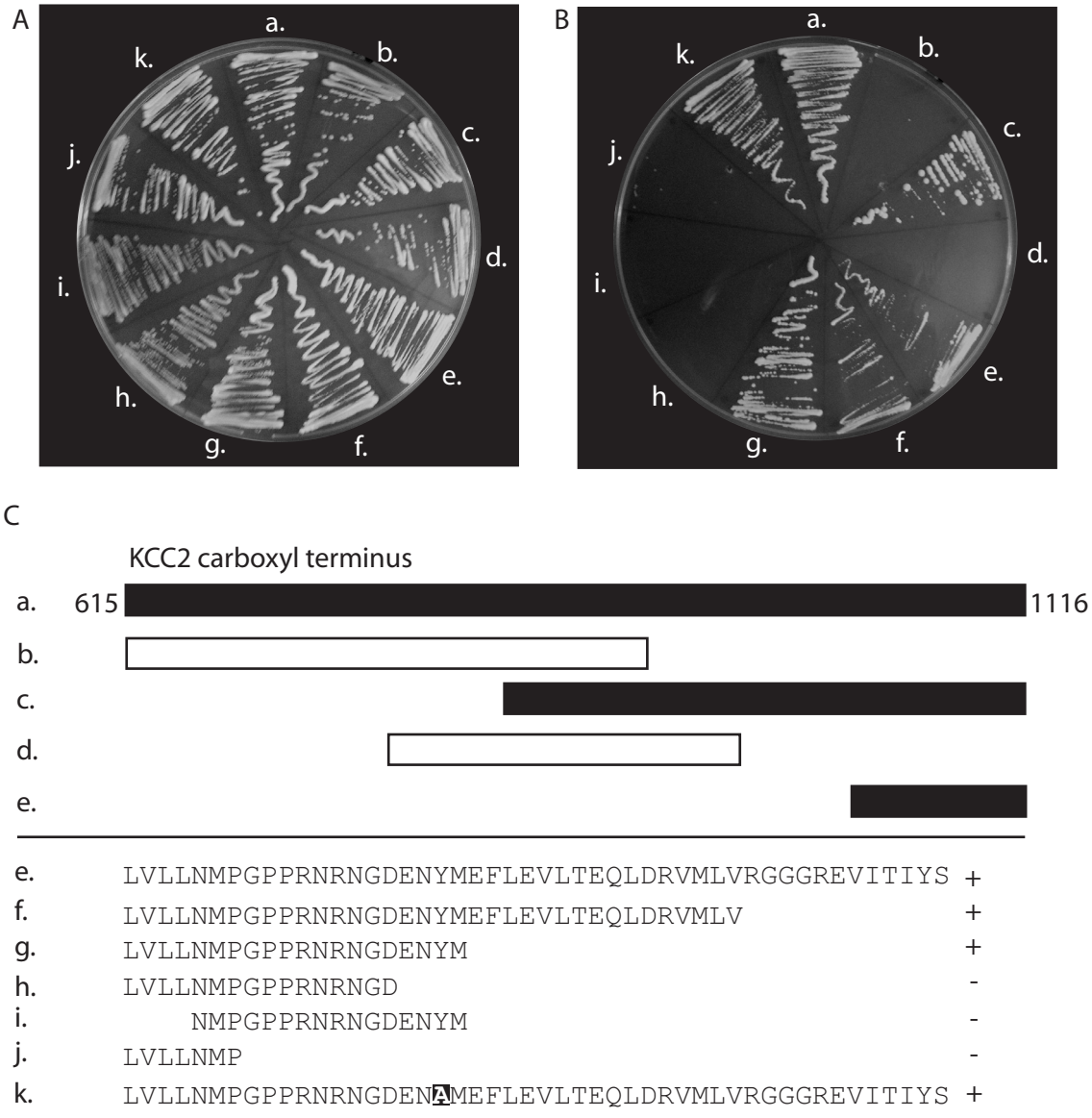

Figure 18. RCC1/PAM interaction narrowed down to 20 amino acids in the carboxyl terminus.

A-C: Truncation mutants of KCC2-CT were used in small scale yeast two-hybrid transformations with RCC1/PAM clone.

A: Restreak on -Uracil, -Leucine media (control plate). B: Restreak on -Uracil, -Leucine, -Histidine + AT media (experimental plate).

C: Schematic/sequences of regions of KCC2-CT used for the truncation mutants. Solid bar/plus sign represents a positive interaction; open bar/minus sign represents a negative interaction.

KCC alignment

The four K-Cl cotransporters generally have highly conserved carboxyl-terminal tails. Since the 20 amino acid sequence we identified did not overlap with the KCC2 specific region, the sequence of the corresponding RCC1/PAM binding region in the three other cotransporters was analyzed. As shown in Figure 19A, the PAM-binding region of KCC2 is very similar to that of the other potassium-chloride cotransporters, differing only by a few amino acid residues.

This similarity is advantageous in that these corresponding regions in the other cotransporters, tested in "small scale" yeast two-hybrid transformation assays, can thus elucidate the specific amino acid residues that are responsible for this protein-protein interaction. As shown in Figure 19A, the RCC1/PAM fragment only interacts with this region in KCC2, but not with the corresponding regions in the other K-Cl cotransporters.

Presence of RXR motif in KCC2 and implications for RCC1/PAM binding

One interesting feature highlighted by the sequence alignment of the KCCs is the presence of a RXR motif within this 20 amino acid region of KCC2. Moreover, this motif is not present in the analogous sequences of the other cotransporters. As described earlier, this observation is particularly interesting because RXR motifs are known to function as ER retention signals. Therefore, in order to explore the importance of the non-conserved residues and the RXR motif, single amino acid mutations were introduced into this region of both KCC2 and KCC3. Disrupting the motif by substituting the second arginine residue into an alanine (RXA) prevented binding to partial RCC1/PAM (Figure 19B). However, introducing an RXR motif into this portion of KCC3 did not confer PAM

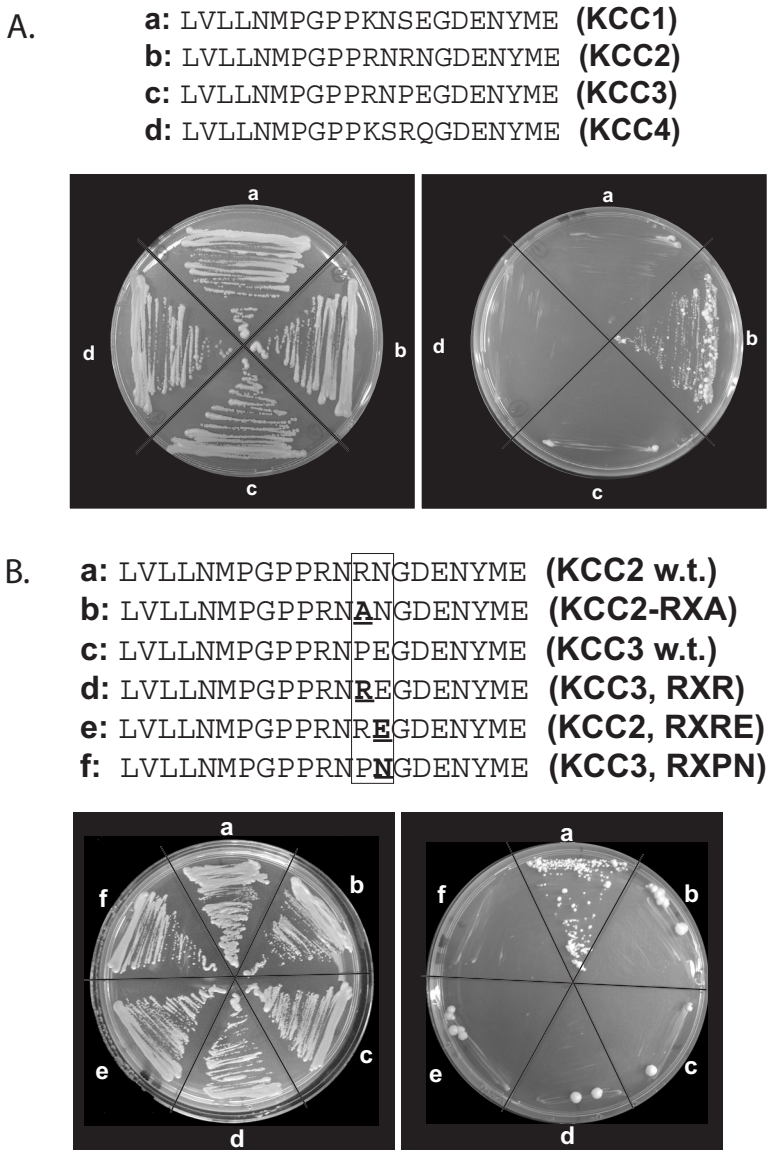

Figure 19. KCC2 point mutant, KCC2-RXA, disrupts RCC1/PAM binding with the minimum 20 amino acid sequence.

A: Small-scale yeast two-hybrid transformation testing interaction between RCC1/PAM against portions of other KCCs homologous to the minimum binding region in KCC2. Top, amino acid sequence alignment. Left, restreak on -Uracil, -Leucine media. Right, restreak on -Uracil, -Leucine, -Histidine + AT media. B: Small-scale yeast two hybrid transformation testing interaction between RCC1/PAM in pACT2, and various mutants of the minimum binding site in KCC2 and homologous region in KCC3. Top, amino acid sequence alignment. Rectangle denotes non-conserved residues between KCC2 and KCC3 in the 20 amino acid region. Bold and underlined residues represent introduced point mutations. Left, restreak on -Uracil, -Leucine media. Right, restreak on -Uracil, -Leucine, -Histidine + AT media.

binding (Figure 19B). This suggests that binding was not only dependent on the RXR motif, but also on neighboring amino acid residues. In support of this idea, introduction of a glutamic acid directly downstream of the RXR motif in KCC2 (thereby mimicking KCC3), was sufficient to disrupt PAM interaction with KCC2 (Figure 19B).

Discussion

Features of RCC1/PAM binding region on KCC2-CT

Truncations of the KCC2-CT and small-scale yeast two-hybrid transformations effectively narrowed down the RCC1-PAM interacting region to rKCC2 residues 1069-1088. This 20 amino acid domain is located between the extreme C-terminus and the region unique to KCC2 which confers constitutive basal activity in isosmotic conditions (Mercado et al., 2006).

The region of KCC2 encompassing this domain and the extreme C-terminus is known to be essential for cotransporter function. In addition to the putative RXR motif described earlier, the 20 amino acid peptide interacting with RCC1/PAM also contains an adjacent putative non-canonical type II Src homology domain 3 (SH3) binding sequence (ϕPxϕPx+) (Barmashenko et al., 2005). SH3 domains are ubiquitous protein interaction modules that are involved in many types of protein-protein interactions. They participate in linking membrane transporters and channels to the cytoskeleton (Choi et al., 2005; Tian et al., 2006), promote protein dimerization (Kristensen et al., 2006), and play a central role in multi-protein scaffolding (Roos and Kelly, 1998; Sheng and Kim, 2000; Xu et al., 2003). However, the fact that all four sequences were identical for the MPGPP[R/K] SH3 putative binding sequence suggested that mutation of this domain

would not likely result in a disruption of binding between RCC1/PAM and KCC2. This does not fully exclude, however, the possibility that this SH3 domain is somehow involved with KCC2 regulation, perhaps via binding to an unknown protein when PAM is not docked or binding to the KCC2-CT.

Significance of RXR motif and residues necessary for RCC1/PAM binding

Despite the high degree of conservation among the four K-Cl cotransporters, it is striking that only the 20 amino acids from KCC2 interacted with the RCC1 domain of PAM in our yeast two-hybrid assay. RCC1/PAM did not promote yeast survival in small-scale yeast two-hybrid tests against the highly homologous region of KCC1, KCC3, and KCC4. The fact that the RXR motif is unique to KCC2 in this region led to the hypothesis that perhaps RCC1/PAM is masking of the motif to allow protein release from the ER. In other RXR-domain containing membrane transport proteins, masking of the RXR motif is done by homomeric or heteromeric subunits, or by ER chaperone proteins (Yuan et al., 2003; Hermosilla et al., 2004; Vivithanaporn et al., 2006). Mutagenesis analysis (Figure 19) revealed that mutating the RXR motif in KCC2 to RXA disrupted RCC1/PAM binding. Mutating the KCC3 sequence to contain an RXR motif did not, however, confer binding to RCC1/PAM. Additionally, mutating the asparagine (N) residue directly after the RXR motif in KCC2 also disrupted RCC1/PAM binding. Taken together, these experiments indicate a role for surrounding residues.

Identification of this pattern of amino acid residues is particularly interesting in light of the previous report of adenylyl cyclases binding and being inhibited by PAM, in particular by the RCC1 domain (Scholich et al., 2001). This interaction was discovered

in a yeast two-hybrid screen using adenylyl cyclase V as a bait protein. An alignment of the 20 amino acid region of KCC2 with adenylyl cyclase V shows conservation of some key residues (Figure 20). This pattern is also present in ACVI, another isoform inhibited by PAM, but is not present in ACII, which is unaffected by PAM. It is possible that there is a common regulation pathway linking these proteins.

The yeast two-hybrid experiments presented here demonstrate the identification of a point mutation which disrupts binding in this particular 20 amino acid region of KCC2-CT. As the ultimate goal is to understand more about the functional effect of PAM binding to the KCC2-CT, the next chapter examines the functional effects of this point mutation in full-length KCC2, in comparison to wild type KCC2.

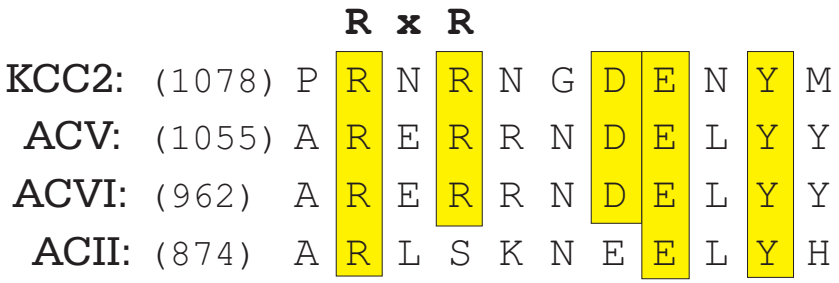

Figure 20. Alignment of homologous portions of adenylyl cyclases V, VI, and II with KCC2.
Numbers in parentheses represent the position of the first amino acid. Yellow boxes indicate amino acid conservation.

CHAPTER V

KCC2 POINT MUTANT AND IMPACT ON KCC2 RCC1/PAM INTERACTION

Introduction

Further examination of the KCC2 point mutant in context

In the experiments described in Chapter III, RCC1/PAM binding to the KCC2 CT was validated. Coexpression of RCC1/PAM with KCC2 in HEK293 cells demonstrated RCC1/PAM's ability to upregulate KCC2 RNA and protein levels, and thus alter KCC2-mediated flux. However, taking into consideration that PAM is a candidate binding partner with KCC2, upregulation of KCC2 transcription is particularly puzzling. So, in order to create a targeted disruption of RCC1/PAM binding on the KCC2-CT, characterization of the RCC1/PAM binding site was performed. As described in Chapter IV, RCC1/PAM binding on the KCC2-CT was narrowed down to 20 amino acids. Furthermore, this led to identification of an arginine residue, unique to KCC2 and located in a putative RXR motif, which, when mutated to alanine, disrupts interaction with these 20 amino acids. In this chapter, this point mutant is introduced into full-length KCC2 and used for several experiments which recapitulate the studies of RCC1/PAM coexpression in Chapter III. The effect of RCC1/PAM on mutant KCC2 RNA and protein expression, as well as mutant KCC2 activity, is examined alongside wild type KCC2 in order to elucidate the functional effects of PAM binding to the KCC2-CT.

N-ethylmaleimide and KCC2 activity

N-ethylmaleimide (NEM) is a known activator of K-Cl cotransport in many cell types (Lauf and Theg, 1980; Adragna et al., 2002; Lauf et al., 2006; Gagnon et al., 2007), including flux by KCC2 heterologous expressed in HEK293 cells (Gillen et al., 1996; Payne, 1997). It has been shown that okadaic acid added prior to NEM inhibits activation of transport. Thus, NEM is believed to act on KCC2 activity via phosphorylation/dephosphorylation pathways (Figure 21). Total net dephosphorylation leading to KCC2 stimulation may be caused by NEM directly acting to dephosphorylate KCC2, or through kinase inhibition, although this is not known (Jennings and Schulz, 1991). NEM is, however, a reliable activator of KCC2 activity. Here, NEM stimulation is used in flux assays in order to tease apart effects of RCC1/PAM specific to RCC1/PAM binding on the KCC2 carboxyl terminus, as opposed to the aforementioned RNA and protein upregulation effects which are not due to the protein interaction originally identified.

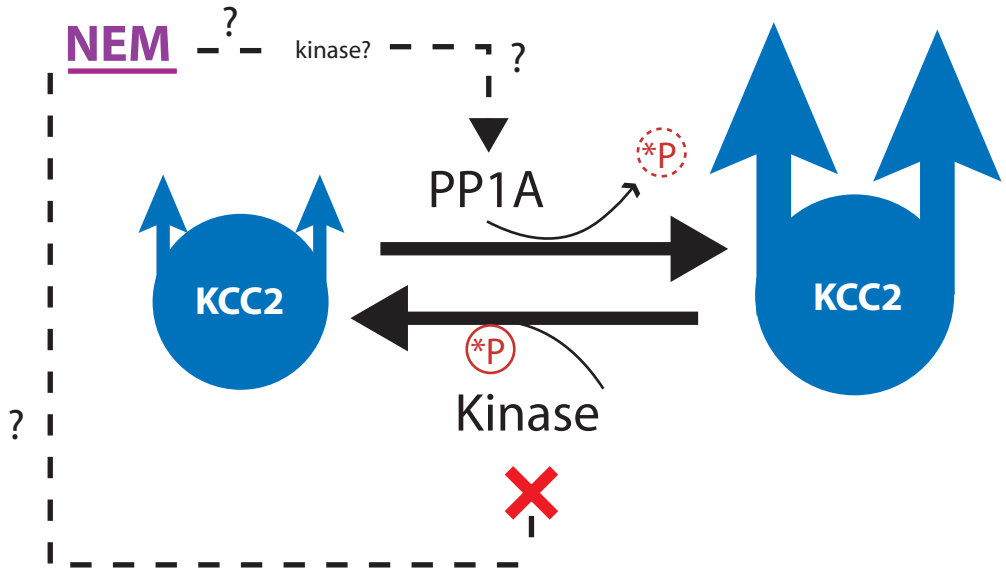

Figure 21. NEM in KCC2 stimulation pathway.
N-ethylmaleimide (NEM) is a potent activator of KCC2 flux activity. It is unknown exactly how NEM activates KCC2 activity, but it likely causes a net dephosphorylation of the cotransporter. NEM could accomplish this by affecting upstream phosphorylation/dephosphorylation pathways, either activating protein phosphatases or inhibiting a regulatory kinase of KCC2.

Methods

Western blotting

In Western Blot assays, proteins were separated by SDS-polyacrylamide gel electrophoresis and transferred to polyvinylidene fluoride membrane (Millipore, Bedford, MA) using a semidry transfer apparatus. Membranes were blocked in 5% non-fat milk/TBST for two hours at room temperature before incubation with antibody in milk/TBST overnight at 4°C. Antibody dilutions: KCC2, 1:1000 dilution; HRP-conjugated HA, 1:1000 (Roche, Indianapolis, IN), human transferrin receptor, 1:2500 (Invitrogen, Carlsbad, CA).

Coimmunoprecipitation

In order to assess the effect of the KCC2 mutation when introduced into full-length KCC2, coimmunoprecipitation assays were used. Once again, transfected HEK293FT cells (Invitrogen) were lysed with 1% Triton X-100 lysis buffer (150 mM NaCl, 10 mM Tris, 2 mM EDTA, 1% Triton X-100) containing protease inhibitors (Roche) for 30 minutes on ice. Lysates were then scraped into 1.5 ml tubes and microcentrifuged for 10 minutes at 14,000 rpm at 4°C. KCC2 was immunoprecipitated from the supernatant with 7 µl of polyclonal KCC2 antibody overnight at 4°C. Protein A-Sepharose beads (Santa Cruz Biotechnology, Santa Cruz, CA), pre-washed with lysis buffer, were incubated with the supernatant for 2 hours at 4°C. Antibody-protein complexes were pulled down by centrifugation for 4 minutes at 4,000 rpm. Pelleted beads were subjected to three spin/washes with 1 ml lysis buffer, then resuspended in sample buffer containing 5% β-mercaptoethanol and denatured at 70°C for 20 minutes.

Semi-quantitative RT-PCR

As described before, semi-quantitative RT-PCR was used to quantitate KCC2 RNA levels in transiently transfected HEK293 cells. RNA was retrieved from HEK293 cells using the QiaShredder and QiaPrep Total RNA extraction kit (Qiagen, Valencia, CA). RNA was then reverse transcribed with Superscript II reverse transcriptase (Invitrogen, Carlsbad CA) using random hexamer primers. PCR was performed on the resulting cDNA, again using primers CC1 and CC2 to amplify a 412 bp region of KCC2. Samples were taken out at various PCR cycles, as indicated in the figures, in order to monitor exponential cDNA amplification before reaching saturation. PCR samples were then run on agarose-TAE gels and visualized by ethidium bromide staining and exposure to UV light.

Biotinylation of proteins

In order to look at cell surface expression of proteins, biotin tagging and pull-down was performed with NHS-S-S-sulfobiotin and NeutrAvidin beads (Pierce). Using a protocol adapted from Daniels and Amara (Daniels and Amara, 1998) cells were washed in ice cold 1x PBS, then incubated with 1mg/ml to 2mg/ml biotin, the maximum recommended concentration, for 25 minutes at 4°C with gentle agitation. Cells were quenched by two washes, followed by a 25 minute incubation in glycine quench buffer (100mM Glycine in 1x PBS), again at 4°C with gentle agitation. Following three washes in 1x PBS, cells were scraped, lysed (1% Triton X-100, 150 mM NaC1, 5 mM EDTA, 50 mM Tris, pH 7.5) and centrifuged as earlier described to clear DNA/unsolubilized fraction. Supernatant containing solubilized proteins was then incubated with

NeutrAvidin beads for one hour at 4°C in an end-over-end rotator. Pull-down of beads was performed by four spin-wash steps, twice in high-salt wash buffer (0.1% TritonX-100, 500mM NaCl, 5mM EDTA, 50mM Tris pH 7.5), followed by twice in no salt buffer (50mM Tris, pH 7.5). Proteins were eluted from beads by addition of sample buffer plus 5% β-mercaptoethanol and denaturing, as previously described.

$^{86}Rb^{+}$ uptake

Once again, the $^{86}Rb^{+}$ uptake assay described earlier was used to measure KCC2 activity. As indicated in figures, flux assays were done with HEK293 cells transfected with either wild type KCC2 or KCC2-RXA, and either RCC1/PAM or empty pCDNA3 vector. N-ethylmaleimide (NEM) stimulation was performed using NEM dissolved in DMSO, and then applied to cells in a final concentration of 1mM, for a total of 15 minutes. As a control, vehicle (DMSO) alone was used in the non-stimulated, NEM-free flux conditions.

Results

Effect of RCC1/PAM on KCC2-RXA mutant protein and RNA levels

To assess the effect of preventing RCC1/PAM interaction with the C-terminal region, the RXA mutation described in Chapter IV was introduced into full-length KCC2. This clone is thus referred to as KCC2-RXA. KCC2-RXA was transfected into HEK293 cells in the presence or absence of the RCC1/PAM fragment, and compared to wild type KCC2, also in the presence and absence of RCC1/PAM, as a control. Interestingly, coexpression of RCC1/PAM with KCC2-RXA resulted in increased KCC2 RNA and protein levels, similar to those observed with wild type KCC2 (Figure 22).

Coimmunoprecipitation of RCC1/PAM and KCC2-RXA

Coimmunoprecipitation experiments were also performed on HEK cells expressing both KCC2-RXA and HA-tagged-RCC1/PAM. As shown in Figure 23, immunoprecipitation of KCC2-RXA with KCC2 antibody still results in pull-down of RCC1/PAM. Thus, it seems that the PAM fragment also interacts elsewhere on KCC2, and not only the carboxyl tail 20 amino acid region identified by yeast two-hybrid.

KCC2-RXA transport activity

$^{86}Rb^{+}$ uptake assays were used to measure KCC2-mediated transport in HEK293 cells transfected with wild type KCC2 and mutant KCC2-RXA. As shown in Figure 24, KCC2-RXA retained flux activity, with a significant increase in flux over the pCDNA3 alone baseline and no significant decrease compared to wild type KCC2 activity.

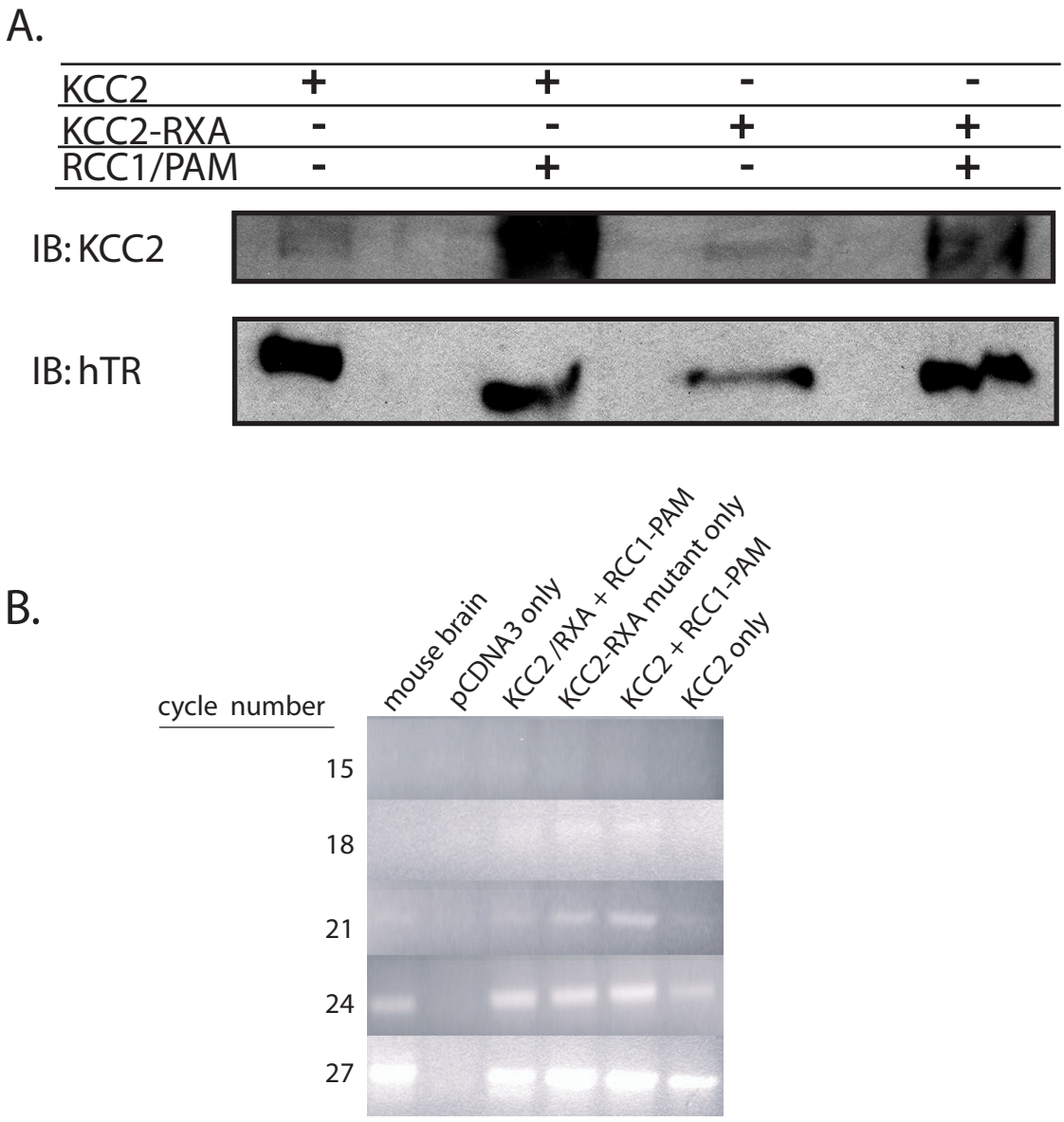

Figure 22. KCC2-RXA, like KCC2, has increased protein and RNA levels when cotransfected with RCC1/PAM.
A: Microsome preparations were made from HEK293 cells transfected with rKCC2-pCDNA3 plus empty pCDNA vector (lane 1), rKCC2 plus RCC1/PAM pCDNA3 (lane 2), KCC2-RXA-pCDNA3 plus empty pCDNA vector (lane 3), and KCC2-RXA plus RCC1/PAM pCDNA3 (lane 4). Western blot was probed with anti-KCC2 antibody and anti-human transferrin receptor antibody. Representative of three separate experiments. B: Semi-quantitative PCR was performed as described earlier, with the indicated HEK cell transfection conditions.

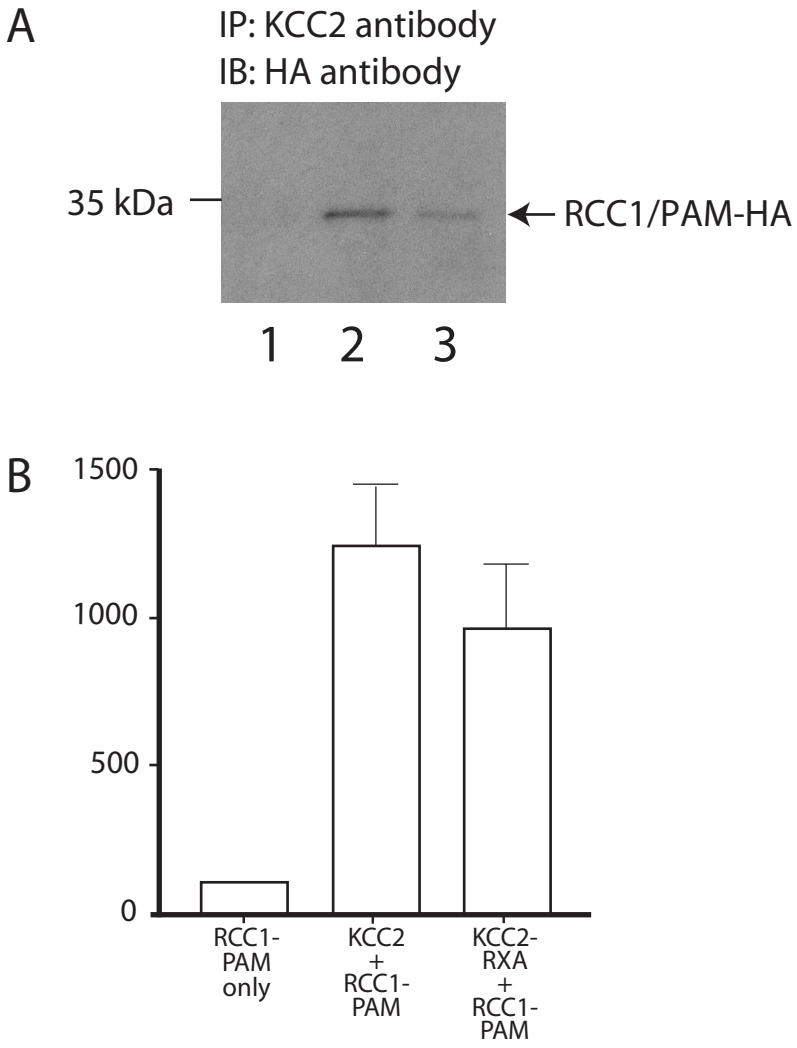

Figure 23. Coimmunoprecipitation of RCC1/PAM with KCC2 and KCC2-RXA. A: Representative Western blot of coimmunoprecipitation experiments. HEK293FT cells were transfected with either RCC1/PAM alone, KCC2 and RCC1/PAM, or KCC2-RXA and RCC1. KCC2 antibody was used for immunoprecipitation and HRP-conjugated anti-HA antibody was used for immunoblotting. B: Coimmunoprecipitation experiments were quantitated by measuring pixel intensity using ImageJ (NIH). Data is normalized to the negative control (RCC1/PAM only condition).

The activity of both wild type and mutant KCC2 was also examined in the presence and absence of coexpressed RCC1/PAM. Interestingly, these functional studies revealed that RCC1/PAM could not increase KCC2-RXA cotransporter function, as is the case with wild type KCC2 (Figure 24).

Considering that KCC2-RXA function did not increase, whereas its RNA and protein levels did increase, one potential explanation is that KCC2-RXA is not expressed in the cell surface to the same extent as wild type KCC2. Thus, biotinylation experiments were used to investigate this idea. Biotin labeling was first performed on cells transiently transfected with KCC2 to mirror the flux experiments previously described. However, weak levels of biotinylated KCC2 signal led to optimization and positive controls of biotinylation technique. These experiments controlling for biotinylation methodology were performed in a HEK293FT cell line which stably overexpresses KCC2. As shown in Figure 25A, the biotinylation method used was successful in specifically labeling cell-surface fractions of transferrin receptor, a widely expressed membrane protein. However, labeling of KCC2 was very inefficient, considering how these cells stably overexpress KCC2. Thus, the aforementioned weak signals of biotinylated KCC2, as depicted in Figure 25B, is likely a function of poor incorporation of biotin label on extracellular KCC2. This led to the following studies of NEM-stimulated K-Cl cotransport, as an alternative way to further examine the effect of the RXA mutation on KCC2 function.

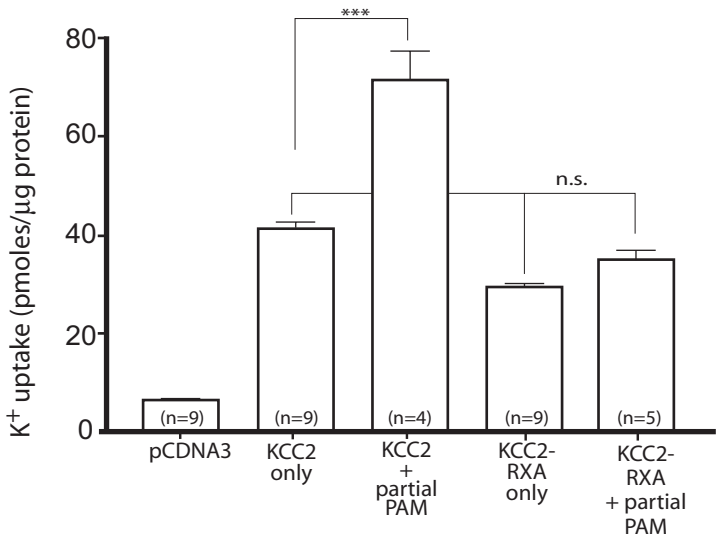

Figure 24. KCC2, but not the mutant KCC2-RXA, has increased activity in the presence of RCC1/PAM. Unidirectional $^{86}Rb^{+}$ uptake in HEK293 cells was measured after 10 minutes of incubation with $^{86}Rb^{+}$. $p < 0.001$ (Tukey post-test) except where indicated.

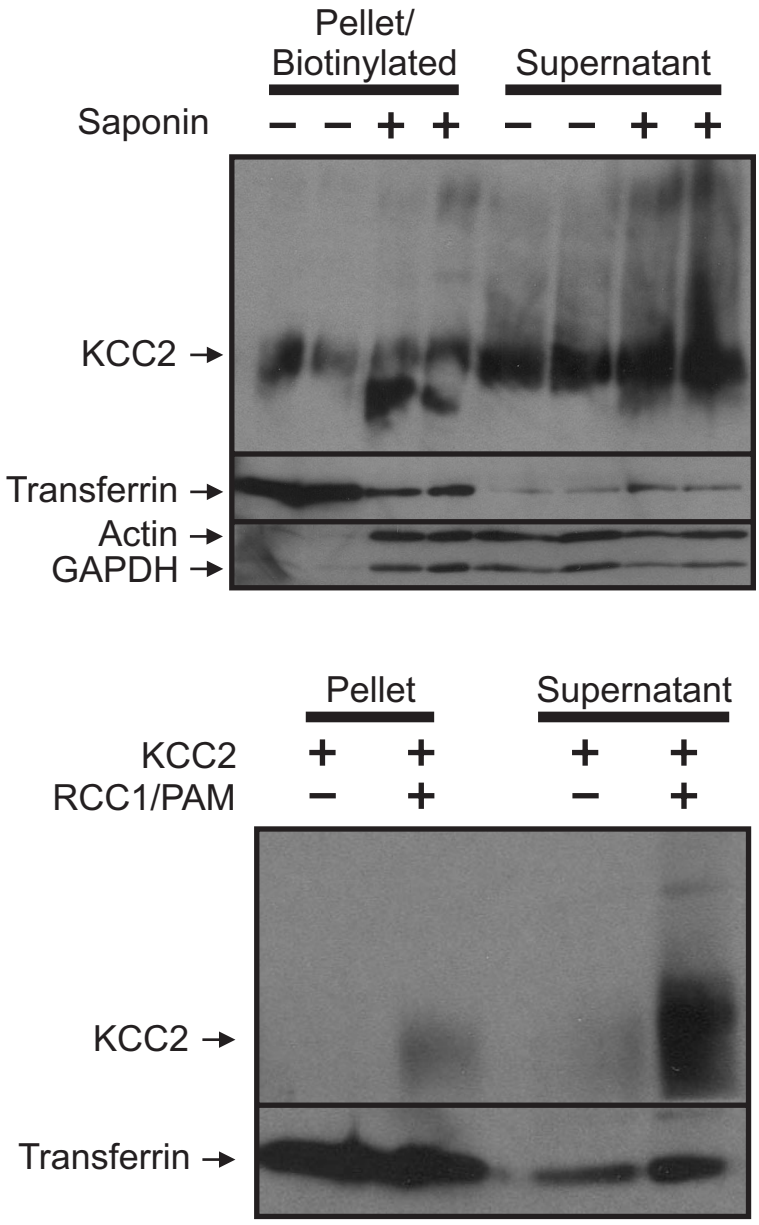

Figure 25. Biotinylation of KCC2.
Upper panel: HEK293 cells stably expressing KCC2 were biotinylated in the presence and absence of a permeabilizing detergent (saponin). Samples were separated by SDS-PAGE and immunoblotted with anti-KCC2, anti-transferrin, anti-actin, and anti-GAPDH antibodies. Lower panel: HEK293 cells transiently transfected with KCC2 in the presence and absence of RCC1/PAM were biotinylated, separated by SDS-PAGE and immunoblotted with anti-KCC2 and anti-transferrin antibodies.

N-ethylmaleimide stimulated flux

NEM is a known activator of KCC2 transport and one possibility is that RCC1/PAM and NEM share a common pathway in KCC2 regulation. Therefore, the effect of NEM was tested on wild type KCC2, in the presence and absence of RCC1/PAM. In agreement with the literature, NEM induced activation of KCC2-mediated K^+ uptake in HEK293 cells (Figure 26). Interestingly, NEM could not further stimulate the KCC2-mediated flux induced by RCC1/PAM coexpression. NEM stimulation of KCC2-RXA function was also examined. As shown in Figure 26, KCC2-RXA was once again demonstrated to be unaffected by RCC1/PAM expression. KCC2-RXA function was also unaffected by NEM treatment of the cells. This lack of NEM sensitivity by KCC2-RXA occurred both in the presence and absence of RCC1/PAM coexpression.

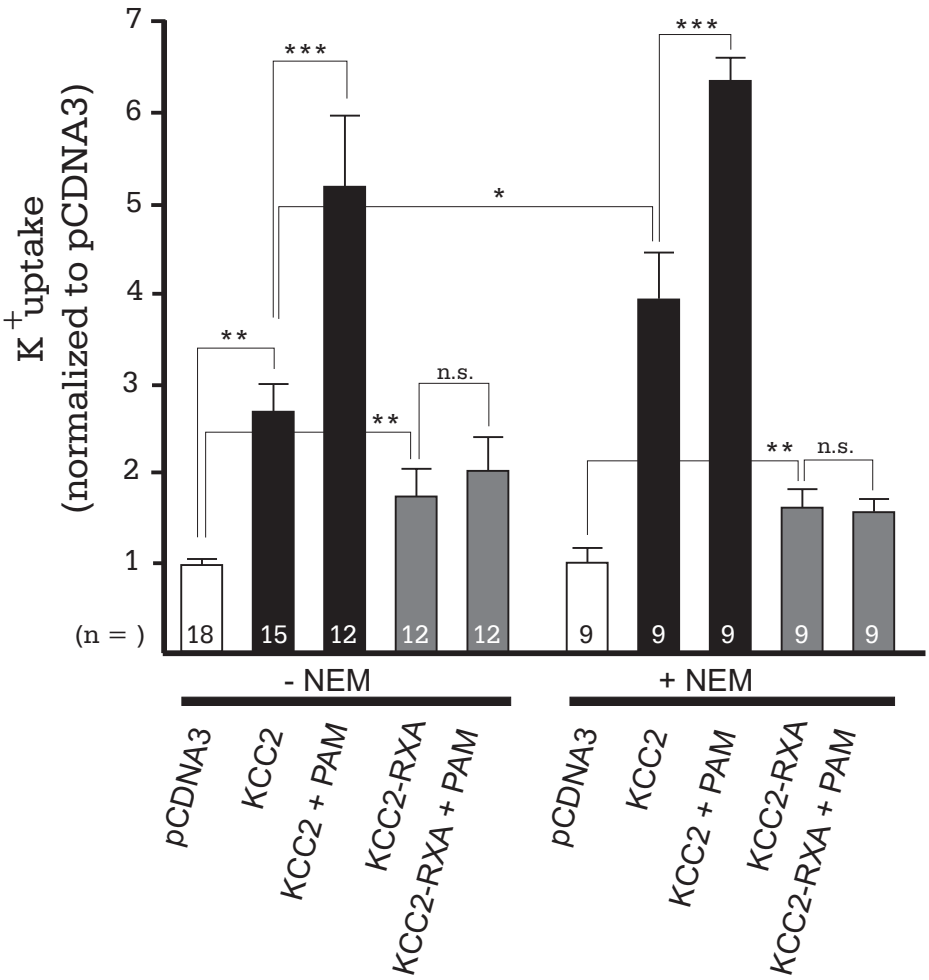

Figure 26. KCC2 mediated flux in the presence and absence of RCC1/PAM and/or N-ethylmaleimide.

HEK293 cells were transfected with KCC2 alone, KCC2 and RCC1/PAM, KCC2-RXA alone, or KCC2-RX A and RCC1/PAM. KCC2 uptake activity was measured using unidirectional $^{86}Rb^{+}$ uptake after 10 minutes of incubation with $^{86}Rb^{+}$. In +NEM conditions, stimulation was performed for 15 minutes total (5 minutes prior to $^{86}Rb^{+}$ incubation, and throughout the 10 minute $^{86}Rb^{+}$ incubation). *** = $P < 0.001$ (ANOVA, Tukey post-test).

Discussion

KCC2-RXA mutant

The RXA point mutation was introduced into full-length KCC2 and expressed in HEK293 cells. Quantitation of KCC2 RNA transcript and protein expression showed that KCC2-RXA, like wild type KCC2, was subject to RNA upregulation, and thus protein upregulation, in the presence of RCC1/PAM. Coimmunoprecipitation experiments with KCC2-RXA showed that this point mutation did not alter the ability of full-length KCC2 to coimmunoprecipitate RCC1/PAM. This suggests that RCC1/PAM binds elsewhere on the transporter, as well. The flux experiments with KCC2-RXA were particularly interesting because they demonstrated that KCC2-RXA still retains levels of transport activity similar to that of wild type KCC2. However, unlike wild type KCC2, KCC2-RXA activity is unaffected by the coexpression of RCC1/PAM. Thus, even though coimmunoprecipitation experiments show that KCC2-RXA binds elsewhere on the cotransporter, the fact that RCC1/PAM does not affect KCC2-RXA function suggests that RCC1/PAM does in fact have a functional impact resulting from binding to this particular region of KCC2.

RCC1/PAM seems to have a general effect on transcription in this experimental model. RCC1/PAM causes similar RNA and protein expression effects on both wild type KCC2 and mutant KCC2-RXA. Additionally, RCC1/PAM causes different functional effects on wild type KCC2 versus mutant KCC2-RXA. These facts together suggest that the effect of RCC1/PAM on transcription can be set aside when assessing the functional role of RCC1/PAM protein binding to the KCC2-CT. It would however be interesting to compare RNA and protein upregulation to assess if the increase in RNA is enough to

equal the increase in protein. It is not likely that this effect on KCC2 transcription would carry over to the natural setting of KCC2, as these KCC2 cDNAs are subcloned into expression vectors without the KCC2 promoter sequence.

In summary, these KCC2-RXA experiments suggest RCC1/PAM affects KCC2 in multiple ways. RCC1/PAM causes an RNA upregulation common to both wild type KCC2 and KCC2-RXA, which can be set aside to study post-translational modulation via RCC1/PAM-KCC2 protein interaction. KCC2 may bind RCC1/PAM on regions other than the KCC2-CT. This binding may or may not account for the fact that KCC2 activity increases in the presence of RCC1/PAM, but this has not been determined. Most significantly, it is clearly demonstrated that a single point mutation in the KCC2-CT can abolish RCC1/PAM-mediated changes in flux activity. The present data, in conjunction with the experiments described in Chapters II and III, provide compelling evidence that RCC1/PAM interacts with KCC2 at this domain on the KCC2-CT, and that this interaction on the KCC2-CT has functional consequences. In conclusion, the mutant KCC2-RXA isoform is a useful tool for examining the role of RCC1/PAM interaction with KCC2.

PAM in relation to RXR motif function

Functional experiments with the full-length RXA KCC2 mutant did not show increased cotransporter function similar to what would be expected if unmasking an RXR motif. Therefore it is questionable whether the RCC1/PAM binding is related to the known function of a bona-fide RXR motif. It is clear, however, that the RXR sequence and surrounding residues participate in the RCC1/PAM binding, and that altering this

motif has functional significance, since unidirectional ion flux experiments demonstrate RCC1/PAM coexpression increases K^+ uptake by wild type KCC2, but not by the KCC2 -RXA mutant.

NEM effect on KCC2 and implications for KCC2 and PAM interaction

NEM is a thiol reactive agent that is known to stimulate KCC function. The most convincing evidence suggests that NEM primarily exerts this effect through a phosphorylation/dephosphorylation pathway. Indeed, NEM is thought to cause net dephosphorylation of an unknown key substrate through kinase inhibition. Subsequent dephosphorylation of this substrate, likely by PP1, allows activation of the cotransporter (Jennings and Schulz, 1991). Although this evidence does not conclusively rule out a direct effect of NEM on KCC2, the fact that NEM has been shown to have opposing effects on NKCCs and KCCs would indicate regulation via upstream signaling pathways as opposed to direct action on the cotransporters (for review, see (Adragna et al., 2004)).

The NEM sensitivity of KCC2 and KCC2-RXA in the presence and absence of RCC1/PAM was tested to examine if the role of PAM binding to KCC2 might share a common pathway as the NEM effect. These studies with NEM, as reported in Figure 26, show that wild type KCC2 coexpressed with RCC1/PAM cannot be further stimulated by the alkylating agent. Additionally, the KCC2-RXA point mutant also cannot be further stimulated by NEM, regardless of whether or not RCC1/PAM is expressed. This indicates that this mutated region of the KCC2 carboxyl terminus is necessary for the pathway involved in NEM-mediated stimulation of KCC2.

The specifics on how PAM is intimately involved in the activity of the cotransporter, apart from binding to it and affecting NEM stimulation, is yet to be determined. In assessing changes in membrane transporter function, one possibility is that RCC1/PAM expression results in an increase in cotransporters present in the cell membrane. If this was the case, NEM stimulation should have an additive effect on RCC1/PAM and KCC2 coexpression. However, NEM stimulation does not have an additive effect with RCC1/PAM. This is particularly important in light of the fact that RCC1/PAM also increases overall KCC2 expression. Therefore, this suggests that the RCC1/PAM effect is not related to an increased number of transporters in the plasma membrane. However, since some change in transporter cell surface expression may make up a statistically insignificant portion of the RCC1/PAM-mediated activity changes, there is still room for further investigation of KCC2 surface expression studies using different extracellular protein labeling techniques.

This then leads to the conclusion that PAM's effect on KCC2 occurs when KCC2 is at the cell membrane. Other reports on PAM and RCC1 domains pose possible roles for PAM. PAM could directly affect kinase activity or GTP-GDP conversion in the vicinity of the cotransporter, as PAM has been shown to inhibit adenylyl cyclase activity (Scholich et al., 2001; Gao and Patel, 2005), and RCC1 domains in other proteins have been shown to have GTPase activity (Ohtsubo et al., 1989; Bischoff and Ponstingl, 1991).

However, the data shown here point strongly to PAM having an effect on KCC2 activity at the cell membrane via the same phosphoregulatory pathway affected by NEM stimulation. A model of this is illustrated in Figure 27. HEK293 cells express

endogenous PAM (Figure 27, panel A), and the transfected RCC1/PAM fragment competes with endogenous PAM for binding on the KCC2 carboxyl terminus (Figure 27B). When RCC1/PAM alone binds to wild type KCC2, it independently causes an increase in KCC2 activity. There are several possibilities why this may happen. RCC1/PAM may cause an allosteric modulation of the cotransporter which endogenous PAM does not. Another possibility is that PAM normally functions as a scaffolding protein, recruiting regulatory proteins to the cotransporter. Thus, when endogenous PAM cannot bind the carboxyl terminus of KCC2, as in the case of KCC2-RXA (Figure 27C) or when the RCC1/PAM fragment is present (Figure 27B), normal KCC2 regulation cannot occur since scaffolded proteins cannot be recruited to KCC2.

This concept of PAM as a scaffolding protein fits well with the NEM data, in that endogenous PAM could also scaffold the kinases or phosphatases which are functionally affected by NEM alkylation. As illustrated in Figure 27, NEM stimulation may require endogenous PAM recruiting phosphatases or kinases to the vicinity of KCC2 (Figure 27A). When endogenous PAM cannot bind the carboxyl terminus of KCC2, as in the case of KCC2-RXA or when the RCC1/PAM fragment is present, NEM stimulation has no effect (Figure 27, panels B and C). Taken altogether, PAM functions as an integral part of the same kinase/phosphatase pathway through which NEM exerts its effect. Thus, PAM binds to the KCC2 carboxyl terminus as an integral part of the phosphoregulation of KCC2 at the cell surface.

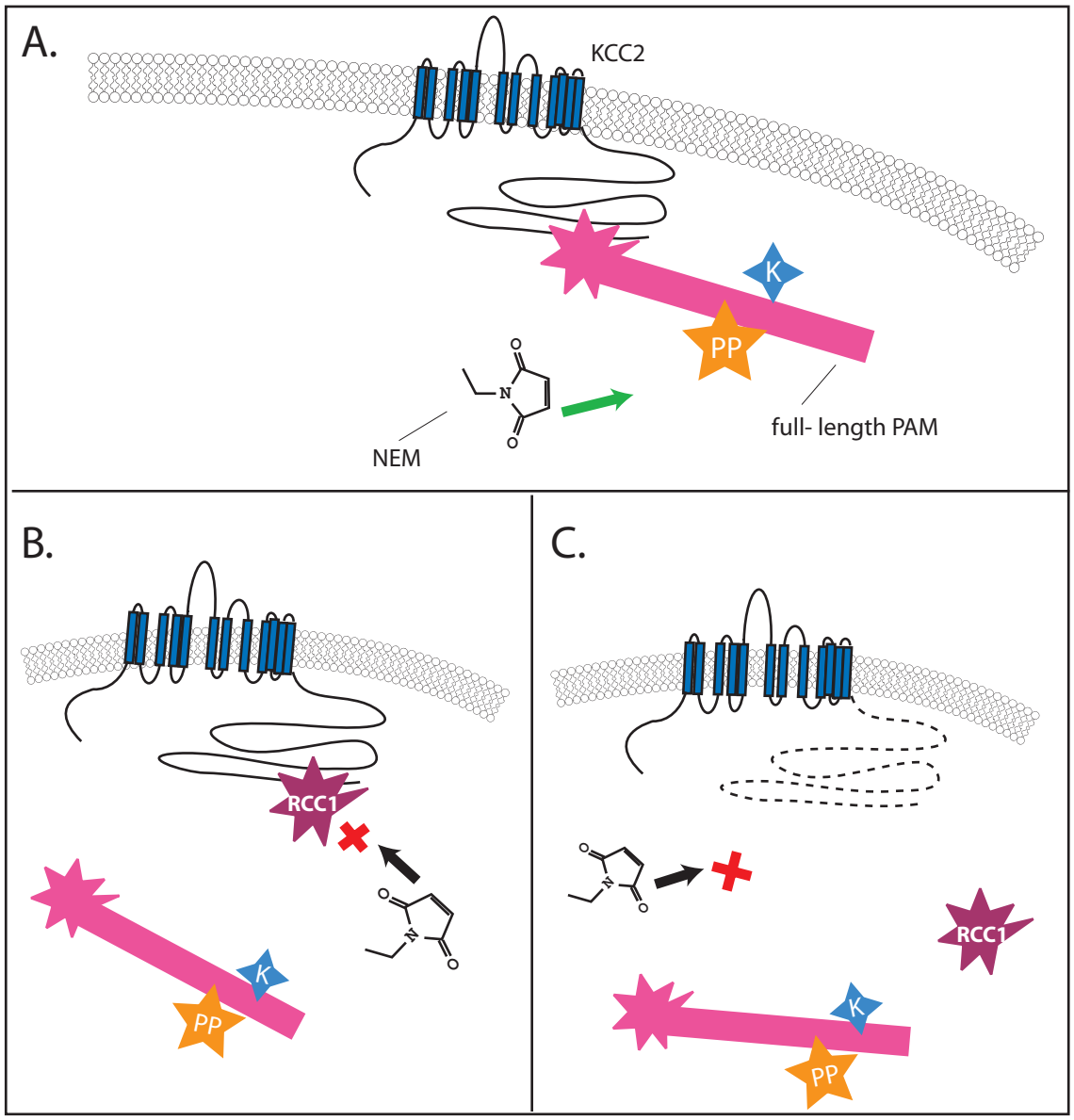

Figure 27. Model of PAM and KCC2 binding and regulation, and NEM stimulation.
Experiments with NEM suggest PAM binding plays a role in phosphoregulation of KCC2. NEM stimulation may involve domains or proteins located or bound on the C-terminal side of endogenous full-length PAM. PAM is depicted here as a scaffolding protein bringing a regulatory kinase (K) and protein phosphatase (PP) to the cotransporter (Panel A). When full-length PAM does not bind to KCC2, either due to blockade by RCC1/PAM (Panel B) or mutation of KCC2-CT (Panel C), this interferes with NEM stimulation of KCC2 activity.

CHAPTER VI

CONCLUSIONS AND FUTURE DIRECTIONS

Summary of work

The neuron-specific K^+-Cl^- cotransporter KCC2 is critical to proper functioning of the nervous system, particularly inhibitory signaling through the neurotransmitter GABA. Little is known about the regulation of this cotransporter, and even less is known about what other proteins interact with KCC2 in order to regulate KCC2-mediated transport activity. Since the carboxyl tail of KCC2 is a cytoplasmic domain, as well as a very large portion of the cotransporter, I hypothesized that proteins could potentially interact with this region of KCC2 to affect KCC2 function and regulation. Therefore, I used the KCC2-CT in a yeast two-hybrid screen of a mouse brain cDNA library to identify novel protein interactors.

This screen identified Protein Associated with Myc (PAM) as a binding partner with the KCC2-CT. Animal models with mutations of PAM and PAM homologues demonstrate that PAM is essential to neurodevelopment. PAM and KCC2 also share overlapping spatial and temporal expression. This led me to pursue studies of the effect of PAM binding to KCC2. Using the RCC1 domain of PAM (RCC1/PAM) I confirmed this newly identified interaction using small-scale yeast two-hybrid, GST pull-down assays, and coimmunoprecipitation of coexpressed full-length KCC2 and RCC1/PAM in HEK293 cells.

Interestingly, I also found that coexpression of RCC1/PAM with KCC2 causes an increase in KCC2 activity, protein expression, and RNA levels. Therefore, in order to isolate the effect of RCC1/PAM coexpression on KCC2 at the protein-protein interaction level, I characterized the binding site of RCC1/PAM on the KCC2-CT. After narrowing down the RCC1/PAM binding site to a 20 amino acid region of the KCC2-CT, I identified an RXR motif in this region of KCC2. Mutagenesis of this RXR motif, as well as the amino acid residue following this motif, are critical to RCC1/PAM binding to this region of KCC2, as demonstrated by yeast two-hybrid.

I introduced the mutated RXR motif, RXA, into full-length KCC2. Like wild type KCC2, KCC2-RXA also has increased RNA and protein levels when coexpressed with RCC1/PAM. Flux experiments showed that KCC2-RXA did not have a significantly different level of transport activity than wild type KCC2. However, unlike wild type KCC2, KCC2-RXA interestingly does not demonstrate increased activity when coexpressed with RCC1/PAM.

In order to further understand how the RXA mutation affects KCC2 function, I tested activity of both the wild type and mutant cotransporter in the presence and absence of RCC1/PAM, as well as when stimulated by the known K-Cl transport activator, N-ethylmaleimide (NEM). NEM most likely exerts its stimulatory effect by causing a net dephosphorylation which results in maximal KCC2 activation. These experiments presented here show that NEM stimulation does not cause an additive increase in KCC2 transport when the transporter and RCC1/PAM are coexpressed. Additionally, KCC2-RXA activity is not significantly stimulated by addition of NEM in either the presence of absence of RCC1/PAM. Taken together, these data suggest that PAM binds to the KCC2

carboxyl terminus as an integral part of the kinase/phosphatase pathway which regulates KCC2 activity.

KCC2 and PAM in the neuron

A critical requirement for the validity of any protein-protein interaction is that both proteins be expressed in the same cellular compartment. Since KCC2 subcellular localization in neurons is predominantly in postsynaptic areas and cell soma (Gulyas et al., 2001; Bartho et al., 2004), it is important that PAM is also expressed in these compartments. Non-mammalian homologues of PAM indicate a presynaptic role of the protein, and the recent work on PAM in Magellan mutant mice by Lewcock et al likewise suggests a presynaptic role (Lewcock et al., 2007). However, mammalian PAM has also been described as being present throughout neurons (Murthy et al., 2004; Szabadics et al., 2006). Thus, it is possible that PAM has numerous roles throughout the cell, as is fitting for a protein with many different functional domains, and only the more visually robust phenotype of axon outgrowth has been reported. It would be interesting to conduct a detailed study of PAM subcellular localization in the cell soma and dendrites, as was done at the growth cone in the studies of neurons from the Magellan mutant mice.

What could be the role of PAM and KCC2 interaction in the neuron? The work presented here shows that PAM binding is somehow tied into the same regulatory pathway as NEM. NEM is suspected to act as a kinase inhibitor resulting in a net dephosphorylation and functional stimulation of KCC2. It is unknown if in this situation the substrate being dephosphorylated is KCC2. I have demonstrated that NEM stimulation of KCC2 cannot occur when RCC1/PAM is expressed, and that NEM cannot

stimulate the mutant cotransporter KCC2-RXA. One potential explanation is that RCC1/PAM is exerting a dominant-negative effect over endogenous PAM. Therefore, in situations when endogenous PAM cannot bind to KCC2, such as during the coexpression of RCC1/PAM, or when the PAM binding site is disrupted on the KCC2 C-terminus, KCC2 activation via net phosphorylation by NEM cannot occur.

Then how does this translate into the native state of the cotransporter, that is, in neurons, and without NEM stimulation? As aforementioned, one possibility is that the role of PAM is to act as a scaffolding protein, recruiting protein kinases or phosphatases to the cotransporter for dephosphorylation and subsequent activation. Other groups have shown that in the axon, PAM works to downregulate kinase activity by ubiquitination of a multi-family kinase, specifically the double-leucine-zipper-kinase, or DLK. A global model integrating my data with this model is shown in Figure 28. Perhaps, in the dendrites, PAM binding to KCC2 exhibits control of K^+-Cl^- transport by recruiting of phosphoregulatory proteins and ubiquitin-mediated downregulation of a kinase in the vicinity of the cotransporter. Downregulation of this unknown kinase could also cause a net dephosphorylation and activate the cotransporter.

In the model presented by Lewcock et al, it is suggested that PAM's absence from the growth cone of developing axons is what allows it to remain fluid and motile (Lewcock et al., 2007). PAM stabilizes microtubules by downregulating DLK. The absence of PAM in the growth cone allows DLK to destabilize microtubules, allowing for extension of the axon via the growth cone. Lewcock et al suggest that, perhaps, when the neuron reaches its target, PAM moves to the distal ends of the axon to tag DLK for degradation, stabilize microtubules, and thus stabilize the synapse. Extrapolating this

idea to PAM's involvement with KCC2 at the dendrites, perhaps in a similar scenario PAM translocates to KCC2, tags a nearby kinase for degradation, thereby enhancing KCC2 activity and stabilizing synapses from a post-synaptic perspective via a shift to inhibitory GABAergic activity (Figure 28). In light of the extensive work done on the influence of GABA signaling in the developing brain, the involvement of KCC2 and PAM in synaptogenesis could be a potentially interesting field of study. This is especially true considering the recently reported interaction between KCC2 and 4.1N protein, and the proposed role of KCC2 as a synchronizing factor in synapse development.

The KCC2 and PAM interaction might be involved in processes beyond neurodevelopment and synaptogenesis. For example, as described in Chapters I and III, both of these proteins are involved in pain signaling pathways. A greater understanding of PAM modulation of KCC2 activity could lead to novel targets for alleviating chronic pain states. Thus, it is highly possible that the link between KCC2 and PAM may prove to be an interesting target for understanding human disease and injury.

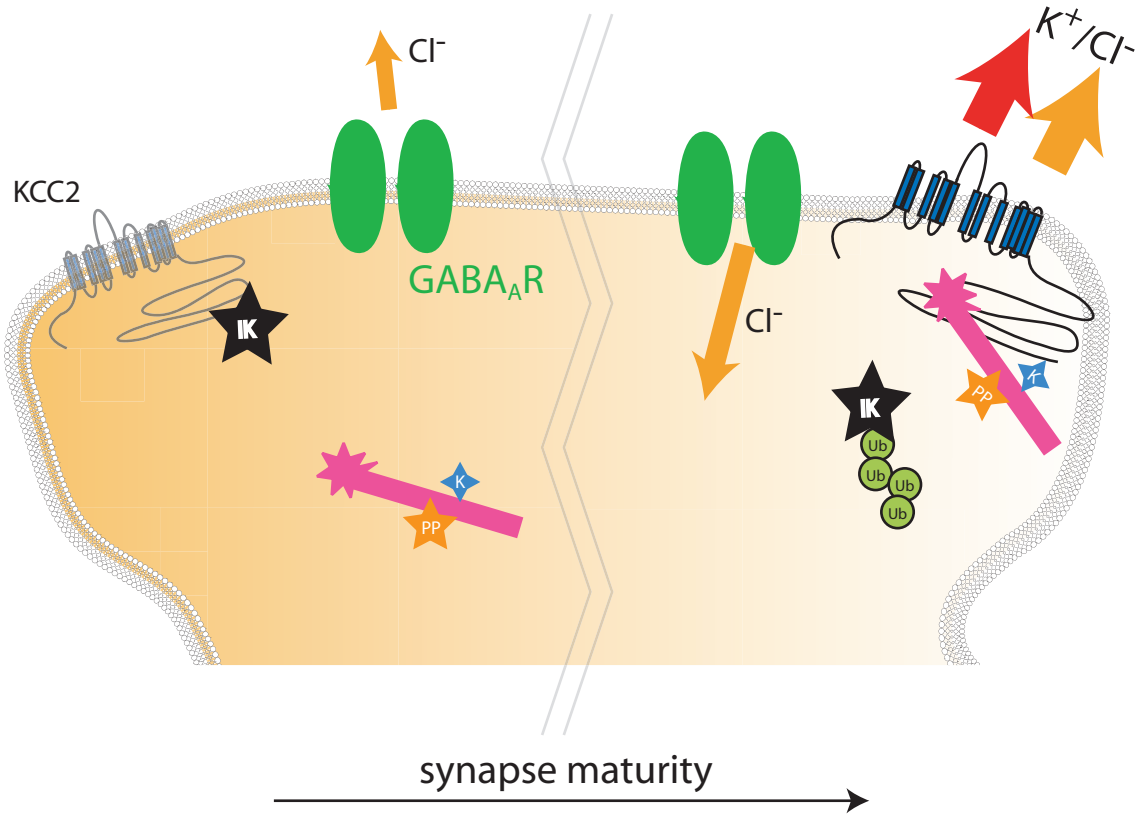

Figure 28. Model of a possible role for KCC2-PAM binding at the synapse. This model depicts a dendritic spine and illustrates a potential role of PAM and KCC2 binding in neurons. As depicted on the left, KCC2 function could be suppressed by cell signaling molecules, such as an inhibitory kinase (IK, black star), and low KCC2 activity leads to a depolarizing GABAergic response. As development proceeds, PAM moves into distal projections of the neuron. In the axon (not shown), PAM has been shown to degrade the DLK kinase by tagging it for ubiquitination, which in turn leads a solidifying of growth cones and development of synapses. Perhaps at this same timepoint PAM also moves into the most distal neuronal projections in the dendrite. PAM binding to KCC2, as depicted on the right, may again lead to kinase inhibition, this time acting on the inhibitory kinase suppressing KCC2 function. By disassociating the inhibitory kinase from KCC2, PAM causes a net dephosphorylation which upregulates KCC2 activity, thereby allowing the inhibitory GABAergic responses characteristic of a mature synapse.

Future directions

Future studies are needed to address the role of PAM on KCC2 function in neurons. One possibility involves examining the effect of PAM deletion on KCC2 function and Cl^- homeostasis. As mentioned above, at the animal level, deletion of PAM results in a phenotype similar to the KCC2 knockout phenotype. A viable mouse expressing PAM without the RCC1 domain (or inactive/mutated RCC1 domain) could represent a useful model for studying the role of PAM-KCC2 interaction in neurons. Another possibility would involve altering PAM expression at the level of the single neuron using RNA interference (RNAi). However, as PAM is a large protein with many domains, it is possible that its down-regulation by RNAi affects neurons beyond any effect related to KCC2. Regardless of whether using cultured cells or whole animal models, the studies presented here provide strong evidence that PAM plays a role in modulating KCC2 function in neurons, thereby affecting neuronal Cl^- concentration and $GABA_A$ and glycine inhibition.

LITERATURE CITED

Adragna NC, Fulvio MD, Lauf PK (2004) Regulation of K-Cl cotransport: from function to genes. J Membr Biol 201:109-137.

Adragna NC, Zhang J, Di Fulvio M, Lincoln TM, Lauf PK (2002) KCl cotransport regulation and protein kinase G in cultured vascular smooth muscle cells. J Membr Biol 187:157-165.

Aguado F, Carmona MA, Pozas E, Aguilo A, Martinez-Guijarro FJ, Alcantara S, Borrell V, Yuste R, Ibanez CF, Soriano E (2003) BDNF regulates spontaneous correlated activity at early developmental stages by increasing synaptogenesis and expression of the K+/Cl- co-transporter KCC2. Development 130:1267-1280.

Akerman CJ, Cline HT (2006) Depolarizing GABAergic conductances regulate the balance of excitation to inhibition in the developing retinotectal circuit in vivo. J Neurosci 26:5117-5130.

Aronica E, Boer K, Redeker S, Spliet WG, van Rijen PC, Troost D, Gorter JA (2007) Differential expression patterns of chloride transporters, Na(+)-K(+)-2Cl(-)-cotransporter and K(+)-Cl(-)-cotransporter, in epilepsy-associated malformations of cortical development. Neuroscience 145:185-196.

Balakrishnan V, Becker M, Lohrke S, Nothwang HG, Guresir E, Friauf E (2003) Expression and function of chloride transporters during development of inhibitory neurotransmission in the auditory brainstem. J Neurosci 23:4134-4145.

Balasubramani M, Day BW, Schoen RE, Getzenberg RH (2006) Altered expression and localization of creatine kinase B, heterogeneous nuclear ribonucleoprotein F, and high mobility group box 1 protein in the nuclear matrix associated with colon cancer. Cancer Res 66:763-769.

Barmashenko G, Schmidt M, Hoffmann KP (2005) Differences between cation-chloride co-transporter functions in the visual cortex of pigmented and albino rats. Eur J Neurosci 21:1189-1195.

Bartho P, Payne JA, Freund TF, Acsady L (2004) Differential distribution of the KCl cotransporter KCC2 in thalamic relay and reticular nuclei. Eur J Neurosci 20:965-975.

Bauer S, Fujita R, Buraczynska M, Abrahamson M, Ehinger B, Wu W, Falls TJ, Andreasson S, Swaroop A (1998) Phenotype of an X-linked retinitis pigmentosa family with a novel splice defect in the RPGR gene. Invest Ophthalmol Vis Sci 39:2470-2474.

Bergeron MJ, Gagnon E, Caron L, Isenring P (2006) Identification of key functional domains in the C terminus of the K+-Cl- cotransporters. J Biol Chem 281:15959-15969.

Bischoff FR, Ponstingl H (1991) Catalysis of guanine nucleotide exchange on Ran by the mitotic regulator RCC1. Nature 354:80-82.

Blaesse P, Guillemin I, Schindler J, Schweizer M, Delpire E, Khiroug L, Friauf E, Nothwang HG (2006) Oligomerization of KCC2 correlates with development of inhibitory neurotransmission. J Neurosci 26:10407-10419.

Blatch GL, Lassle M (1999) The tetratricopeptide repeat: a structural motif mediating protein-protein interactions. Bioessays 21:932-939.

Bloom AJ, Miller BR, Sanes JR, DiAntonio A (2007) The requirement for Phr1 in CNS axon tract formation reveals the corticostriatal boundary as a choice point for cortical axons. Genes Dev 21:2593-2606.

Booth RF, Clark JB (1978) Studies on the mitochondrially bound form of rat brain creatine kinase. Biochem J 170:145-151.

Buraczynska M, Wu W, Fujita R, Buraczynska K, Phelps E, Andreasson S, Bennett J, Birch DG, Fishman GA, Hoffman DR, Inana G, Jacobson SG, Musarella MA, Sieving PA, Swaroop A (1997) Spectrum of mutations in the RPGR gene that are identified in 20% of families with X-linked retinitis pigmentosa. Am J Hum Genet 61:1287-1292.

Burgess RW, Peterson KA, Johnson MJ, Roix JJ, Welsh IC, O'Brien TP (2004) Evidence for a conserved function in synapse formation reveals Phr1 as a candidate gene for respiratory failure in newborn mice. Mol Cell Biol 24:1096-1105.

Castegna A, Aksenov M, Aksenova M, Thongboonkerd V, Klein JB, Pierce WM, Booze R, Markesbery WR, Butterfield DA (2002) Proteomic identification of oxidatively modified proteins in Alzheimer's disease brain. Part I: creatine kinase BB, glutamine synthase, and ubiquitin carboxy-terminal hydrolase L-1. Free Radic Biol Med 33:562-571.

Casula S, Shmukler BE, Wilhelm S, Stuart-Tilley AK, Su W, Chernova MN, Brugnara C, Alper SL (2001) A dominant negative mutant of the KCC1 K-Cl cotransporter: both N- and C-terminal cytoplasmic domains are required for K-Cl cotransport activity. J Biol Chem 276:41870-41878.

Choi WS, Khurana A, Mathur R, Viswanathan V, Steele DF, Fedida D (2005) Kv1.5 surface expression is modulated by retrograde trafficking of newly endocytosed channels by the dynein motor. Circ Res 97:363-371.

Coull JA, Boudreau D, Bachand K, Prescott SA, Nault F, Sik A, De Koninck P, De Koninck Y (2003) Trans-synaptic shift in anion gradient in spinal lamina I neurons as a mechanism of neuropathic pain. Nature 424:938-942.

D'Souza J, Hendricks M, Le Guyader S, Subburaju S, Grunewald B, Scholich K, Jesuthasan S (2005) Formation of the retinotectal projection requires Esrom, an ortholog of PAM (protein associated with Myc). Development 132:247-256.

Daniels GM, Amara SG (1998) Selective labeling of neurotransmitter transporters at the cell surface. Methods Enzymol 296:307-318.

DeFazio RA, Keros S, Quick MW, Hablitz JJ (2000) Potassium-coupled chloride cotransport controls intracellular chloride in rat neocortical pyramidal neurons. J Neurosci 20:8069-8076.

Delpire E (2000) Cation-Chloride Cotransporters in Neuronal Communication. News Physiol Sci 15:309-312.

Delpire E, Gagnon KB (2006) SPAK and OSR1, key kinases involved in the regulation of chloride transport. Acta Physiol (Oxf) 187:103-113.

Delpire E, Gagnon KB (2007) Genome-wide analysis of SPAK/OSR1 binding motifs. Physiol Genomics 28:223-231.

Devon RS, Orban PC, Gerrow K, Barbieri MA, Schwab C, Cao LP, Helm JR, Bissada N, Cruz-Aguado R, Davidson TL, Witmer J, Metzler M, Lam CK, Tetzlaff W, Simpson EM, McCaffery JM, El-Husseini AE, Leavitt BR, Hayden MR (2006) Als2-deficient mice exhibit disturbances in endosome trafficking associated with motor behavioral abnormalities. Proc Natl Acad Sci U S A 103:9595-9600.

DiAntonio A, Haghighi AP, Portman SL, Lee JD, Amaranto AM, Goodman CS (2001) Ubiquitination-dependent mechanisms regulate synaptic growth and function. Nature 412:449-452.

Ehnert C, Tegeder I, Pierre S, Birod K, Nguyen HV, Schmidtko A, Geisslinger G, Scholich K (2004) Protein associated with Myc (PAM) is involved in spinal nociceptive processing. J Neurochem 88:948-957.

Feng XH, Derynck R (2001) Mammalian two-hybrid assays. Analyzing protein-protein interactions in transforming growth factor-beta signaling pathway. Methods Mol Biol 177:221-239.

Gagnon KB, England R, Delpire E (2006) Volume sensitivity of cation-Cl- cotransporters is modulated by the interaction of two kinases: Ste20-related proline-alanine-rich kinase and WNK4. Am J Physiol Cell Physiol 290:C134-142.

Gagnon KB, Adragna NC, Fyffe RE, Lauf PK (2007) Characterization of glial cell K-Cl cotransport. Cell Physiol Biochem 20:121-130.

Galanopoulou AS, Moshe SL (2003) Role of sex hormones in the sexually dimorphic expression of KCC2 in rat substantia nigra. Exp Neurol 184:1003-1009.

Ganguly K, Schinder AF, Wong ST, Poo M (2001) GABA itself promotes the developmental switch of neuronal GABAergic responses from excitation to inhibition. Cell 105:521-532.

Gao X, Patel TB (2005) Histidine residues 912 and 913 in protein associated with Myc are necessary for the inhibition of adenylyl cyclase activity. Mol Pharmacol 67:42-49.

Gillen CM, Brill S, Payne JA, Forbush B, 3rd (1996) Molecular cloning and functional expression of the K-Cl cotransporter from rabbit, rat, and human. A new member of the cation-chloride cotransporter family. J Biol Chem 271:16237-16244.

Gros-Louis F, Gaspar C, Rouleau GA (2006) Genetics of familial and sporadic amyotrophic lateral sclerosis. Biochim Biophys Acta 1762:956-972.

Gulledge AT, Stuart GJ (2003) Excitatory actions of GABA in the cortex. Neuron 37:299-309.

Gulyas AI, Sik A, Payne JA, Kaila K, Freund TF (2001) The KCl cotransporter, KCC2, is highly expressed in the vicinity of excitatory synapses in the rat hippocampus. Eur J Neurosci 13:2205-2217.

Guo Q, Xie J, Dang CV, Liu ET, Bishop JM (1998) Identification of a large Myc-binding protein that contains RCC1-like repeats. Proc Natl Acad Sci U S A 95:9172-9177.

Hadano S, Kunita R, Otomo A, Suzuki-Utsunomiya K, Ikeda JE (2007) Molecular and cellular function of ALS2/alsin: implication of membrane dynamics in neuronal development and degeneration. Neurochem Int 51:74-84.

Hadano S, Benn SC, Kakuta S, Otomo A, Sudo K, Kunita R, Suzuki-Utsunomiya K, Mizumura H, Shefner JM, Cox GA, Iwakura Y, Brown RH, Jr., Ikeda JE (2006) Mice deficient in the Rab5 guanine nucleotide exchange factor ALS2/alsin exhibit age-dependent neurological deficits and altered endosome trafficking. Hum Mol Genet 15:233-250.

Hadano S, Hand CK, Osuga H, Yanagisawa Y, Otomo A, Devon RS, Miyamoto N, Showguchi-Miyata J, Okada Y, Singaraja R, Figlewicz DA, Kwiatkowski T, Hosler BA, Sagie T, Skaug J, Nasir J, Brown RH, Jr., Scherer SW, Rouleau GA, Hayden MR, Ikeda JE (2001) A gene encoding a putative GTPase regulator is mutated in familial amyotrophic lateral sclerosis 2. Nat Genet 29:166-173.

Haskins WE, Kobeissy FH, Wolper RA, Ottens AK, Kitlen JW, McClung SH, O'Steen BE, Chow MM, Pineda JA, Denslow ND, Hayes RL, Wang KK (2005) Rapid discovery of putative protein biomarkers of traumatic brain injury by SDS-PAGE-capillary liquid chromatography-tandem mass spectrometry. J Neurotrauma 22:629-644.

He S, Parapuram SK, Hurd TW, Behnam B, Margolis B, Swaroop A, Khanna H (2008) Retinitis Pigmentosa GTPase Regulator (RPGR) protein isoforms in mammalian retina: insights into X-linked Retinitis Pigmentosa and associated ciliopathies. Vision Res 48:366-376.

Hegedus T, Aleksandrov A, Cui L, Gentzsch M, Chang XB, Riordan JR (2006) F508del CFTR with two altered RXR motifs escapes from ER quality control but its channel activity is thermally sensitive. Biochim Biophys Acta 1758:565-572.

Hekmat-Scafe DS, Lundy MY, Ranga R, Tanouye MA (2006) Mutations in the K+/Cl- cotransporter gene kazachoc (kcc) increase seizure susceptibility in Drosophila. J Neurosci 26:8943-8954.

Helms C, Pelsue S, Cao L, Lamb E, Loffredo B, Taillon-Miller P, Herrin B, Burzenski LM, Gott B, Lyons BL, Keppler D, Shultz LD, Bowcock AM (2005) The Tetratricopeptide repeat domain 7 gene is mutated in flaky skin mice: a model for psoriasis, autoimmunity, and anemia. Exp Biol Med (Maywood) 230:659-667.

Hendricks M, Mathuru AS, Wang H, Silander O, Kee MZ, Jesuthasan S (2008) Disruption of Esrom and Ryk identifies the roof plate boundary as an intermediate target for commissure formation. Mol Cell Neurosci 37:271-283.

Hermosilla R, Oueslati M, Donalies U, Schonenberger E, Krause E, Oksche A, Rosenthal W, Schulein R (2004) Disease-causing V(2) vasopressin receptors are retained in different compartments of the early secretory pathway. Traffic 5:993-1005.

Hiki K, D'Andrea RJ, Furze J, Crawford J, Woollatt E, Sutherland GR, Vadas MA, Gamble JR (1999) Cloning, characterization, and chromosomal location of a novel human K+-Cl- cotransporter. J Biol Chem 274:10661-10667.

Hirosawa M, Nagase T, Ishikawa K, Kikuno R, Nomura N, Ohara O (1999) Characterization of cDNA clones selected by the GeneMark analysis from size-fractionated cDNA libraries from human brain. DNA Res 6:329-336.

Holtzman D, Meyers R, Khait I, Jensen F (1997) Brain creatine kinase reaction rates and reactant concentrations during seizures in developing rats. Epilepsy Res 27:7-11.

Hubner CA, Stein V, Hermans-Borgmeyer I, Meyer T, Ballanyi K, Jentsch TJ (2001) Disruption of KCC2 reveals an essential role of K-Cl cotransport already in early synaptic inhibition. Neuron 30:515-524.

Inoue K, Ueno S, Fukuda A (2004) Interaction of neuron-specific K+-Cl- cotransporter, KCC2, with brain-type creatine kinase. FEBS Lett 564:131-135.

Inoue K, Yamada J, Ueno S, Fukuda A (2006) Brain-type creatine kinase activates neuron-specific K+-Cl- co-transporter KCC2. J Neurochem 96:598-608.

Jacquier A, Buhler E, Schafer MK, Bohl D, Blanchard S, Beclin C, Haase G (2006) Alsin/Rac1 signaling controls survival and growth of spinal motoneurons. Ann Neurol 60:105-117.

Jennings ML, Schulz RK (1991) Okadaic acid inhibition of KCl cotransport. Evidence that protein dephosphorylation is necessary for activation of transport by either cell swelling or N-ethylmaleimide. J Gen Physiol 97:799-817.

Jennings ML, Adame MF (2001) Direct estimate of 1:1 stoichiometry of K(+)-Cl(-) cotransport in rabbit erythrocytes. Am J Physiol Cell Physiol 281:C825-832.

Jin ZB, Liu XQ, Uchida A, Vervoort R, Morishita K, Hayakawa M, Murakami A, Matsumoto N, Niikawa N, Nao-i N (2005) Novel deletion spanning RCC1-like domain of RPGR in Japanese X-linked retinitis pigmentosa family. Mol Vis 11:535-541.

Kaddurah-Daouk R, Lillie JW, Daouk GH, Green MR, Kingston R, Schimmel P (1990) Induction of a cellular enzyme for energy metabolism by transforming domains of adenovirus E1a. Mol Cell Biol 10:1476-1483.

Kakazu Y, Akaike N, Komiyama S, Nabekura J (1999) Regulation of intracellular chloride by cotransporters in developing lateral superior olive neurons. J Neurosci 19:2843-2851.

Kakazu Y, Uchida S, Nakagawa T, Akaike N, Nabekura J (2000) Reversibility and cation selectivity of the K(+)-Cl(-) cotransport in rat central neurons. J Neurophysiol 84:281-288.

Karadsheh MF, Delpire E (2001) Neuronal restrictive silencing element is found in the KCC2 gene: molecular basis for KCC2-specific expression in neurons. J Neurophysiol 85:995-997.

Kelsch W, Hormuzdi S, Straube E, Lewen A, Monyer H, Misgeld U (2001) Insulin-like growth factor 1 and a cytosolic tyrosine kinase activate chloride outward transport during maturation of hippocampal neurons. J Neurosci 21:8339-8347.

Khanna H, Hurd TW, Lillo C, Shu X, Parapuram SK, He S, Akimoto M, Wright AF, Margolis B, Williams DS, Swaroop A (2005) RPGR-ORF15, which is mutated in retinitis pigmentosa, associates with SMC1, SMC3, and microtubule transport proteins. J Biol Chem 280:33580-33587.

Kristensen O, Guenat S, Dar I, Allaman-Pillet N, Abderrahmani A, Ferdaoussi M, Roduit R, Maurer F, Beckmann JS, Kastrup JS, Gajhede M, Bonny C (2006) A unique set of SH3-SH3 interactions controls IB1 homodimerization. EMBO J 25:785-797.

Kunita R, Otomo A, Mizumura H, Suzuki-Utsunomiya K, Hadano S, Ikeda JE (2007) The Rab5 activator ALS2/alsin acts as a novel Rac1 effector through Rac1-activated endocytosis. J Biol Chem 282:16599-16611.

Kuzhikandathil EV, Molloy GR (1994) Transcription of the brain creatine kinase gene in glial cells is modulated by cyclic AMP-dependent protein kinase. J Neurosci Res 39:70-82.

Kuzhikandathil EV, Molloy GR (1999) Proximal promoter of the rat brain creatine kinase gene lacks a consensus CRE element but is essential for the cAMP-mediated increased transcription in glioblastoma cells. J Neurosci Res 56:371-385.

Lai C, Xie C, McCormack SG, Chiang HC, Michalak MK, Lin X, Chandran J, Shim H, Shimoji M, Cookson MR, Huganir RL, Rothstein JD, Price DL, Wong PC, Martin LJ, Zhu JJ, Cai H (2006) Amyotrophic lateral sclerosis 2-deficiency leads to neuronal degeneration in amyotrophic lateral sclerosis through altered AMPA receptor trafficking. J Neurosci 26:11798-11806.

Lamb JR, Tugendreich S, Hieter P (1995) Tetratrico peptide repeat interactions: to TPR or not to TPR? Trends Biochem Sci 20:257-259.

Lauf PK, Theg BE (1980) A chloride dependent K^+ flux induced by N-ethylmaleimide in genetically low K^+ sheep and goat erythrocytes. Biochem Biophys Res Comm 70:221-242.

Lauf PK, Adragna NC (2000) K-Cl cotransport: properties and molecular mechanism. Cell Physiol Biochem 10:341-354.

Lauf PK, Adragna NC, Dupre N, Bouchard JP, Rouleau GA (2006) K-Cl cotransport in red blood cells from patients with KCC3 isoform mutants. Biochem Cell Biol 84:1034-1044.

Lauf PK, Bauer J, Adragna NC, Fujise H, Zade-Oppen AM, Ryu KH, Delpire E (1992) Erythrocyte K-Cl cotransport: properties and regulation. Am J Physiol 263:C917-932.

Le Guyader S, Maier J, Jesuthasan S (2005) Esrom, an ortholog of PAM (protein associated with c-myc), regulates pteridine synthesis in the zebrafish. Dev Biol 277:378-386.

Leupen SM, Tobet SA, Crowley WF, Jr., Kaila K (2003) Heterogeneous expression of the potassium-chloride cotransporter KCC2 in gonadotropin-releasing hormone neurons of the adult mouse. Endocrinology 144:3031-3036.

Lewcock JW, Genoud N, Lettieri K, Pfaff SL (2007) The Ubiquitin Ligase Phr1 Regulates Axon Outgrowth through Modulation of Microtubule Dynamics. Neuron 56:604-620.

Li H, Khirug S, Cai C, Ludwig A, Blaesse P, Kolikova J, Afzalov R, Coleman SK, Lauri S, Airaksinen MS, Keinanen K, Khiroug L, Saarma M, Kaila K, Rivera C (2007) KCC2 Interacts with the Dendritic Cytoskeleton to Promote Spine Development. Neuron 56:1019-1033.

Linari M, Ueffing M, Manson F, Wright A, Meitinger T, Becker J (1999) The retinitis pigmentosa GTPase regulator, RPGR, interacts with the delta subunit of rod cyclic GMP phosphodiesterase. Proc Natl Acad Sci U S A 96:1315-1320.

Lu J, Karadsheh M, Delpire E (1999) Developmental regulation of the neuronal-specific isoform of K-Cl cotransporter KCC2 in postnatal rat brains. J Neurobiol 39:558-568.

Mahadevan LC, Whatley SA, Leung TK, Lim L (1984) The brain isoform of a key ATP-regulating enzyme, creatine kinase, is a phosphoprotein. Biochem J 222:139-144.

Margeta-Mitrovic M, Jan YN, Jan LY (2000) A trafficking checkpoint controls GABA(B) receptor heterodimerization. Neuron 27:97-106.

McCabe BD, Hom S, Aberle H, Fetter RD, Marques G, Haerry TE, Wan H, O'Connor MB, Goodman CS, Haghighi AP (2004) Highwire regulates presynaptic BMP signaling essential for synaptic growth. Neuron 41:891-905.

McCarthy MM, Auger AP, Perrot-Sinal TS (2002) Getting excited about GABA and sex differences in the brain. Trends Neurosci 25:307-312.

Meindl A, Dry K, Herrmann K, Manson F, Ciccodicola A, Edgar A, Carvalho MR, Achatz H, Hellebrand H, Lennon A, Migliaccio C, Porter K, Zrenner E, Bird A, Jay M, Lorenz B, Wittwer B, D'Urso M, Meitinger T, Wright A (1996) A gene (RPGR) with homology to the RCC1 guanine nucleotide exchange factor is mutated in X-linked retinitis pigmentosa (RP3). Nat Genet 13:35-42.

Mercado A, Broumand V, Zandi-Nejad K, Enck AH, Mount DB (2006) A C-terminal domain in KCC2 confers constitutive K+-Cl- cotransport. J Biol Chem 281:1016-1026.

Miano MG, Testa F, Strazzullo M, Trujillo M, De Bernardo C, Grammatico B, Simonelli F, Mangino M, Torrente I, Ruberto G, Beneyto M, Antinolo G, Rinaldi E, Danesino C, Ventruto V, D'Urso M, Ayuso C, Baiget M, Ciccodicola A (1999) Mutation analysis of the RPGR gene reveals novel mutations in south European patients with X-linked retinitis pigmentosa. Eur J Hum Genet 7:687-694.

Miletic G, Miletic V (2007) Loose ligation of the sciatic nerve is associated with TrkB receptor-dependent decreases in KCC2 protein levels in the ipsilateral spinal dorsal horn. Pain.

Mockli N, Deplazes A, Hassa PO, Zhang Z, Peter M, Hottiger MO, Stagljar I, Auerbach D (2007) Yeast split-ubiquitin-based cytosolic screening system to detect interactions between transcriptionally active proteins. Biotechniques 42:725-730.

Moore-Hoon ML, Turner RJ (2000) The structural unit of the secretory Na+-K+-2Cl-cotransporter (NKCC1) is a homodimer. Biochemistry 39:3718-3724.

Mount DB, Mercado A, Song L, Xu J, George AL, Jr., Delpire E, Gamba G (1999) Cloning and characterization of KCC3 and KCC4, new members of the cation-chloride cotransporter gene family. J Biol Chem 274:16355-16362.

Munoz A, Mendez P, DeFelipe J, Alvarez-Leefmans FJ (2007) Cation-chloride cotransporters and GABA-ergic innervation in the human epileptic hippocampus. Epilepsia 48:663-673.

Murthy V, Han S, Beauchamp RL, Smith N, Haddad LA, Ito N, Ramesh V (2004) Pam and its ortholog highwire interact with and may negatively regulate the TSC1.TSC2 complex. J Biol Chem 279:1351-1358.

Nabekura J, Ueno T, Okabe A, Furuta A, Iwaki T, Shimizu-Okabe C, Fukuda A, Akaike N (2002) Reduction of KCC2 expression and GABAA receptor-mediated excitation after in vivo axonal injury. J Neurosci 22:4412-4417.

Neidhardt J, Glaus E, Barthelmes D, Zeitz C, Fleischhauer J, Berger W (2007) Identification and characterization of a novel RPGR isoform in human retina. Hum Mutat 28:797-807.

Nomura H, Sakai A, Nagano M, Umino M, Suzuki H (2006) Expression changes of cation chloride cotransporters in the rat spinal cord following intraplantar formalin. Neurosci Res 56:435-440.

Nunez JL, McCarthy MM (2007) Evidence for an extended duration of GABA-mediated excitation in the developing male versus female hippocampus. Dev Neurobiol 67:1879-1890.

Ohtsubo M, Okazaki H, Nishimoto T (1989) The RCC1 protein, a regulator for the onset of chromosome condensation locates in the nucleus and binds to DNA. J Cell Biol 109:1389-1397.

Otomo A, Hadano S, Okada T, Mizumura H, Kunita R, Nishijima H, Showguchi-Miyata J, Yanagisawa Y, Kohiki E, Suga E, Yasuda M, Osuga H, Nishimoto T, Narumiya S, Ikeda JE (2003) ALS2, a novel guanine nucleotide exchange factor for the small GTPase Rab5, is implicated in endosomal dynamics. Hum Mol Genet 12:1671-1687.

Palma E, Amici M, Sobrero F, Spinelli G, Di Angelantonio S, Ragozzino D, Mascia A, Scoppetta C, Esposito V, Miledi R, Eusebi F (2006) Anomalous levels of Cl- transporters in the hippocampal subiculum from temporal lobe epilepsy patients make GABA excitatory. Proc Natl Acad Sci U S A 103:8465-8468.

Payne JA (1997) Functional characterization of the neuronal-specific K-Cl cotransporter: implications for [K+]o regulation. Am J Physiol 273:C1516-1525.

Payne JA, Stevenson TJ, Donaldson LF (1996) Molecular characterization of a putative K-Cl cotransporter in rat brain. A neuronal-specific isoform. J Biol Chem 271:16245-16252.

Pearson MM, Lu J, Mount DB, Delpire E (2001) Localization of the K(+)-Cl(-) cotransporter, KCC3, in the central and peripheral nervous systems: expression in the choroid plexus, large neurons and white matter tracts. Neuroscience 103:481-491.

Perrot-Sinal TS, Sinal CJ, Reader JC, Speert DB, McCarthy MM (2007) Sex differences in the chloride cotransporters, NKCC1 and KCC2, in the developing hypothalamus. J Neuroendocrinol 19:302-308.

Peterson KA, King BL, Hagge-Greenberg A, Roix JJ, Bult CJ, O'Brien TP (2002) Functional and comparative genomic analysis of the piebald deletion region of mouse chromosome 14. Genomics 80:172-184.

Piechotta K, Lu J, Delpire E (2002) Cation chloride cotransporters interact with the stress-related kinases Ste20-related proline-alanine-rich kinase (SPAK) and oxidative stress response 1 (OSR1). J Biol Chem 277:50812-50819.

Piechotta K, Garbarini N, England R, Delpire E (2003) Characterization of the interaction of the stress kinase SPAK with the Na+-K+-2Cl- cotransporter in the nervous system: evidence for a scaffolding role of the kinase. J Biol Chem 278:52848-52856.

Pierre SC, Hausler J, Birod K, Geisslinger G, Scholich K (2004) PAM mediates sustained inhibition of cAMP signaling by sphingosine-1-phosphate. Embo J 23:3031-3040.

Pramfalk C, Lanner J, Andersson M, Danielsson E, Kaiser C, Renstrom IM, Warolen M, James SR (2004) Insulin receptor activation and down-regulation by cationic lipid transfection reagents. BMC Cell Biol 5:7.

Price TJ, Cervero F, de Koninck Y (2005) Role of cation-chloride-cotransporters (CCC) in pain and hyperalgesia. Curr Top Med Chem 5:547-555.

Race JE, Makhlouf FN, Logue PJ, Wilson FH, Dunham PB, Holtzman EJ (1999) Molecular cloning and functional characterization of KCC3, a new K-Cl cotransporter. Am J Physiol 277:C1210-1219.

Reid KH, Guo SZ, Iyer VG (2000) Agents which block potassium-chloride cotransport prevent sound-triggered seizures in post-ischemic audiogenic seizure-prone rats. Brain Res 864:134-137.

Reid KH, Li GY, Payne RS, Schurr A, Cooper NG (2001) The mRNA level of the potassium-chloride cotransporter KCC2 covaries with seizure susceptibility in inferior colliculus of the post-ischemic audiogenic seizure-prone rat. Neurosci Lett 308:29-32.

Renault L, Nassar N, Vetter I, Becker J, Klebe C, Roth M, Wittinghofer A (1998) The 1.7 A crystal structure of the regulator of chromosome condensation (RCC1) reveals a seven-bladed propeller. Nature 392:97-101.

Rivera C, Voipio J, Kaila K (2005) Two developmental switches in GABAergic signalling: the K+-Cl- cotransporter KCC2 and carbonic anhydrase CAVII. J Physiol 562:27-36.

Rivera C, Voipio J, Payne JA, Ruusuvuori E, Lahtinen H, Lamsa K, Pirvola U, Saarma M, Kaila K (1999) The K+/Cl- co-transporter KCC2 renders GABA hyperpolarizing during neuronal maturation. Nature 397:251-255.

Rivera C, Voipio J, Thomas-Crusells J, Li H, Emri Z, Sipila S, Payne JA, Minichiello L, Saarma M, Kaila K (2004) Mechanism of activity-dependent downregulation of the neuron-specific K-Cl cotransporter KCC2. J Neurosci 24:4683-4691.

Rivera C, Li H, Thomas-Crusells J, Lahtinen H, Viitanen T, Nanobashvili A, Kokaia Z, Airaksinen MS, Voipio J, Kaila K, Saarma M (2002) BDNF-induced TrkB activation down-regulates the K+-Cl- cotransporter KCC2 and impairs neuronal Cl- extrusion. J Cell Biol 159:747-752.

Roepman R, Bernoud-Hubac N, Schick DE, Maugeri A, Berger W, Ropers HH, Cremers FP, Ferreira PA (2000) The retinitis pigmentosa GTPase regulator (RPGR) interacts with novel transport-like proteins in the outer segments of rod photoreceptors. Hum Mol Genet 9:2095-2105.

Roos J, Kelly RB (1998) Dap160, a neural-specific Eps15 homology and multiple SH3 domain-containing protein that interacts with Drosophila dynamin. J Biol Chem 273:19108-19119.

Sandrock B, Tirode F, Egly JM (2001) Three-hybrid screens. Inducible third-party systems. Methods Mol Biol 177:271-289.

Santos TM, Han S, Bowser M, Sazani K, Beauchamp RL, Murthy V, Bhide PG, Ramesh V (2006) Alternative splicing in protein associated with Myc (Pam) influences its binding to c-Myc. J Neurosci Res 83:222-232.

Schaefer AM, Hadwiger GD, Nonet ML (2000) rpm-1, a conserved neuronal gene that regulates targeting and synaptogenesis in C. elegans. Neuron 26:345-356.

Scholich K, Pierre S, Patel TB (2001) Protein associated with Myc (PAM) is a potent inhibitor of adenylyl cyclases. J Biol Chem 276:47583-47589.

Scott DB, Blanpied TA, Swanson GT, Zhang C, Ehlers MD (2001) An NMDA receptor ER retention signal regulated by phosphorylation and alternative splicing. J Neurosci 21:3063-3072.

Sheng M, Kim E (2000) The Shank family of scaffold proteins. J Cell Sci 113 (Pt 11):1851-1856.

Simard CF, Bergeron MJ, Cotton-Frenette R, Carpentier GA, Pelchat ME, Caron L, Isenring P (2007) Homooligomeric and heterooligomeric associations between K-Cl cotransporter isoforms and between K-Cl and Na-K-Cl cotransporters. J Biol Chem.

Somer H, Kaste M, Troupp H, Konttinen A (1975) Brain creatine kinase in blood after acute brain injury. J Neurol Neurosurg Psychiatry 38:572-576.

Stein V, Hermans-Borgmeyer I, Jentsch TJ, Hubner CA (2004) Expression of the KCl cotransporter KCC2 parallels neuronal maturation and the emergence of low intracellular chloride. J Comp Neurol 468:57-64.

Strange K, Singer TD, Morrison R, Delpire E (2000) Dependence of KCC2 K-Cl cotransporter activity on a conserved carboxy terminus tyrosine residue. Am J Physiol Cell Physiol 279:C860-867.

Streck EL, Amboni G, Scaini G, Di-Pietro PB, Rezin GT, Valvassori SS, Luz G, Kapczinski F, Quevedo J (2008) Brain creatine kinase activity in an animal model of mania. Life Sci 82:424-429.

Szabadics J, Varga C, Molnar G, Olah S, Barzo P, Tamas G (2006) Excitatory effect of GABAergic axo-axonic cells in cortical microcircuits. Science 311:233-235.

Thaminy S, Miller J, Stagljar I (2004) The split-ubiquitin membrane-based yeast two-hybrid system. Methods Mol Biol 261:297-312.

Tian L, Chen L, McClafferty H, Sailer CA, Ruth P, Knaus HG, Shipston MJ (2006) A noncanonical SH3 domain binding motif links BK channels to the actin cytoskeleton via the SH3 adapter cortactin. FASEB J 20:2588-2590.

Toyoda H, Ohno K, Yamada J, Ikeda M, Okabe A, Sato K, Hashimoto K, Fukuda A (2003) Induction of NMDA and GABAA receptor-mediated Ca2+ oscillations with KCC2 mRNA downregulation in injured facial motoneurons. J Neurophysiol 89:1353-1362.

Tudor EL, Perkinton MS, Schmidt A, Ackerley S, Brownlees J, Jacobsen NJ, Byers HL, Ward M, Hall A, Leigh PN, Shaw CE, McLoughlin DM, Miller CC (2005) ALS2/Alsin regulates Rac-PAK signaling and neurite outgrowth. J Biol Chem 280:34735-34740.

Ueno T, Okabe A, Akaike N, Fukuda A, Nabekura J (2002) Diversity of neuron-specific K+-Cl- cotransporter expression and inhibitory postsynaptic potential depression in rat motoneurons. J Biol Chem 277:4945-4950.

Uvarov P, Pruunsild P, Timmusk T, Airaksinen MS (2005) Neuronal K+/Cl- co-transporter (KCC2) transgenes lacking neurone restrictive silencer element recapitulate CNS neurone-specific expression and developmental up-regulation of endogenous KCC2 gene. J Neurochem 95:1144-1155.

Uvarov P, Ludwig A, Markkanen M, Rivera C, Airaksinen MS (2006) Upregulation of the neuron-specific K+/Cl- cotransporter expression by transcription factor early growth response 4. J Neurosci 26:13463-13473.

Uvarov P, Ludwig A, Markkanen M, Pruunsild P, Kaila K, Delpire E, Timmusk T, Rivera C, Airaksinen MS (2007) A novel N-terminal isoform of the neuron-specific K-Cl cotransporter KCC2. J Biol Chem 282:30570-30576.

Van Criekinge W, Beyaert R (1999) Yeast Two-Hybrid: State of the Art. Biol Proced Online 2:1-38.

Vardi N, Zhang LL, Payne JA, Sterling P (2000) Evidence that different cation chloride cotransporters in retinal neurons allow opposite responses to GABA. J Neurosci 20:7657-7663.

Vervoort R, Wright AF (2002) Mutations of RPGR in X-linked retinitis pigmentosa (RP3). Hum Mutat 19:486-500.

Vervoort R, Lennon A, Bird AC, Tulloch B, Axton R, Miano MG, Meindl A, Meitinger T, Ciccodicola A, Wright AF (2000) Mutational hot spot within a new RPGR exon in X-linked retinitis pigmentosa. Nat Genet 25:462-466.

Vivithanaporn P, Yan S, Swanson GT (2006) Intracellular trafficking of KA2 kainate receptors mediated by interactions with coatomer protein complex I (COPI) and 14-3-3 chaperone systems. J Biol Chem 281:15475-15484.

Wan HI, DiAntonio A, Fetter RD, Bergstrom K, Strauss R, Goodman CS (2000) Highwire regulates synaptic growth in Drosophila. Neuron 26:313-329.

White RA, McNulty SG, Nsumu NN, Boydston LA, Brewer BP, Shimizu K (2005) Positional cloning of the Ttc7 gene required for normal iron homeostasis and mutated in hea and fsn anemia mice. Genomics 85:330-337.

Williams JR, Sharp JW, Kumari VG, Wilson M, Payne JA (1999) The neuron-specific K-Cl cotransporter, KCC2. Antibody development and initial characterization of the protein. J Biol Chem 274:12656-12664.

Willis D, Parameswaran B, Shen W, Molloy GR (1999) Conditions providing enhanced transfection efficiency in rat pheochromocytoma PC12 cells permit analysis of the activity of the far-upstream and proximal promoter of the brain creatine kinase gene. J Neurosci Methods 92:3-13.

Woo NS, Lu J, England R, McClellan R, Dufour S, Mount DB, Deutch AY, Lovinger DM, Delpire E (2002) Hyperexcitability and epilepsy associated with disruption of the mouse neuronal-specific K-Cl cotransporter gene. Hippocampus 12:258-268.

Wu C, Wairkar YP, Collins CA, DiAntonio A (2005) Highwire function at the Drosophila neuromuscular junction: spatial, structural, and temporal requirements. J Neurosci 25:9557-9566.

Xu Z, Kukekov NV, Greene LA (2003) POSH acts as a scaffold for a multiprotein complex that mediates JNK activation in apoptosis. Embo J 22:252-261.

Yamanaka K, Vande Velde C, Eymard-Pierre E, Bertini E, Boespflug-Tanguy O, Cleveland DW (2003) Unstable mutants in the peripheral endosomal membrane component ALS2 cause early-onset motor neuron disease. Proc Natl Acad Sci U S A 100:16041-16046.

Yang H, Scholich K, Poser S, Storm DR, Patel TB, Goldowitz D (2002) Developmental expression of PAM (protein associated with MYC) in the rodent brain. Brain Res Dev Brain Res 136:35-42.

Yang Y, Hentati A, Deng HX, Dabbagh O, Sasaki T, Hirano M, Hung WY, Ouahchi K, Yan J, Azim AC, Cole N, Gascon G, Yagmour A, Ben-Hamida M, Pericak-Vance M, Hentati F, Siddique T (2001) The gene encoding alsin, a protein with three guanine-nucleotide exchange factor domains, is mutated in a form of recessive amyotrophic lateral sclerosis. Nat Genet 29:160-165.

Yuan H, Michelsen K, Schwappach B (2003) 14-3-3 dimers probe the assembly status of multimeric membrane proteins. Curr Biol 13:638-646.

Zerangue N, Schwappach B, Jan YN, Jan LY (1999) A new ER trafficking signal regulates the subunit stoichiometry of plasma membrane K(ATP) channels. Neuron 22:537-548.

Zhao J, Schmieg FI, Simmons DT, Molloy GR (1994) Mouse p53 represses the rat brain creatine kinase gene but activates the rat muscle creatine kinase gene. Mol Cell Biol 14:8483-8492.

Zhen M, Huang X, Bamber B, Jin Y (2000) Regulation of presynaptic terminal organization by C. elegans RPM-1, a putative guanine nucleotide exchanger with a RING-H2 finger domain. Neuron 26:331-343.

Zhu L, Lovinger D, Delpire E (2005) Cortical neurons lacking KCC2 expression show impaired regulation of intracellular chloride. J Neurophysiol 93:1557-1568.